AN ABSTRACT OF THE DISSERTATION OF

Jason K. Stowers for the degree of Doctor of Philosophy in Chemistry presented on August 14, 2008.

Title: Direct Patterning of Solution Deposited Metal Oxides.

Abstract approved: ____

Douglas A. Keszler

Patterning of metal oxides typically involves a multi step process, involving depositing a resist, patterning that resist with some form of lithography, etching the oxide through the resist, and finally removing. This process can be simplified if the resist is removed and replaced with a metal oxide that can be directly patterned. Solution deposition of metal oxides allows the possibility of depositing materials that are responsive to traditional lithographic patterning methods. A directly patterned resist can be integrated into devices with less difficulty. It is also possible, with a directly patterned metal oxide, to consider this material also as a resist for the patterning of another material. This metal oxide can then be considered an inorganic resist. Inorganic resists have proven to offer a higher resolution and etch resistance than a comparable polymer resist. The work presented here represents efforts to develop directly patterned metal oxides that exhibits these desired resist properties, but which also competes with polymer resist in terms of sensitivity, the one area inorganic resists have always performed unsuitably. An inorganic resist has been developed that exhibits excellent performance in these important metrics, as well as others which are

required of state-of-the-art resists. This inorganic resist has shown sensitivity to a variety of modern exposure sources. The patterning chemistry which has been develop is adaptable to a large number of metal oxides. Direct pattern of metal oxides also offers potential for the modification of the material through solution based or solid state methods in order to access a variety of material properties not found in the initial metal oxide.

©Copyright by Jason K. Stowers
August 14, 2008
All Rights Reserved

Direct Patterning of Solution Deposited Metal Oxides

by
Jason K. Stowers

A DISSERTATION

submitted to

Oregon State University

in partial fulfillment of
the requirements for the
degree of

Doctor of Philosophy

Presented August 14, 2008
Commencement June 2009

Doctor of Philosophy dissertation of Jason K. Stowers presented on August 14, 2008.

APPROVED:

Major Professor, representing Chemistry

Chair of the Department of Chemistry

Dean of the Graduate School

I understand that my dissertation will become part of the permanent collection of Oregon State University libraries. My signature below authorizes release of my dissertation to any reader upon request.

Jason K. Stowers, Author

ACKNOWLEDGMENTS

I would like to acknowledge the single most important person to the completion of this body of research, my wife, Avie Meadows. She has been my side through the majority of my graduate education and she has waited patiently for the completion of this dissertation. She has focus my efforts and motivated me through the last few months of my Ph.D. work. With the end of my time in graduate school I hope to be able to provide for her as she truly deserves.

Dr. Jeanette Roberts and Dr. Pooya Tadayon are both responsible for the path I have chosen since completing my undergraduate education. They were in part responsible for convincing me to go to graduate school and receive my doctorate. They have continued to serve as mentors through the start of my career.

Dr. Douglas Keszler deserves significant recognition for his roll as my advisor. He has contributed to both my scientific knowledge and education about how business and academics function. His remarkable ability to find funding has assured me the opportunity to focus on my research.

Many members of the Keszler Group deserve recognition. Heather A. S. Platt is a dedicated member of the group. She deserves significant credit for volunteering in maintaining various pieces of equipment essential to every member of the group. I was fortunate to work with her during the very end of my time in graduate school. That experience was rewarding and produced a significant volume of successful results in a short amount of time. Kai Jiang has continuously impressed me with the quality of research he has produced. My brief collaboration with him was quite successful. He provided me with knowledge to expand my effort to new materials.

Dr. Stephen Meyers has always been the most pragmatic of scientists in the group. I have always used Stephen as a sounding board for ideas. This contribution to my research has been invaluable. My conversations with Dr. Jeremy Anderson proved to be transformative. Jeremy is in large part responsible for effecting my change from the mindset of an engineer to that of a scientist. Much of the research I have done is base on material systems he first developed. His generous sharing of knowledge regarding these materials has made my results possible.

Several past members of the Keszler Group deserve acknowledgment. One of the kindest men I have known, Dr. Cheol Hee Park, assisted me with much of my early research. Dr. Pete Hersh and I collaborated early in my graduate work. Together we learn how do deal with unsuccessful avenues of research. While in the group Pete was also largely responsible for maintaining equipment that keeps the group functioning. Dr. Jao Young Jeong keep me company with pleasant conversation on many late nights during the waning part of my graduate education.

Since our first months in graduate school together, Dr. Paul Newhouse, has proven to be a successful collaborator. More importantly he became a remarkable friend. We have shared much over the past years. For our early collaborations, his more recent help in making electrical measurements, and most importantly for his friendship over the past many years I am grateful.

Last but not least I would like to acknowledge Porter Henry Stowers who has been waiting his entire life for his father to finish this dissertation. With its completion I have promised to spend more time with him and to read to him all the books he desires.

CONTIBUTION OF AUTHORS

There are several fellow researchers that have made contributions to material contained within this dissertation. Dr. Jeremy Anderson needs to be credited for his indirect contribution to chapters 2, 3, and 4. These chapters are based on a material system originally developed by Dr. Anderson. His vast knowledge of this system, generously shared, served as a foundation for the work contained within these chapters.

Kai Jiang developed the method to deposit high quality TiO_2 found in chapter 5. This chapter has been excerpted from a larger publication with co-authors Kai Jiang, Andriy Zakutayev, Dr Douglas Keszler, Dr Janet Tate, Dr David McIntyre, and Jason Stowers. Only sections pertaining to film deposition and patterning have been excerpted, thus Kai Jiang is to only relevant co-author for the contents of this chapter. The topic of patterning has been expanded upon within this chapter.

The contents of Chapter 6 were produced in collaboration with Heather A. S. Platt. Her knowledge of solid-state synthesis was brought to bear on the reduction of the MoO_x materials.

Dr. Douglas Keszler has made numerous contributions in suggesting experiments, interpreting of results, and editing through the entirety of this dissertation.

TABLE OF CONTENTS

	Page
CHAPTER 1: INTRODUCTION	1
Introduction to Photolithography	3
The Photolithography Process	3
Photoresist Characterization	15
History of Organic Resist Research	19
Inorganic Resists	26
References	32
Figures	36
CHAPTER 2: PHOTO INDUCED DIFFUSION OF METAL OXIDE BILAYERS	37
Abstract	38
Introduction	39
Experimental	40
Results	41
Conclusion	41
References	43
Figures	44
CHAPTER 3: PHOTO PATTERNING OF SOLUTION DEPOSITED METAL OXIDES	48
Abstract	49
Introduction	50
Experimental	51

TABLE OF CONTENTS (Continued)

Page

Results 53

Conclusion 56

References 57

Figures 58

CHAPTER 4: NOVEL INORGANIC RESIST FOR NANOMETER SCALE PATTERNING 65

Abstract 66

Introduction 67

Experimental 71

Results 72

Conclusion 79

References 80

Figures 81

CHAPTER 5: DIRECTLY PATTERNED SOLUTION DEPOSITED TITANIA 87

Abstract 88

Introduction 89

Experimental 90

Results 91

Conclusion 94

References 94

Figures 95

TABLE OF CONTENTS (Continued)

Page

CHAPTER 6: SOLUTION DEPOSITION AND SOLID STATE MODIFICATION OF MOLYBDENUM OXIDES............... 101

Abstract.. 102

Introduction.. 103

Experimental... 104

Results.. 106

Conclusion.. 112

References... 113

Figures... 115

CHAPTER 7: CONCLUSION.. 126

BIBLIOGRAPHY.. 129

LIST OF FIGURES

Figure		Page
1-1	Typical characteristic contrast curves for photoresists.....................	36
2-1	Process flow for photolithography or electron beam lithography.....	44
2-2	Thermal ink jet based patterning..	45
2-3	Optical microscope image of photographically patterned HafSOx through photo induced diffusion..	46
2-4	Electron beam lithography patterning of copper formate/HafSOx bilayer..	47
3-1	Extinction Coefficients for HafSOx and ZircSOx...........................	58
3-2	Time dependent characteristic contrast curve for UV exposed ZircSOx..	59
3-3	Optical microscope image of UV patterned negative-tone ZircSOx..	60
3-4	Optical microscope image of UV patterned positive-tone ZircSOx..	61
3-5	SEM of EUV exposed sample degradation......................................	62
3-6	Contrast curve for EUV exposed HafSOx.......................................	63
3-7	SEM of 30-nm lines and spaces patterned by EUV interference lithography...	64
4-1	Contrast curve for a HafSOx film developed in 12 M HCl..............	81
4-2	Contrast curve for a ZircSOx film developed in 20% TMAH.........	82
4-3	SEM image of 100-nm lines and spaces patterned in HafSOx...........	83
4-5	SEM image of 30-nm isolated lines..	84
4-6	SEM image of a 16-nm isolate line...	85
4-4	SEM image of 28-nm lines printed on a 100 nm period..................	86

LIST OF FIGURES (Continued)

Figure Page

5-1 XRD patterns of TiO_2 films annealed at different temperatures....... 95

5-2 SEM images of TiO_2 thin films... 96

5-3 Patterned TiO_2 films of varying exposure time................................ 97

5-4 Photolithographically patterned TiO_2.. 98

5-5 AFM image of an electron beam lithography pattern....................... 99

5-6 Contrast curve for electron-beam patterned TiO_2............................ 100

6-1 Optical microscope image of photolithographically patterned peroxopolymolybdate... 115

6-2 XRD data for peroxopolymolybdate films, as deposited and annealed in air.. 116

6-3 SEM image of an oriented MoO_3 film from a peroxopolymolybdate film annealed in air to 325ºC for 5 minutes.. 117

6-4 SEM image of an oriented MoO_3 film from a peroxopolymolybdate film annealed in air to 600ºC for 5 minutes.. 118

6-5 TGA data for peroxopolymolybdate powders prepared from solutions of three different ages... 119

6-6 XRD of peroxopolymolybdate films reduced in flowing H2 at various temperatures... 120

6-7 XRD of peroxopolymolybdate films reduced to MoO2 at 450ºC for 10 or 30 minutes.. 121

6-8 Thermoelectric data for a peroxopolymolybdate reduced at 450ºC for 30 minutes after an exposure to UV light for 10 minutes........... 122

6-9 SEM image of peroxopolymolybdate after reduction at 450ºC in flowing H_2 for 30 minutes... 123

6-10 SEM image of peroxopolymolybdate after exposure to UV light for 10 minutes followed by reduction at 450ºC in flowing H_2 for 30 minutes.. 124

6-11 Optical Transmission for exposed and unexposed films reduced in flowing H_2 at 450ºC for 30 minutes.. 125

LIST OF TABLES

Table	Page
4-1 EPMA data for HafSOx/ZircSOx under varying processing conditions..	76
6-1 Electrical data for peroxopolymolybdate films reduced to MoO_2....	110

DIRECT PATTERNING OF SOLUTION DEPOSITED METAL OXIDES

CHAPTER 1

INTRODUTION

In the course of this dissertation the use of lithography for the direct patterning of metal oxide thin films will be discussed. The metal oxide films in question are all deposited from aqueous solution. This direct patterning does not employ a polymer material to transfer the pattern to the metal oxides. Instead the metal oxide film interacts directly with the exposure source of the lithography patterning process. Direct patterning of solution deposited metal oxides eliminates the need for a high energy plasma etch to transfer the pattern to the oxide. Because of this, direct patterning is significantly easier to integrate in to a multilayer process.

Work in direct patterning was initiated after the development of the thin-film chemistry of the material HafSOx [1]. HafSOx is an aqueous solution-deposited material based on various compositions of hafnium oxide sulfate that was initially designed as a high-k dielectric. HafSOx, and its zirconium analog ZircSOX, can be deposited in films ranging in thickness from 2 to 500 nm. The films are characterized by being atomically smooth surfaces. Taken together, these properties serve as an excellent starting point for the development of a directly patterned metal oxide. Furthermore, with the proper patterning characteristics this material could be adapted as a high quality inorganic resist.

The modern lithography process will be discussed to provide background for understanding the implications of this dissertation. To provide perspective a brief review of organic resists is made followed by a detailed consideration of inorganic resists. These topics are addressed in Chapter 1. A new bilayer lithographic process involving only inorganic solutions is detailed in Chapter 2, and a straight forward

negative-tone photolithographic process is detailed in Chapter 3. The use of the photoactive process has been extended to electron-beam lithography for image formation at the nanometer scale. By using electron-beam lithography, the directly patterned metal oxide is demonstrated to function as a high quality inorganic resist. The electron beam lithography results are presented in Chapter 4. The concept of direct patterning the HafSOx/ZircSOx systems extended to the direct patterning of TiO_2 in Chapter 5. Another aspect of the functionality of directly patterned metal oxides is the ability to modify their chemical composition. Results on the reduction of a Mo^{6+} (aq) peroxo precursor to MoO_2 are presented in Chapter 6.

Introduction to Photolithography

The digital age in which we live is powered by microprocessors and other integrated circuits that are the brains of the modern devices affecting our everyday lives. The operating speed of these devices has progressively increased with each generation. This increase in performance is reflected by an observation made by Gordon Moore [2], now known as Moore's Law, which states that every two years the density of transistors on a integrated circuit will double. The maintenance of this extraordinary growth rate has been largely predicated on the development of advanced manufacturing processes associated with photolithography. Photolithography is a process by which a pattern is optically transferred onto a substrate. Every layer of an integrated circuit is defined by this pattern-transfer process, and it has driven the number of transistors on a processor to increase from 275,000 on an Intel X386

processor circa 1986 to 820,000,000 in an Intel Penryn chip of today [3, 4].

Photolithography Process

In a standard photolithographic process, the layer to be patterned is coated with a thin layer of a photoactive polymer, known as the resist. Nine basic steps are associated with first patterning the resist and transferring the pattern into the underlying substrate. They are, in order of processing: adhesion promotion, coating, pre-exposure bake, exposure, post-exposure bake, development, hard bake, image transfer, and strip. The purpose of adhesion promotion is to clean the wafer and prepare it suitably for application of the resist. The coating process is the actual deposition of the resist; a softbake is used next to drive off the excess solvent from the film. During the exposure step an image is projected onto the resist. Following this step, a post-exposure bake is performed to initiate the necessary chemistries that lead to high differential solubilities between exposed and unexposed regions. During development, areas of the resist are dissolved depending on the image that was transferred during the exposure step. After development, a hardbake is done to cure and harden the film for the image transfer. During this step the pattern previously created in the resist is transferred to the underlying film or substrate through an etch process. The final step is removal of the resist so that it does not interfere with later processing. Though generalized here for photolithography, the process differs little for other forms of exposure, e.g., electron beam or extreme ultra violet (EUV). This brief description provides a simple, aggregate view of the processes, but it is

beneficial to also describe the nuances of each step in more detail.

Preparing the substrate for coating is analogous to preparing a surface before painting. To produce a smooth coat of paint that will not flake off, the surface needs to be clean, dry, and primed to enable the paint to stick. The first part of adhesion promotion involves a high temperature bake to remove environmental contaminants and to remove all water and dangling hydroxyl groups from the silicon or silicon dioxide surface. At high temperatures, hydroxyl groups on a silicon dioxide surface will combine and release water. A hydroxlated silicon dioxide surface will be hydrophilic, and once most of the hydroxyl groups are removed the surface becomes hydrophobic. A surface typically needs to be hydrophobic for an organic resist to adhere. Even a thoroughly clean and dry substrate can be difficult to coat, necessitating the use of an appropriate adhesion layer. The most common adhesion promoter is hexamethyldisilazane, commonly known as HMDS. This primer works by attacking any silanol groups that survived the high-temperature bake, replacing the hydroxyl group with an organic functional group, thereby producing a hydrophobic surface and improved adhesion of the resist.

Depositing a thin uniform coating of photoresist is generally a straight forward process. The photoresist, dissolved in an appropriate solvent, is deposited onto the surface of a wafer located on a turntable. The wafer is then spun to a high RPM, which ejects excess material from the lip of the wafer to leave a thin and uniform film layer that is depleted in solvent. While appearing simple, this process has a large number of variables that affect the film quality and characteristics. The resist may be dispensed

statically or dynamically. Static dispensing means the resist is applied before wafer spinning is initiated while dynamic dispensing means the resist is applied while the wafer is spinning at some low RPM. The spin rates and times must be optimized to provide the desired film thickness, and for each target spin rate the acceleration must also be optimized. Environmental conditions like exhaust, humidity, and temperature also all affect film quality. Significant consideration must be given to characteristics of the resist at the wafer edge. During spinning, excess photoresist is pushed to the edge of the wafer, where it is ejected, but, after most of the material has been removed a small bead will remain. This bead will cover both the top and the bottom the wafer, and it will be much thicker than the film covering the interior of the substrate. If not removed this bead of material will be the source of many defects as the wafer is heated and handled through the rest of the process. Edge bead removal is typically performed in industry with a controlled solvent spray while the wafer is spinning at a high RPM.

After the photoresist is spin coated onto the wafer, it still retains 20-40% by weight of solvent. The remaining solvent is removed in a low-temperature bake referred to as a softbake or prebake. The prebake will stabilize the characteristics of the film over time, reduce the thickness of the film, increase adhesion, and decrease tackiness, which limits particle adhesion and subsequent defects. While the prebake is highly advantageous, a bake temperature that is too high can produce undesirable results. The photoreactive components of the resist can begin to break down, and other parts of the resist can begin to crosslink or oxidize. The prebake must be optimized to maximize the benefits from solvent loss while minimizing the thermal-degradation

effects.

The next step in the lithographic process is alignment and exposure. During exposure, a spatially varying light intensity incident on the film chemically induces a corresponding spatially varying solubility difference in the film. This can happen in two tones. In a positive-tone resist, the chemical reaction makes the film more soluble upon exposure, so that after development the areas that were not exposed remain on the substrate. In a negative-tone material, a reactions make the exposed regions less soluble, so that after development the exposed regions remain on the substrate.

The spatially varying light intensity that is required to form an image in a resist generally results from passing light through a photomask. A photomask is typically a pattern of chromium on a transparent substrate. This image-transfer process can be done with contact or proximity lithography. In contact lithography, the mask is brought into direct contact with the resist. This process allows resolution near the wavelength of the light source, but it creates a high probability of contamination from the mask, leading to low device yields. As a result, contact lithography does not typically find use in manufacturing. In proximity lithography, the mask is held a very small distance above the photoresist, typically 2 to 4 mm. This distance greatly reduces the chances of contamination from the mask, but it comes with a price in terms of resolution.

To circumvent the problems associated with contact and proximity methods, all modern manufacturing methods rely on the use of projection techniques. In projection lithography, optical elements are used to project the image of the mask onto the resist

from a large distance.

Two classes of projection-lithography systems are in use today: scanners and steppers. In a scanner, the mask holds the image of the entire wafer, and mirrors are used to create a slit of light. The mask and wafer are then rastered through this slit of light in unison, allowing the entire wafer to be exposed in one pass. This can allow for fast throughput of wafers but it requires a large and complicated mask. In a stepper, an image of a single chip is projected across a field of one to several square centimeters in size. The wafer is the fully exposed by stepping the image across the entire surface. While the mask needed in a stepper is smaller than that for a scanner, a stepping system can be highly complex. Though scanners were initially used in production, steppers became more prevalent because of their ability to include optical reduction of the mask image. As resolution requirements dropped below 2 microns, industry moved completely to stepper systems. In the early 1990s, hybrid step and scan systems were developed. These systems use a small slit of light rastered across a single field to expose one chip. The process is then repeated as in a traditional stepper. Hybrid step and scan systems allow for a simpler lens design at the expense of more complicated mask and wafer stages. They are the primary design used in modern lithography tools.

Over the years, the wavelength of the exposure source has dropped to shorter and shorter wavelengths. The older lithography tools are operated with high-pressure mercury vapor lamps and chromatic filters to select the g-line, h-line, or i-line (436, 405, or 365 nm, respectively). More advanced tools use KrF excimer lasers (248 nm),

while state-of-the-art tools used in production employ ArF excimer lasers (193 nm). The selection of the exposure wavelength is dictated by the desired resolution in relation to the Rayleigh equation,

$$R = k_1 \frac{\lambda}{n \cdot \sin(\theta_{max})}$$

where R is minimum resolution; k_1 is a constant with a minimum theoretical value of 0.5 (typically in the range 0.7-1); λ is the wavelength of the exposure source; n is the index of refraction of the medium between the mask and objective lens; and θ_{max} is the maximum half-angle of light that can enter the objective lens. From the Rayleigh equation, R is directly proportional to λ, so the desire to realize submicron features has driven the use of short exposure wavelengths.

Following exposure of the resist, another bake step is done. The purpose of this is dependent on the type of resist, and it can be optional. Under some exposure conditions a standing-wave effect is observed. When monochromatic light strikes a resist from multiple angles, it approximates a plane wave. If the substrate is reflective, then the reflected light can interfere with the incoming light, setting up a standing wave of high and low intensity through the thickness of the resist. At the edges of exposed regions, this standing wave can translate to sidewalls that undulate with the standing wave pattern. The most effective way to remove the standing wave effect is to use a bottom anti-reflective coating (BARC), which prevents reflection of light back into the resist. If a BARC is not used, the post-exposure bake can smooth the effects of the standing wave by causing diffusion of the photoactive components. In the

specialized chemically amplified resists used today, the post-exposure bake (PEB) is where all of the significant chemical changes occur. In these resists, the exposure only releases a strong acid that does not in itself affect solubility. During the PEB, this acid diffuses through the resist and catalyzes deprotection reactions that change the solubility of the film. In either case, the diffusion that occurs is dependent on the residual solvent content of the film. To maximize the gains of diffusion, the PEB must be optimized along with prebake.

The next step in the photolithography process is to develop the latent image in the resist. Most resists are developed with aqueous bases. Because of the wide spread use of novolac-based 436-nm wavelength resists in the past, the developer 0.26 N tetramethylammonium hydroxide (TMAH) has been adopted as the industry standard. TMAH in particular was chosen as a developer because it is a strong aqueous base that has no metal content while still having a low vapor pressure. The choice of this developer has been thoroughly entrenched in industry, because it is plumbed in wafer fabs and photolithography process tracks all over the world. Because the use of this developer is so ingrained, it is the de-facto developer for all industrial resist applications, even though the concentration of TMAH may not produce optimized results for a given resist. The development can be done in batch processing or through a single wafer, inline process. In batch processing, 10 to 25 wafers are immersed in a bath of developer while the bath is agitated. In-line development is more prevalent, because it is integrated into the same equipment used to spin coat the photoresist. This allows all photolithography-related wafer processing to be automated on the same set

of equipment. In-line wafer development comes in three flavors - spin, spray and puddle -, but it is common practice to use some combination of all three. Spin development involves applying a stream of developer to a wafer that is spinning at a low speed. This method offers the advantage of a constant refresh of the developer. While the wafer is still spinning the developer is replaced with a water rinse. The wafer is then spun up in speed to dry. In spray development the developer is uniformly applied to the surface of the wafer from a mist, greatly reducing the amount of developer. In puddle develop, developer is applied to the top of a stationary wafer until if forms a puddle all the way to the edge; it is then spin rinsed.

After the wafer is developed the resist must go through one more bake cycle. This postbake, sometimes called the hard bake, serves to harden the resist to later processing. The resist is heated to a temperature below its glass transition temperature to induce crosslinking. This crosslinking can be further induced by UV or plasma hardening. If the resist is heated above its glass transition temperature, flow of the resist can smear features, although it has been shown that a tightly controlled heating cycle above the transition point can induce just enough flow to reduce line edge roughness.

After features are made in the resist layer it is necessary to transfer the pattern into the underlying material. This transfer can take the form of a subtractive process, an additive process, or impurity doping. Subtractive processes are most common, being implemented through etching. To etch a substrate or a uniformly deposited layer, the photolithography process is performed such that the material selected for removal is

uncovered during the development process. The etch step then removes material from the uncovered areas, while the photoresist "resists" the etch and protects the covered material. The etch process can be a wet process using solutions of strong acids or bases. Wet etching is usually an isotropic process, where the resist is undercut the same distance as the depth of material removed. In some cases, crystalline materials will etch anisotropically along certain crystalline planes. For example, in concentrated KOH(aq) silicon will etch anisotropically to produce pyramidal instead of round etch profiles. In either case, the undercutting limits the aspect ratio of features, making wet etching unsuitable for high resolution applications. For demanding high-resolution applications, dry etching is preferred. A dry etch requires a gaseous etchant which is activated by a plasma, and the process progresses in a line-of-sight fashion from the source of the plasma. The main advantage of dry etching is that it can produce features with very high aspect ratios. An example of additive pattern transfer is electroplating of copper. To make copper interconnects, holes are created in a resist layer, and copper is electrolessly grown up from the substrate. When the resist is removed copper is left as a negative image of the developed resist. The final form of pattern transfer is ion implantation, which serves to modify the impurity level in a semiconductor and change the carrier type or concentration. Again, holes are created in the resist where implantation is desired, and then dopant ions are accelerated at the substrate. Where the resist has been removed, these ions deposit into the substrate where, after thermal annealing, they are incorporated into the structure. The remaining resist traps the accelerated ions and prevents them from reaching the

substrate, preserving the initial electrical properties. In some cases, a polymer photoresist is unable to withstand the energetics of the pattern-transfer process necessitating a hard mask. A hard mask is an intermediary sacrificial layer used to transfer the pattern to its final destination. Examples of a hard mask includes thermally grown SiO_2 and CVD deposited silicon nitride. This material must be patterned with a technique that a polymer photoresist can withstand, but the hard-mask must be resistant to the subsequent final patterning process. Once patterned the remaining resist is stripped before the final pattern transfer.

In every case, after the photoresist has served to transfer its pattern to another layer, it must then be removed. The resist may be stripped from the substrate by either a wet or dry etch. In a laboratory setting acetone is typically used to remove the residual photoresist, but in the manufacturing environment acetone is unsuitable, because it leaves an organic scum on the wafer. Alternative organic solvents and some inorganic acids remove greater amounts of residual photoresist, but scum is a constant issue as the last monolayer of resist can be quite difficult to remove. Typically, a final oxygen plasma etch of short duration must be done, effectively removing organic material without affecting the underlying inorganic materials.

This general description applies to photolithography. There may be variations to the process when dealing with other exposure tools such as EUV and electron beam, but these are largely restricted to adjustment of the process parameters of each step. These variations apply to the exposure process, while the rest of the process remains identical. Electron-beam lithography is different from other forms of lithography in

that the pattern is exposed serially with a rastered electron beam. This side steps the restrictions of the Rayleigh criterion, but it comes at the expense of significantly lengthened exposure times. In the exposure tool, the electron beam is extracted from a filament, then focused and rastered by electromagnetic lenses. The exposure is done at high vacuum, requiring the use of resists that do not out-gas organics, which could contaminate the imaging elements. The limitation of resolution in an electron-beam system arises from coulombic repulsion, which sets the focusing limit of the beam diameter. With electron-beam lithography, features have been patterned at 1 nm. One of the major limitations to the use of electron beam is the proximity effect. As the primary beam of electrons hits the resist, it can be scattered both forward and backward, broadening a point source into a Gaussian distribution. The proximity effect can be limited by using very thin resist films, exposing on thin membrane substrates, and using a very high acceleration voltage for the electrons (100 keV). Even though electron beam lithography has severe limitations in terms of writing speeds, photolithography is entirely dependent on it for fabrication of the necessary masks. Mask fabrication is not a minor concern for the semiconductor industry, as a single mask can cost as much as $100,000. A set of 30 masks may be required to complete the fabrication of an IC.

In EUV lithography, 13.5-nm light is used for exposure. Though technically photolithography, the exposure mechanism is similar to electron-beam lithography. The reduction in wavelength by over an order of magnitude from 193 nm, also effectively sidesteps the Rayleigh criterion. At this wavelength, the photons have

sufficient energy to remove core electrons from atoms in the resist. The energy of the resulting secondary electrons can then activate the chemical processes that are necessary for image formation. For this reason, resists that function well for electron beam lithography are often good candidates for EUV lithography. A major stumbling block for the development of EUV lithography is the lack of an inexpensive, high-intensity light source. Because all materials are opaque to EUV light, optical elements in an EUV system must be reflective. These reflective optics have a maximum reflectivity of 70%, while the whole optical system including the condenser allow only around 4% of the total EUV light to be delivered to the wafer. The low source intensity, compounded by the low reflectivity of the optic system, places high requirements on the resists used for EUV lithography. The International Technology Roadmap for Semiconductors, requires EUV resists to have a sensitivity of 10 mJ/cm^2. While EUV lithography has been used to pattern 20 nm lines and spaces at a dose of 20-25 mJ/cm^2, it remains to be seen if EUV can be adapted for full production use.

Photoresist characteristics

A good photoresist is defined by three main characteristics; high contrast, high resolution, and fast photospeed. Achieving all three properties at the same time can prove difficult, especially since the requirements are constantly tightening as lithography technology advances. In addition, there are several other significant characteristics that are important for features < 100 nm.

Resists generally function in either positive or negative tone, although under

certain conditions some can work in both tones. A positive-tone resist becomes more soluble in a developer when exposed to light. After development the resist forms a positive image of the mask. A negative-tone resist becomes less soluble in a developer upon exposure, and after development a negative-tone image of the mask is produced.

The contrast, γ, of a resist is a measure of the range of exposure dose that is necessary to transition from unexposed to fully exposed. This resist characteristic is heavily influenced by the processing conditions. For simplicity, the following discussion will be limited to consideration of a negative-tone resist as an example; but the concepts also apply to a positive-tone resist. Ideally, a perfect resist would have a very fast development rate when unexposed and at a full exposure would have a zero development rate. A step-like transition between unexposed rate and exposed rate would yield an infinite contrast. In practice, a resist will transition from unexposed to exposed over a range of doses and even at a high dose the resist would experience a slow but measurable development rate. The sharpness of this transition is modeled by the contrast. By plotting the natural log of exposure dose versus development rate this resist property can be quantified. Because it is often difficult to measure development rates, the rate can be replaced by considering film thickness remaining after a set development time. The afore mentioned plot then becomes the natural log of exposure dose versus the normalized thickness, Figure 1-1. In the region around E_o, the plot can be approximated as a linear function with the slope defined as the contrast. The contrast can then be represented in an equation of this linear region as follows:

$$\frac{T_E(E)}{T_o} = \gamma \ln\left(\frac{Eo}{E}\right)$$

$T_E(E)$ is the thickness remaining after development for dose E; T_o is the thickness of the resist before development; E_o is the minimum dose for a nonzero (negative-tone) resist thickness; and γ is the experimentally determined contrast.

The importance of contrast becomes apparent in considering the image that is being projected onto the resist by the lithography system. The image is commonly referred to as the aerial image. An ideal aerial image would have zero intensity in the unexposed region and an infinitely sharp transition to the desired dose in the exposed region. In practice, all aerial images are significantly degraded from this ideal case and in the most extreme cases, the aerial image is modeled as a sine wave. It is the contrast of a resist that defines how the aerial image is reproduced in the resist. A poor aerial image and a low-contrast resist will produce only a spatially varying thickness, while a high-contrast resist can compensate for the poor aerial image and produce a resist profile with a nearly ideal binary thickness. In addition, a dose fluctuation for a poor aerial image will result in an off-target line width for a low contrast material. Furthermore. a poor aerial image and a low contrast will also limit the resolution that can be printed when features are close together.

When considering resolution of patterned features, there are two basic types of resolution that must be considered, dense resolution and isolated resolution. Dense resolution is defined as the smallest repeating lines and spaces of equal width that can be printed. This resolution determines the packing density of transistors on a chip. It

is a function of the contrast of the resist and the quality of the aerial image that the lithography system can produce. For the best aerial image, this resolution is still limited by the wavelength of the exposure light. Isolated resolution is the smallest isolated feature size that can be produced in the resist. This resolution determines, for example, the characteristics of the transistors being produced and it has a considerable effect on processor speed and power consumption. It also serves as an upper limit for the dense resolution. This isolated resolution is limited by the size of the molecular species in the resist, anisotropy of their distribution, and their interaction volumes. Attempts to increase isolated resolution in organic resists are generally targeted at narrowing the distribution of molecular weights and lowering the average molecular size of the resist.

The photospeed of the resist represents the time at a given exposure intensity to produce full exposure. The photospeed can also be represented as the sensitivity, the amount of energy per unit area needed to expose the resist. For useful application, the sensitivity of a photoresist should be as high as possible. This requirement is driven by the low intensity of exposure sources and the need to maximize throughput of lithography tools. In state-of-the-art photolithography tools, 300-mm diameter wafers are exposed at 131/hr, corresponding to 25.7 cm^2/sec.

Though measured independently, contrast, resolution, and photospeed are all interrelated. A resist cannot achieve its resolution limit without a suitable contrast to replicate the aerial image of the lithography system. There is often a trade-off between use of an aggressive developer, which can result in a better contrast, and a

less aggressive developer, which can lower the photospeed.

As advances in photolithography have pushed the resolution of developed features to the nanometer scale, the roughness of the edges of these features is now important. This roughness is know as line edge roughness (LER) or if taken across both sides of a line as the line width roughness (LWR). When resist features are smaller than one or two hundred nanometers, the roughness of the edges of these features becomes a significant contribution to the width of these features. If the resist feature is being used to define a transistor channel width, a high roughness will induce significant variation in transistor performance. Across the millions of transistors that exist on a chip this performance variation can have large negative effects. The LWR is defined as the 3σ standard deviation of the width of a line. This roughness can have many sources, including defects on the mask level or inhomogeneously distributed resist constituents. Once feature sizes fall below about one hundred nanometers, the size of the actual resist molecule comes into play. Resists are typically comprised of long organic polymers with molecular weights on the order of 10^4 grams/mol. When these materials are spincoated, the long polymer chains curl with a radius of gyration of 2 to 6 nm [5]. Consequently, a 100-nm wide line could be measured as approximately 10 molecules wide. The variation of a single molecule then becomes a significant part of the overall feature size. For this reason, research on organic resists is being directed to small molecular-weight options [6] .

Organic Resist History

Photolithography resist research has a long history, and its roots are shared with those of photography. In fact, the first photography was also an example of photolithography. In 1826, Nicéphore Niépce created the first photograph from bitumen on pewter [7-10]. Bitumen is the residual collection of hydrocarbons from the distillation of petroleum, and it is commonly used in tar paper and asphalt as well as in sealants for roofs. By dissolving bitumen in lavender oil, Niépce was able to make high-quality coatings on polished pewter plates. He placed one of these coated plates into a simple camera obscura and exposed an image of his courtyard over the course of eight hours. He then developed the bitumen with a mix of lavender oil and white petroleum. Those portions of the bitumen exposed to sunlight became less soluble, so that upon development the underlying pewter plate was revealed to different degrees, depending on the amount of sunlight seen by the bitumen film. Thus the first permanent photography was created.

Niépce's other work provides a good example of photolithography: by placing a velum drawing on top of a bitumen-coated tin plate and exposing it to the sun for several hours. Again, by using lavender oil diluted with white petroleum, he was able to dissolve the areas of the bitumen that were shadowed by the drawing on the velum, while the areas of the bitumen that were exposed to sunlight through the velum were insoluble. The remaining bitumen coating that held the image of the drawing served to protect parts of the tin plate, while the exposed areas were etched in acid. Thus an image that was photolithographically made in the bitumen was transferred into a metal substrate. When the bitumen was removed, the original image could be seen in relief

on the tin surface. This process is analogous to the modern use of photolithography in integrated circuit fabrication.

Because of the many hours needed to make an exposure with bitumen, a more sensitive material was desired. In 1852, William Fox Talbot patented a process of using ammonium dichromate in gelatin. Dichromate gelatin was readily cast into quality films, and its sensitivity was an order of magnitude greater than that of bitumen. This resist system, though not without problems, sparked the industry of photolithography. Dichromate gelatin became the standard for the photolithographic manufacture of stone and metal printing plates for the next 100 years [11].

In the early 1950s, when William Shockley and his co-workers at Bell Labs began to work on integrated circuits, they turned to dichromated gelatin, at the time it was their only option for a photoresist. Dichromated gelatin proved to be unsuitable, because it was not resistant to the hydrofluoric acid, which was used to etch silicon dioxide, an essential part of their process. The Bell Labs group contacted researchers at Eastman Kodak for help. Eastman Kodak had already been working on a replacement for dichromate gelatin for application in the manufacture of lithographic printing plates. The only known photodimerization known at the time was that of cinnamic acid [12]. The polymer poly(vinylcinnamate) was brought forward, preforming at a level that allowed Bell Labs to initiate a pilot program. Even though fine patterns were produced with poly(vinylcinnamate), the resulting yield of the process proved to be too low because of the poor adhesion of the polymer to the silicon dioxide surface. Researchers at Bell Labs returned to Kodak, seeking an

improved process. Several attempts were made to improve the adhesion of poly(vinylcinnamate) but it became apparent that another approach was needed. Kodak researchers suggested the use of a light sensitive rubber adhesive. Research at the time into the photolysis of azide-compounds lead to the idea of synthesizing bis-azides and formulating them with a low moleculer weight rubber. The first attempt produced excellent patterns, while eliminating the adhesion problems on silicon dioxide surfaces. Though many other bis-azide compounds were tried in this application, none were able to best the first which was tried, 2,6-bis(4-azidobenzal)-4-methlycyclohexane. On the basis of this formulation Kodak began selling “Kodak Thin Film Resist” (KTFR), which was the dominate resist material for the semiconductor industry from 1957 until 1972. At the end of those fifteen years, device dimensions had been reduced to 2 μm, which was the resolution limit of KTFR [13].

An exhaustive examination of various photosensitive coatings began for a material having higher resolution than KTFR. This search eventually settled on diazonapthoquinone/novolac resin resists from the Kalle company in Wiesbaden, Germany. Kalle had been in the business of graphics reproduction for a long time. Their core business consisted of copying engineering drawings, the original blueprint. For blueprints, the paper used was coated with a diazonium salt and an azo coupling agent. As light was passed through the original drawing and the image was transferred to the copy paper, the incident light induced decomposition of the diazonium salts. In unexposed regions of the paper, during a following ammonia treatment, the remaining

diazonium salt would bind with the azo coupling agent to form a blue azodye. This formed on the paper a blue positive tone copy of the original drawing, hence the name blueprint.

In the late 1940s, Kalle began experimenting with binders for diazonapthoquinone (DNQ), their most successful diazo salt, in the hope of being able to form films of their material and improve its image-forming properties. One of these binders was novolac resin, which was commercially known in the US as Bakelite, having been sold in products since the 1920s. The combination of DNQ and novolac upon exposure resulted in a dull reddish color change, not the bright blue hoped for. However it was found that diazo salts made the novolac resin less soluble in aqueous base, while decomposition of the diazo salts increased novolac solubility [14]. This chemistry was applied to the manufacture of positive-tone lithographic plates, which were desirable, because in the lithographic printing process they allowed the direct reproduction of an original without the need to first make a negative photographic image. In 1950, Kalle began selling anodized aluminum sheets with a DNQ/novolac coating to the lithographic print making industry. Their product was immediately successful.

In photolithography, DNQ/Novolac resists, when compared to KTFR, offered a higher contrast and lack of swelling during development. DNQ/novolac was introduced to the semiconductor industry in 1972, and within one year, it almost totally replaced KTFR causing considerable turmoil among both resist and mask manufacturers [15]. For the next twenty five years, DNQ/novolac resists dominated over 90% of the world-wide resist market. The lasting success of this resist system has

been aided by its additional characteristics of high etch resistance and an environmentally friendly aqueous base developer. The ultimate resolution of this system was found to be around 250 nm with near UV (λ = 350-450 nm) Hg i-line, high numerical aperture tools.

As resolution requirements pushed photolithographic light sources into the deep UV (λ = 240-260 nm) new resists were developed [16-19]. The light source in these tools, a high pressure mercury vapor lamp, produce only about 10% of the intensity that they do at near UV. To maintain the same productivity levels, a new resist was needed with an order-of-magnitude greater sensitivity. DNQ/novolac are incapable of achieving this as, theoretically, it takes more than 3 photons to trigger the decomposition of DNQ. This dilemma led to the concept of chemically amplified resists.

In a chemically amplified resist system, a photochemical reaction generates a catalyst. This catalyst then propagates through the film, initiating secondary reactions that modify the solubility of the film. The effective quantum efficiency of this system is then the product of the quantum efficiency of the initial photochemical reaction and the number of sites the catalyst activates until it is destroyed. In this way a single photon activation event can be amplified in effect and area. In practice the catalyst is a sulfonic acid group and the catalyst precursor is call a photo-acid generator (PAG). The first successful chemically amplified resist was developed by Wilson, Frechet, and Ito at IBM [20]. They synthesized a poly(t-boc styrene) (PBOCST) as a possible replacement to novolac resin. In this process they discovered that t-butylcarbonate

groups attached to the chain served to protect the material from solvation better than the unprotected p-hydroxostyrene. A deprotection transition could be rendered by treatment of the t-butylcarbonate with an acid. By formulating PAG molecules with PBOCST, upon exposure the acid generated by the PAG can diffuse through the film and decompose the t-buytlcarbonate to carbon dioxide and isobutylene, which escape the film as gases. Interestingly the PBOCST can be used in either a positive or negative tone depending on the solvent. In an aqueous basic solvent the deprotected regions are soluble making a positive tone image and in a nonpolar solvent, like anisole, the unmodified protected regions are soluble making a negative-tone image. The more environmentally benign basic developer led this system to be used primarily as a negative-tone resist. The PBOCST system showed a two order of magnitude increase in sensitivity allowing the gain in resolution from lower wavelength tools to be realized. It was expected that the sensitivity gain would come with a trade off in ultimate resolution, but it was found with electron-beam exposures on thin-membrane substrates that the intrinsic resolution limit in both positive and negative tones to be around 20 nm, the same resolution as the best electron beam resist at the time, PMMA [21].

In recent years, industry has made yet another progressive move for lithography tools from 248 to 193-nm light. This presented an interesting challenge because novolac, p-hydroxostyrene and all the other aromatic materials become opaque at short the wavelengths such as 193 nm. The first 193-nm resist was borrowed from a process to pattern circuit boards with visible light. Allen, Wallraff, and their co-

workers at IBM had previously made an acrylate analog to PBOCST which was dye-sensitized to function with 514-nm light. After the dye was removed, the polyacrylate was transparent to light at 193 nm, producing excellent patterning results as a host resin for a chemically amplified resist [22].

The next step for high production lithography tools remains unclear. There are four main contenders vying for use in the coming generations of tools: 193 nm immersion lithography with double patterning, EUV Lithography, multiple-beam electron-beam lithography, and nanoimprint lithography [3]. Today the advancement of resist technology continues on both the 193 nm platform and on EUV lithography. This brief history hides the monumental amount of work that has been devoted to developing organic resists, and it serves to illustrate the comparably small amount of research done on developing inorganic resists.

Inorganic Resists

In the 50+ years since the advent of photolithography in the semiconductor industry, the vast majority of resist development has been done in the area of organic chemistry. Presently, only small efforts have been put into the development of inorganic resists. That effort will be reviewed in detail here. Only in the last few years have the requirements of the semiconductor industry begun pushing on the theoretical limits of organic resists. Inorganic resists hold promise to exceed the performance of organic resists in several key areas. Inorganic materials can have a fundamentally smaller unit size, which impacts resolution and line edge roughness. Most inorganic

resist materials also exhibit a much higher etch resistance than organic resists, allowing the use of much thinner layers. Despite the advantages inorganic resists demonstrate, they are generally hampered by low sensitivity.

The highest resolution features ever patterned have been with resist systems based on metal halides in electron-beam lithography systems [23-25] . Most of the research on metal halides has been targeted at AlF_3 and AlF_3/LiF mixed systems [26, 27]. AlF_3 acts as a self-developing positive resist under ultra-high vacuum with a very high dose of 20 C/cm^2. The reaction mechanism for self development is understood to take place in two steps. First the high-energy, direct-beam electrons induce dissociation of the metal fluoride, with subsequent desorption of flourine. This is followed by the remaining metal either partial evaporating or diffusing into surrounding grain boundaries. In a negative-tone operation, a dose of 1-3 C/cm^2 results in desorption of the fluorine while leaving metal in the exposed regions. Only the direct beam has sufficient energy to induce metal halide decomposition, making these materials insensitive to the much wider area effect of low-energy secondary electrons. In either positive or negative tone, AlF_3 resists offer excellent fluorine base dry-etch resistance. Though mixed AlF_3/LiF systems often lower the sensitivity, ~100 mC/cm^2, the required dose is still far too high to receive more than passing interest.

Metal bilayers have also been investigated as a thermal resist [28]. This technique relies on binary alloys with eutectic points below about 150 ºC. The model system is Indium/Bismuth, which has a eutectic at 72 ºC. These two metals are deposited as a bilayer via DC sputtering at a thickness ratio to make the overall composition match

the eutectic point on the indium/bismuth phase diagram. A laser pulse is used to induce melting at the interface between the metals. At the end of the pulse, rapid cooling commences, resulting in a binary alloy. This process is invariant to the wavelength used to initiate mixing. This thermal resist system has shown sensitivity comparable to chemically amplified resists, 7 mJ/cm^2, although the dose is highly dependent on laser power. This system has shown suitable resistance to wet etching, but resolution significantly beyond the micron range has not been realized. Additionally, this system is incompatible with standard step-and-flash lithography systems and vacuum-based, electron-beam lithography.

Inorganic chalcogenide photoresists have been studied for some time. It has been shown that As_2S_3, AsSe, and GeSe amorphous glasses, deposited via physical vapor deposition in vacuum, can be utilized as photoresists in both positive and negative tones [29-32]. Of these materials, the deposition of As_2S_3 is flexible in that it can be deposited via physical vapor deposition or by spin coating [32]. The photoactive behavior of these chalcogenide resists is quite complex. The mechanism involves a structural change that is thermally reversible and correlates to a photodarkening effect, but the exact mechanism of this structural change is ambiguous [33, 34]. It has also been shown that the sensitivity of this process is highly dependent on the power levels of the exposure dose. An increase in sensitivity of as much as a 10^3-10^4 can be achieved for very short laser pulses versus a continuous-wave laser [30]. The sensitivity of the negative-tone image can be as low as 24 mJ/cm^2. The tone of the photolithographic image is dependent on the type of developer used with either tone

accessible under the same exposure conditions. The negative-tone process yields a significantly higher sensitivity and higher contrast. The photodarkening effect, which accompanies the photo induced structural change, limits the effect of this system as a positive resist. As the exposure proceeds, the photodarkening reduces the transparency of the film from the top down, causing a lower dose to be delivered to the bottom of the resist. In positive tone, this darkening means the top of the film will be more soluble than the bottom, which lowers contrast. These chalcogenide photoresists can also be used to produce negative-tone images through photo-induced doping with silver [35-37]. Before exposure, a thin layer of Ag or AgTe is either deposited by PVD or electroless methods. Upon exposure, the incident light induces diffusion of the Ag into the chalcogenide glass, rendering the exposed regions insoluble in aqueous bases. This Ag based chalcogenide resist has exhibited sensitivities as low as 8 mJ/cm^2, but the dose must be delivered in multiple pulses and at higher power densities than normally used in lithography [37]. It is believed that a thermal component of the exposure contributes to this behavior. The chalcogenide inorganic resists exhibit excellent resolution because of their amorphous nature, but they have not proven to be sufficiently sensitive to replace organic resists [38]. These materials also face a significant hurdle in the high toxicity of the component elements. Furthermore, Ag acts as a recombination site and dopant in silicon, limiting its use in mainstream semiconductor processing.

Peroxopolymetalates, particularly the peroxopolytungstate, have demonstrated application as inorganic photoresists [39]. The peroxopolymetalates are all prepared

by dissolving the target metal powder in concentrated hydrogen peroxide. Once the excess peroxide is catalytically removed, the solution is readily spin coated. This system has exhibited sensitivity to UV, X-ray, and electron-beam exposures. Peroxopolytungstate has exhibited a sensitivity to UV light of 1 J/cm^2. This sensitivity can be lowered to 150 mJ/cm^2 by substituting Nb for part of the W [40]. The mechanism of photoactivity has be shown to be the decomposition of peroxide groups within the film and subsequent condensation of adjacent WO_6 octahedra [41, 42]. Unlike the solvents required by organic resists, these films are simply developed in water. While the environmentally benign nature of the elements and developer as well as the excellent oxygen plasma etch resistance are promising, the photo sensitivity is not competitive with organic photoresists. This system does show a significantly high sensitivity in electron-beam lithography of 15 μC/cm^2 [39]. The resolution of this system has not be investigated. Why this system never received more traction is unclear, but it is likely associated with poor resolution caused by heavy crystallization during post exposure thermal treatment. Furthermore at the time the system was developed, high-resolution electron-beam lithography did not have wide application.

Sol-gel synthesis is a commonly attempted way to spin coat metal oxide thin films. Sol-gel based systems have been investigated as a means to directly patterned metal oxides. Al_2O_3, ZrO_2, and TiO_2 systems, all based on n-butoxide organo-metallics, have been developed as electron-beam resists [43-45]. These systems are all limited in application due to sensitivities of ~10-200 mC/cm^2. Furthermore, during exposure these systems suffer serious out gassing of organic molecules as the organic

part of the resist decomposes. While hampered by these limitations, the sol-gel resists have exhibited the advantages common to inorganic resists, including high resolution and high etch resistance. The zirconia based system has exhibited a resolution of 9 nm for isolated features. The titania based system has demonstrated an ability to act as a hard mask for the plasma-etching conditions required for semiconductors fabrication.

The inorganic resist most widely used today is hydrogen silsesquioxane (HSQ), an inorganic polymer. HSQ is only sensitive to an electron beam and high energy photons, e.g., EUV. It is sold by Dow Corning Co. under the trade name FOx as a spin on glass for semiconductor packaging, low-k interlayer dielectric, and planarization applications. Dow Corning sells a variety of HSQ formulas at difference concentrations with a choice of methyl isobutyl ketone (MIBK) or methyl siloxane as the solvent. For electron-beam lithography, the thinnest formulation is selected and then further diluted with its solvent to achieve the desired thickness in the range of 10-100 nm [46]. Resolution for this system has been demonstrated as low as 6 nm for isolated lines and 10 nm for dense lines and spaces by using electron-beam lithography at doses of 5.5 mC/cm^2 and 33 mC/cm^2, respectively [47]. By using EUV interference lithography, 20-nm dense lines and spaces have been printed at a dose of ~20 mJ/cm^2 [48]. In both cases, HSQ exhibits significant promise because of a low line edge roughness. Though this resist does have a low sensitivity in comparison to chemically amplified resists, its resolution and small LER make it a possible candidate for future semiconductor industry adoption. It is assumed that EUV lithography, which has hit many development stumbling blocks, will eventually make its way to

production.

There remains a very significant advantage of inorganic-resist materials in comparison to organic materials. With an inorganic resist the deposited material can have a functional application. In this manner, these systems can be considered directly patterned functional materials. Furthermore, once metal oxides have been deposited and patterned, traditional solid-state chemical techniques can be applied to modify the functionality of the materials. For example, by using a hydrogen-gas stream as a reducing agent, a metal oxide ca be reduced to a lower valent state oxide or even its base metal. The aforementioned peroxopolytungstic acid has been used to convert from patterned WO_3 to patterned W metal [49]. More advanced methods can be used to exchange components to alter properties.

The work outlined in this thesis represents significant new advances in the field of inorganic resists. The theoretical advantages of inorganic resists over organic resist now hold the possibility to be realized. The new inorganic resist presented here holds promise for surpassing HSQ in terms of resolution, sensitivity, and etch resistance.

References

[1] J.T. Anderson, C.L. Munsee, C.M. Hung, T.M. Phung, G.S. Herman, D.C. Johnson, J.F. Wager, D.A. Keszler, Adv. Funct. Mater, 17 (2007) 2117-2124.

[2] G.E. Moore, Electronics,, 38 (1965).

[3] C. Mack, Future Fab International, (2007).

[4] “Intel Technology Journal”; http://www.intel.com/technology/itj/2008/v12i1/7-evaluation/2-intro.htm.

[5] J.A. Liddle, G.M. Gallatin, L.E. Ocola, Three-Dimensional Nanoengineered Assemblies as held at the 2002 MRS Fall Meeting, (2002) 19-30.

[6] S.W. Chang, R. Ayothi, D. Bratton, D. Yang, N. Felix, H.B. Cao, H. Deng, C.K. Ober, Journal of Materials Chemistry, 16 (2006) 1470-1474.

[7] H. Gernsheim, A. Gernsheim, *The History of Photography: From the Camera Obscura to the Beginnings of the Modern Era*, McGraw Hill, New York, NY, 1969.

[8] J.L. Marignier, in: V.V. Krongauz, A.D. Trifunac (Eds.), Processes in Photoreactive Polymers, Springer, 1995, p. 409.

[9] W.S. Deforest, *Photoresist: Materials and Processes*, Mcgraw-Hill (Tx), 1975.

[10] A. Reiser, *Photoreactive Polymers: The Science and Technology of Resists*, John Wiley & Sons, 1989.

[11] J.G. Jorgensen, H.M. Bruno, *The Sensitivity of Bichromated Coatings*, Lithographic Technical Foundation, New York, NY, 1954.

[12] H. Stobbe, A. Lehfeldt, Ber, 58 (1925) 2418.

[13] R.K. Agnihorti, F. D.L, F.P. Hood, L.G. Lesoine, C.D. Needham, J.A. Offenbach, Photogr. Sci. Eng., 16 (1954) 443.

[14] O. Süss, Liebeg's Ann. Chem., 566 (1944) 65-84.

[15] O. Süss, M. Schmidt, U.S. Patent 2 766 118, (1956).

[16] J.P. Fouassier, J.F. Rabek, *Radiation Curing in Polymer Science and Technology*, Springer, 1993.

[17] T. Iwayanagi, S. Ueno, H. Nonogaki, C.G. Willson, in: M. Bowden, S. Turner (Eds.), Electronic and Photonic Applications of Polymers, American Chemical Society, 1988, p. 372.

[18] S.A. MacDonald, C.G. Willson, J.M.J. Frechet, Accounts of Chemical Research, 27 (1994) 151-158.

[19] E. Reichmanis, L.F. Thompson, Chemical Reviews, 89 (1989) 1273-1289.

[20] J.M.J. Frechet, H. Ito, E. Eichler, C.G. Wilson, Polymer, 24 (1983) 995-1000.

[21] C.P. Umbach, A.N. Broers, C.G. Willson, R. Koch, R.B. Laibowitz, Journal of

Vacuum Science & Technology B: Microelectronics and Nanometer Structures, 6 (1988) 319.

[22] G. Wallraff, R. Allen, W. Hinsberg, C. Willson, L. Simpson, S. Webber, J. Sturtevant, Journal of imaging science and technology, 36 (1992) 468-476.

[23] M. Isaacson, A. Muray, M. Scheinfein, A. Adesida, E. Kratschmer, Microelectronic Engineering, 2 (1984) 58-64.

[24] E. Kratschmer, M. Isaacson, Journal of Vacuum Science & Technology B: Microelectronics and Nanometer Structures, 4 (1986) 361.

[25] E. Kratschmer, M. Isaacson, Journal of Vacuum Science & Technology B: Microelectronics and Nanometer Structures, 5 (1987) 369.

[26] W. Langheinrich, A. Vescan, B. Spangenberg, H. Beneking, Microelectronics Eng, 23 (1994) 287.

[27] J. Fujita, H. Watanabe, Y. Ochiai, S. Manako, J.S. Tsai, S. Matsui, Applied Physics Letters, 66 (1995) 3064.

[28] G.H. Chapman, Y. Tu, M.V. Sarunic, J. Dhaliwal, 2001, pp. 557-568.

[29] H. Nagai, A. Yoshikawa, Y. Toyoshima, O. Ochi, Y. Mizushima, Appl. Phys. Lett., 28 (1976) 145-147.

[30] V. Lyubin, M. Klebanov, I. Bar, S. Rosenwaks, N.P. Eisenberg, M. Manevich, J. Vac. Sci. Technol. B , 15 (1997) 823-827.

[31] J. Teteris, Journal of Non-Crystalline Solids, 299 (2002) 978-982.

[32] G.C. Chern, I. Lauks, J. Appl. Phys., 53 (1982) 6979-6982.

[33] S. Shtutina, M. Klebanov, V. Lyubin, S. Rosenwaks, V. Volterra, Thin Solid Films, 261 (1995) 263-265.

[34] K. Tanaka, Current Opinion in Solid State and Materials Science, 1 (1996) 567-571.

[35] A. Yoshikawa, O. Ochi, H. Nagai, Y. Mizushima, Applied Physics Letters, 29 (1976) 677.

[36] M. Frumar, T. Wagner, Current Opinion in Solid State and Materials Science, 7 (2003) 117-126.

[37] J.M. Lavine, M.J. Buliszak, J. Vac. Sci. Technol. B, 14 (1996) 3489-3491.

[38] A. Yoshikawa, S. Hirota, O. Ochi, A. Takeda , Y. Mizushima , Jpn. J. Appl. Phys. , 20 (1981) L81-L83.

[39] H. Okamoto, T. Iwayanagi, K. Mochiji, H. Umezaki, T. Kudo, Appl. Phys. Lett., 49 (1986) 298-300.

[40] H. Okamoto, A. Ishikawa, T. Kudo, Thin Solid Films, 172 (1989) L97-L99.

[41] H. OKAMOTO, A. ISHIKAWA, T. KUDO, Journal of photochemistry and photobiology. A, Chemistry, 49 (1989) 377-385.

[42] H. Okamoto, A. Ishikawa, T. Kudo, Journal of The Electrochemical Society, 136 (1989) 2646.

[43] M.S.M. Saifullah, K. Kurihara, C.J. Humphreys, J. Vac. Sci. Technol. B, 18 (2000) 2737-2744.

[44] K.R.V. Subramanian, M.S.M. Saifullah, E. Tapley, D. Kang, M.E. Welland, M. Butler, Nanotechnology, 15 (2004) 158-162.

[45] M. Saifullah, K. Subramanian, E. Tapley, D. Kang, M. Welland, M. Butler, Nano Lett., 3 (2003) 1587-1591.

[46] H. Namatsu, Y. Takahashi, K. Yamazaki, T. Yamaguchi, M. Nagase, K. Kurihara, J. Vac. Sci. Technol. B, 16 (1998) 69-76.

[47] A.E. Grigorescu, M.C. van der Krogt, C.W. Hagen, P. Kruit, Microelectronic Engineering, 84 (2007) 822-824.

[48] Y. Ekinci, H.H. Solak, C. Padeste, J. Gobrecht, M.P. Stoykovich, P.F. Nealey, Microelectronic Engineering, 84 (2007) 700-704.

[49] H. Okamoto, A. Ishikawa, Appl. Phys. Lett., 55 (1989) 1923-1925.

Figures

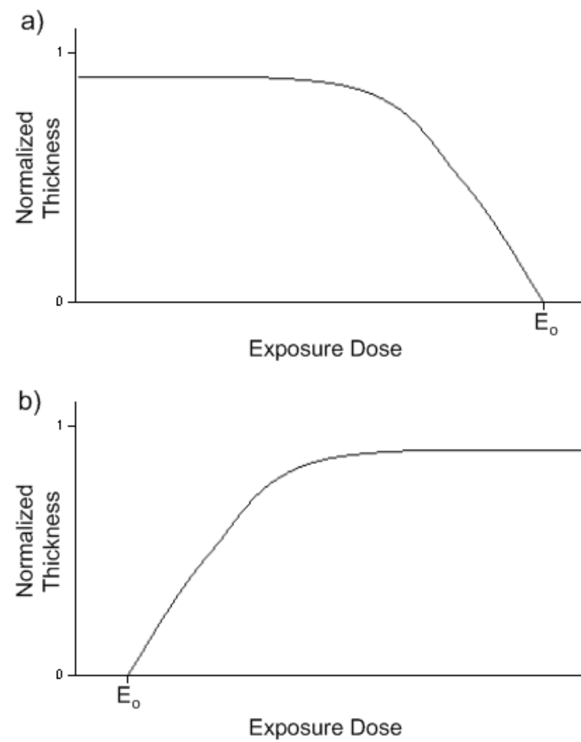

Figure 1. Typical characteristic curves for photoresists, showing photoresist thickness remaining after development as a function of exposure dose for (a) a positive resist and (b) a negative resist. The exposure dose is plotted on a logarithmic scale to produce a curve that is approximately linear in the vicinity of E_o.

CHAPTER 2

DIFFUSION PATTERNING

Abstract

A bilayer system for patterning a solution deposited metal oxide is presented. The pattern process relies on selective diffusion between two hydrated metal oxides precursors. Where the bilayer interdiffuses, the combined layer is made soluble in strong inorganic acid. The diffusion based patterning process is initiated with UV light and electron-beam exposure.

Introduction

For the past four decades, photolithographic processing has been the driving force for improvements in resolution and dimensional control that have made possible the extension of Moore's Law in semiconductor manufacturing[1-3]. In a modern fabrication facility, photolithography is responsible for patterning billions of transistors every second. These transistors are responsible for the personal computers, cell phones, and innumerable advanced electronic products that are now essential parts of our lives. The photolithographic advances making these products possible have centered on the development of short-wavelength exposure tools and an extraordinary extension in the feature-size and resolution capabilities of polymer resists [4, 5]. As the quest for ever smaller feature sizes continues, the limitations and inefficiencies of polymer-based resist technology are becoming more evident [6], prompting considerable interest in possible alternatives.

The smallest feature sizes produced via lithography have been realized by electron-beam writing of inorganic materials [7]. The beam doses required to produce these features, however, have been much too high to receive more than passing interest for use in a manufacturing environment. Herein, we describe a new and general approach to lithography with inorganic materials, demonstrating versatility for applications covering a length scale from macro to nano. We illustrate here applications in ink-jet printing, photolithography, and electron-beam writing.
This approach derives from our recent demonstration of the solution deposition and processing of homogeneously and atomically dense oxide films as thin as 3 nm [8].

The films can be stacked to form nanolaminates exhibiting atomically abrupt interfaces, and more importantly the degree of hydration of the films can be controlled through processing. This variation in hydration provides a method for controlling the interdiffusion of stacked films and their resulting physical and chemical properties. This interdiffusion, attendant modification in material solubility, and high-film quality have provided means to realize this new lithographic process.

Bilayer photo induced diffusion has been previously used for lithographic patterning. Chalcogenide glasses like As_2S_3, AsSe, and GeSe exhibit photo induced diffusion from a top coat of Ag metal or AgTe [9-11]. Silver, which diffuses into the chalcogenide glass renders the film insoluble in an alkaline solution. These chalcogenide systems can be used in both photolithography and electron beam lithography [12].

Results & Discussion

The technique is exemplified by considering the bilayer film system HafSOx [8] (hafnium oxide sulfate) and copper formate. HafSOx is a high-performance dielectric used in transistors, and it can readily be spin-coated onto a substrate and gently heated to produce an insoluble solid acid. The HafSOx film can then be coated with copper formate, and induced decomposition of the copper formate leads to interdiffusion of the “Cu” and HafSOx layers. Following a cure, the resulting interdiffused bilayer readily dissolves in aqueous acid. A diagram of this process is givenr in Figure 2-1.

A simple, visual example of the use of the interdiffusion in patterning is demonstrated in Figure 2-2. Here, HafSOx is first cast onto a SiO_2/Si substrate. The substrate is placed on the heated platen of a printer, and lines or dots of copper formate are then written via a thermal ink-jet head. As the copper source meets the surface, the copper formate begins to decompose and interdiffuse with the HafSOx layer, effectively rendering the HafSOx film soluble. Following a cure and development in acid, drawn lines and dots are clearly evident.

As shown in Figures 2 and 3, similar patterning has been achieved by using UV photolithography and electron-beam writing. As shown in Figure 2-3, exposure of the same bilayer to UV radiation through a mask readily leads to pattern development. In a similar way, nanoscale feature sizes can be written with electron-beam writing, Figure 2-4. In single passes with the electron beam, lines as narrow as 22 ± 3 nm have been achieved, already indicating small feature-size capabilities for the technique. In addition, charge doses as low as 150 $\mu C/cm^2$ for pattern development represent a sensitivity similar to that of many polymer resists and an enhancement of $> 10^3$ relative to other inorganic approaches.

Conclusion

This diffusion patterning system bears some similarities to chalcogenide resists which rely on photoinduced doping of the chalcogenide glass by a silver bilayer [12]. While the system presented here also relies on an induced doping effect, it functions at a significantly lower dose and it is not hampered by highly toxic constituents.

A simple mutual interdiffusion has been used to form patterns at multiple feature sizes. Relative to conventional lithographic processing and patterning of inorganic materials, the film application, baking, and etching steps of the polymer resist as well as the vacuum and high-temperature annealing steps associated with deposition of the inorganic material have been eliminated. Except for the electron-beam exposure all processing is conducted in a normal laboratory environment in air. The process is quite efficient as a functional material, e.g., HafSOx, directly participates in its own patterning. Considering the simplicity of the technique and the reduction of processing steps relative to conventional methods, continued development could provide routes to improved device production yields and lower fabrication costs. Relying on the exclusive use of aqueous chemistries, the procedures are also environmentally friendly; washed products can readily be reclaimed and recycled for additional use.

The process has relevance to many advancing technologies. Its use is not restricted to the chemical systems described here. We believe the film chemistries can be extended to 50 or more elements in the periodic table, greatly increasing opportunities in lithography beyond the common five-element set of organic polymer resists. Our technique provides a method for patterning printed all-oxide electronic devices and circuits, which have recently been demonstrated to have performance characteristics superior to those of amorphous Si and organics in flexible macroelectronics [13]. Also, a new chemical toolbox is now available to examine high-refractive index inorganic materials for a variety of uses, including extension of

optical lithography to smaller critical dimensions, augmenting printing and imprinting technologies, and advancing future-generation lithographic methods by providing new means to tune and optimize material-beam interactions.

References

[1] C.G. Willson, R.R. Dammel, A. Reiser, Proc. SPIE, 3049 (1997), 28-41.

[2] C. Mack, Future Fab International, (2007).

[3] A.E. Grigorescu, M.C. van der Krogt, C.W. Hagen, (2007).

[4] C. Mack, *Fundamental Principles of Optical Lithography: The Science of Microfabrication*, Wiley-Interscience, 2008.

[5] H.J. Levinson, *Principles of Lithography, Second Edition*, 2nd ed., SPIE Publications, 2005.

[6] R.P. Meagley, Future Fab International, (2006).

[7] M. Isaacson, A. Muray, M. Scheinfein, A. Adesida, E. Kratschmer, Microelectronic Engineering, 2 (1984) 58-64.

[8] J.T. Anderson, C.L. Munsee, C.M. Hung, T.M. Phung, G.S. Herman, D.C. Johnson, J.F. Wager, D.A. Keszler, Adv. Funct. Mater, 17 (2007) 2117-2124.

[9] A. Yoshikawa, O. Ochi, H. Nagai, Y. Mizushima, Applied Physics Letters, 29 (1976) 677.

[10] J. Teteris, Journal of Non-Crystalline Solids, 299 (2002) 978-982.

[11] J.M. Lavine, M.J. Buliszak, J. Vac. Sci. Technol. B, 14 (1996) 3489-3491.

[12] G.H. Bernstein, W.P. Liu, Y.N. Khawaja, M.N. Kozicki, D.K. Ferry, L. Blum, J. Vac. Sci. Technol. B, 6 (1988) 2298-2302.

[13] K. Nomura, H. Ohta, A. Takagi, T. Kamiya, M. Hirano, H. Hosono, Nature, 432 (2004) 488-492.

Figures

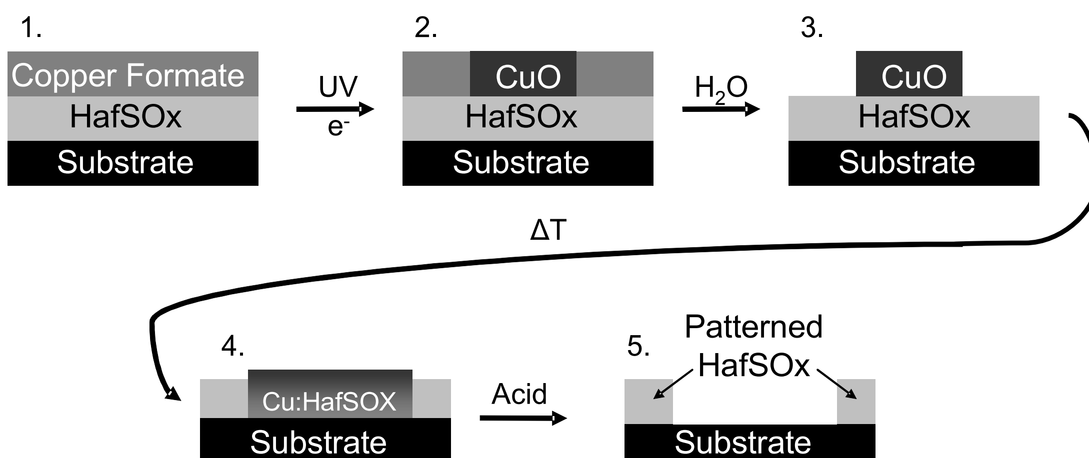

Figure 2-1. Process flow for photolithography or electron beam lithography; 1.) A bilayer of HafSOx and copper formate is deposited. 2.) Where HafSOx is to be removed the formate is selectivly decomposed by UV light or electron beam. 3.) Excess formate is rinsed away to form a selective bilayer. 4.) The film stack is annealed which results in diffusion of the Cu into the Hafsox. 5.) The regions of the film that contain Cu are removed with a strong inorganic acid.

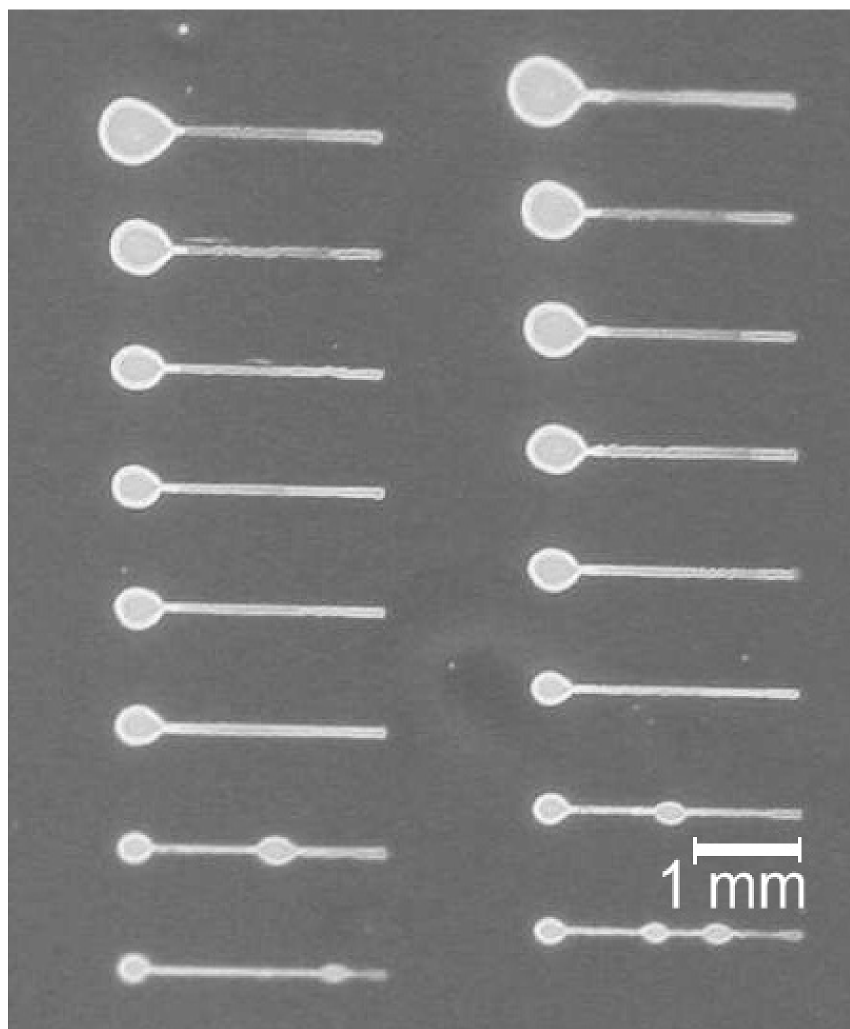

Figure 2-2. Thermal ink jet based patterning. Printing copper formate to form a bilayer with blanket coated HafSOx, which after interdiffusion renders the HafSOx locally soluble.

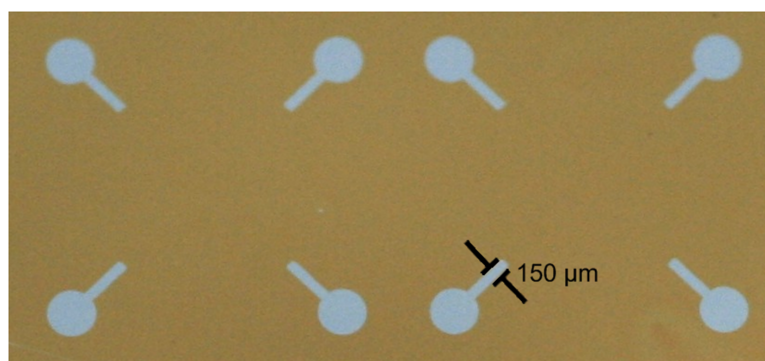

Figure 2-3. Optical microscope image of photographically patterned HafSOx via photo induced interdiffusion. The dark area is HafSOx and the light area is the substrate.

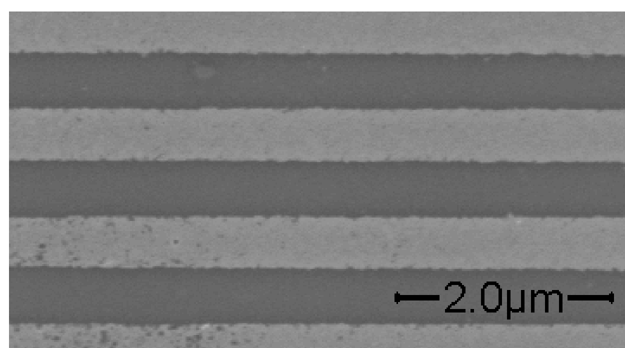

Figure 2-4. Electon beam lithography patterning of copper formate/HafSOx bilayer. (500 nm wide lines and spaces)

CHAPTER 3

PHOTOLITHOGRAPHIC PATTERNING OF SOLUTION DEPOSITED SOx MATERIALS

Abstract

A new system for directly patterning functional metal oxides by UV and EUV exposuresis demonstrated. The materials are deposited from aqueous solutions, and they exhibit excellent film quality. While the systems were originally designed as high-k dielectrics, they also display considerable potential for application as inorganic photoresists.

Introduction

Inorganic resists have for some time demonstrated a potential for high resolution patterning. The highest resolution features obtained with lithography, using electron beam lithography, have been obtained with metal flouride resist systems [1-3]. However, metal fluorides function at a dose that is impractical for wide scale use. Hydrogen silsesquioxane (HSQ), available from Dow Corning under the trade name FOx, is an inorganic resist that functions at a significantly lower dose than metal fluorides while only making a small trade off in resolution. Using HSQ, isolated lines as small as 6 nm and dense lines and spaces of 10 nm have been produced [4]. The doses required to print these features were 5.5 and 33 mC/cm^2, respectively. While these results represent an improvement of several orders of magnitude over the sensitivity of the metal flourides, they are still moderately high in comparison to traditional organic resists. Aside from the sensitivity HSQ has another inherent limitation. The exposure mechanism is only sensitive to high energy electrons; typically from electron-beam lithography or from the photoelectrons generated through extreme ultra violet (EUV) lithography.

Photolithography, a primary fabrication tool of the semiconductor industry, is the predominant form of lithography. A few inorganic resists have exhibited photo sensitivity, but in comparison to polymer resists the dose required to pattern with photons is much higher than for electron-beam exposure. The various chalcogenide based inorganic resists are all photo sensitive to some degree. These systems have demonstrated a sensitivity of ~24 mJ/cm^2 and by including a thin layer of Ag as low as

8 mJ/cm^2 [5, 6]. In both cases there is a non-linear response to exposure power , necessitating the use of very high exposure powers. At the lower power normally found in photolithography systems, the required dose is higher. These chalcogenide materials become opaque to light in the visible spectrum [7]. Since the choice of exposure wavelength is limited to the visible spectrum, the patterns able to be printed in chalcogenide materials are severely limited by the diffraction limit.

Another inorganic resist, peroxopolytungstate, has exhibited a photosensitivity to deep ultraviolet light. This material has exhibited a sensitivity to 248-nm light of 1 J/cm^2. This sensitivity can be lowered to 150 mJ/cm^2 by substituting Nb for part of the W [8]. This sensitivity is still far too high to be selected in applications where a chemically applified polymer resist would suffice. One advantage of this system is a high oxygen plasma etch resistance. In a bilayer process, where the peroxopolytungstate is deposited on top of an organic material, this high etch resistance allows high aspect ratio structures to be generated. Peroxopolytungstate does not suffer from the same laser power dependency as the chalcogenides.

The work here represents a new addition to the small number of inorganic resists that are photosensitive. More importantly, this resist shows sensitivity to 193-nm light, the exposure wavelength that is currently at the cutting edge in semiconductor fab lithography tools.

Experimental

Solutions for spincoating are prepared from dry chemicals and concentrated stock

solutions. Aqueous precursor solutions of 1 M $ZrOCl_2$ (aq), 1M $HfOCl_2$ (aq), 2 M H_2SO_4 (aq), and 2 M H_2O_2 (aq) were prepared from $ZrOCl_2 \cdot 8(H_2O)$ (Alfa Aesar, 98%), $HfOCl_2 \cdot 8(H_2O)$ (Alfa Aesar, 99+ % excluding 1.5%Zr), H_2SO_4 (EMD, 17.8M), and H_2O_2 (Mallinckrodt, 30%) with 18-MΩ purified water. These precursor solutions were combined to produce a working solution which were directly spin coated. Working solutions were prepared by combining the $ZrOCl_2$ (aq) or $HfOCl_2$ (aq) with H_2O_2 (aq) to give a metal to peroxide ratio of 1 to 0.75. The solution was allowed to rest for 15 min. to enable ligand exchange to approach equilibrium. Following this, H_2SO_4 (aq) was added to give a metal to sulfate ratio of 1 to 0.5-0.7. Again the solution was allowed to rest for 15 min to enable ligand exchange to reach equilibrium. Solutions were diluted with 18 MΩ purified water to give a final metal concentration of 0.5 M.

Substrates were either silicon wafer chips (n^+ heavily doped) or silicon coupons with 200 nm of thermal oxide. The substrates for UV exposure were prepared for spincoating by sonication in Decon Labs, Contrad 70 at 45°C for 60 min. Substrates for EUV exposure were prepared by immersion in a fresh piranha etch solution (3 parts H_2SO_4 to 2 parts H_2O_2) for 1 min. Working solutions were spin coated at 3000 rpm for 30 seconds resulting in films 30 to 35-nm thick.

Patterning by UV light was achieved by exposing films through a chrome-on-silica mask, placed in contact with the films. The exposure source was an Oriel Series Q 30-W deuterium lamp. The images were developed by immersion in .05-1 M HCl. Blanket exposures were performed across samples in a stepwise manner by sliding a opaque mask across the surface at regular time intervals. After patterning the films

were annealed at 300 °C for 5 minutes to fully cure them.

Patterning by EUV light was conducted at the XIL beam-line of the Swiss Light Source at the Paul Scherrer Institute in Villigen, Switzerland. An interference setup was used to produce high resolution and high contrast aerial images at the plane of the resist. Blanket exposures were also conducted to generate characteristic contrast curves. The images were developed by immersion in 12 M HCl.

Contrast curves were generated from step heights measured by atomic force microscope (AFM). The AFM data was collected on an Asylum Research MFP-3D instrument. Images were taken on a Zeiss Ultra field-emission gun scanning electron microscope (SEM).

Results and Discussion

Though both ZircSOx and HafSOx are UV sensitive, ZircSOx exhibits a greater sensitivy with the deuterium exposure source. When comparing the fully annealed materials, ZircSOx begins adsorbing about 30 nm higher in the UV spectrum. The extinction coefficients of these materials have previously been determined; the values are plotted in Figure 3-1. It is expected that these extinction coefficients will be different with the presence of peroxide in the as-deposited material, but the separation between the two materials is expected to remain. As a result, ZircSOx has more available spectrum for exposure in the lamp output and consequently is easier to pattern. Though the extinction coefficients are not known it should be noted that as-deposited peroxide containing HafSOx and ZircSOx are not sensitive to $\lambda > 254$ nm.

The UV exposure setup use does not allow for a quantitative analysis of sensitivities. The power density of the lamp output, which could be used to calculated exposure dose is not known. This limits the usefulness of a characteristic contrast curve to determine sensitivity. Considering that exposure time is proportional to the exposure dose at a given power density this curve can still be used to accurately determine the contrast of the resist. A time dependent contrast curve for ZircSOx can be found in Figure 3-2. This curve shows a contrast a 0.7, a relatively low contrast. To improve the contrast it will be necessary to find a different developer.

It was found that ZircSOx could be patterned by UV light in either positive or negative tone. An example of negative-tone patterning can be found in Figure 3-3 and positive-tone in Figure 3-4. Positive-tone patterning could be achieved by subjecting the resist to a prebake of 100 ºC for 2 min. With a lower bake step negative-tone patterning is achieved. Negative tone patterning can be enhanced by applying a mild post-exposure bake of 50 ºC for 30 s. Negative-tone is the preferred mode of patterning as positive-tone patterning suffers from a very low contrast. The dual tone of this resist system will still need to be further investigated, as it may prove enlightening to the exposure and development mechanisms.

Under different processing conditions the photoactive element of the resist is either increasing or decreasing the solubility of the exposed region relative to the unexposed region. To pattern in negative tone, the exposure has to make the film more resistant to dissolution than the unexposed region. Conversely, to pattern in the positive tone the exposure has to make the film less resistant to dissolution than the

unexposed region. Understanding this exposure mechanism is critical to understanding how to optimize resist performance. Analytical methods for detecting changes induced by this exposure are complicated by the amount of material in question. Films on the order of 30-nm thick do not have sufficient volume per unit area to generate a signal large enough to be measured under most analyses. Typical surface analysis, like x-ray photoelectron spectroscopy, is too energetic to measure reactive species without destroying them. There are three tools necessary to characterize this exposure mechanism and future work should be directed to obtaining access to this analysis. The peroxide stretch is a Raman active vibration, but for the thickness of films used, there insufficient material to detect a response with standard Raman spectroscopy. Tip Enhanced Raman Spectroscopy (TERS), a modification of Surface Enhanced Raman Spectroscopy (SERS), uses gold antenna placed on the flattened tip of an AFM probe to generate a local field enhancement to the Raman cross section that can boost the Raman signal as much as 10^{10}. TERS be used to examine the vibration modes of peroxide in the SOx materials and how these modes change under processing conditions and exposure dose. The reaction products of the exposure mechanism, if release into vacuum, can be captured and analyzed. By using the appropriate mass spectrometer, the species evolved during exposure can be determined. Additionally, a Thermally Programmed Desorption (TPD) Mass Spectrometer would enable the correlation of the exposure products to those produced via thermal decomposition. TPD would also clarify the influence of the prebake and postbake. Taken together, these experiment would enable the proper determination of

the exposure mechanism in both the positive and negative tone.

Films were also subject to EUV interference exposures. This research did not generate significant results because of processing errors. Following exposure and development, films were not annealed to fully cure them. During the three week interim, while the samples were shipped from Switzerland, they absorbed moisture from the air and degraded significantly. An example of this degradation can be seen in Figure 3-5. Because of this problem, only a single set of samples generated measurable results. This sample set underwent a prebake for 30 s at 100 ºC. This partial annealing made the films less subject to moisture during transit. Unfortunately, it is apparent that a prebake at this temperature is detrimental to the patterning process.

Contrast data were collected from this single sample set. These data have been plotted in Figure 3-6. Under these processing conditions, HafSOx exhibited a contrast of 0.3 and a sensitivity of 194 mJ/cm^2. These values represent very poor resist performance, but considering the circumstances, these results indicate the need for more EUV exposures. Even with the errors in processing and poor resist performance, nano-scale features were patterned with EUV lithography. An example of 30 nm lines and spaces can be found in Figure 3-7. The low contrast of the process is reflected in the poor edge definition of the lines. Were these exposure to be repeated, given the revisions to the patterning process, it is expected that results would be vastly improved.

Conclusion

A method for directly patterning a metal oxide has been presented. The patterning

performance exhibited by these materials indicates they could have usefulness as inorganic photoresists. The performance of these materials to exposure by deep ultraviolet light has initially been evaluated. Coincidentally, the exposure wavelength which would best be used with these materials is 193-nm, the wavelength which is currently the exposure wavelength in state of the art lithography tools in the semiconductor industry. A low contrast of 0.7 was demonstrated with UV patterning. Experiments were conducted to evaluate this material under exposure to EUV light. These experiments were hampered by an error in processing, and thus generated unoptimized results. Even with these errors, a contrast of 0.3 and a sensitivity of 194 mJ/cm^2 were demonstrated.

References

[1] M. Isaacson, A. Muray, M. Scheinfein, A. Adesida, E. Kratschmer, Microelectronic Engineering, 2 (1984) 58-64.

[2] E. Kratschmer, M. Isaacson, Journal of Vacuum Science & Technology B: Microelectronics and Nanometer Structures, 4 (1986) 361.

[3] E. Kratschmer, M. Isaacson, Journal of Vacuum Science & Technology B: Microelectronics and Nanometer Structures, 5 (1987) 369.

[4] A.E. Grigorescu, M.C. van der Krogt, C.W. Hagen, P. Kruit, Microelectronic Engineering, 84 (2007) 822-824.

[5] V. Lyubin, M. Klebanov, I. Bar, S. Rosenwaks, N.P. Eisenberg, M. Manevich, J. Vac. Sci. Technol. B , 15 (1997) 823-827.

[6] J.M. Lavine, M.J. Buliszak, J. Vac. Sci. Technol. B, 14 (1996) 3489-3491.

[7] S. Shtutina, M. Klebanov, V. Lyubin, S. Rosenwaks, V. Volterra, Thin Solid Films, 261 (1995) 263-265.

[8] H. Okamoto, A. Ishikawa, T. Kudo, Thin Solid Films, 172 (1989) L97-L99.

Figures

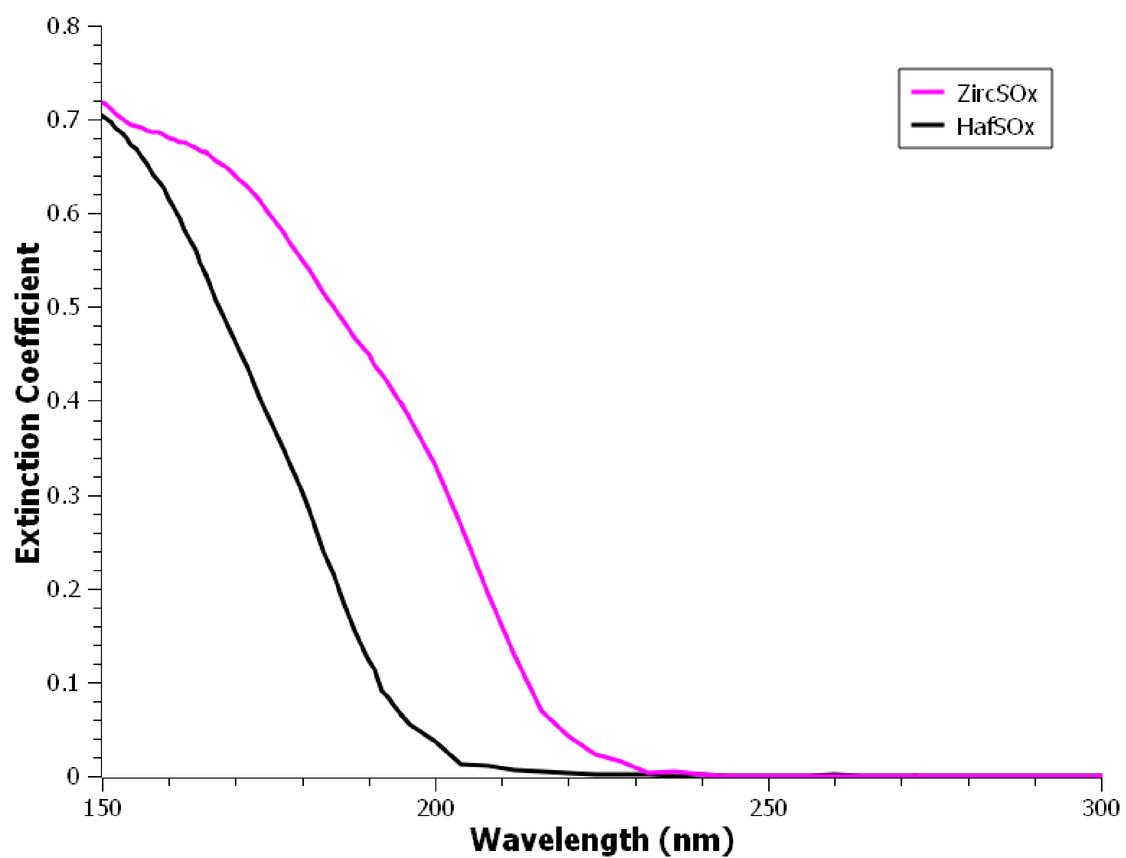

Figure 3-1. Extinction coefficients for HafSOx and ZircSOx films after anneal at 325 ºC.

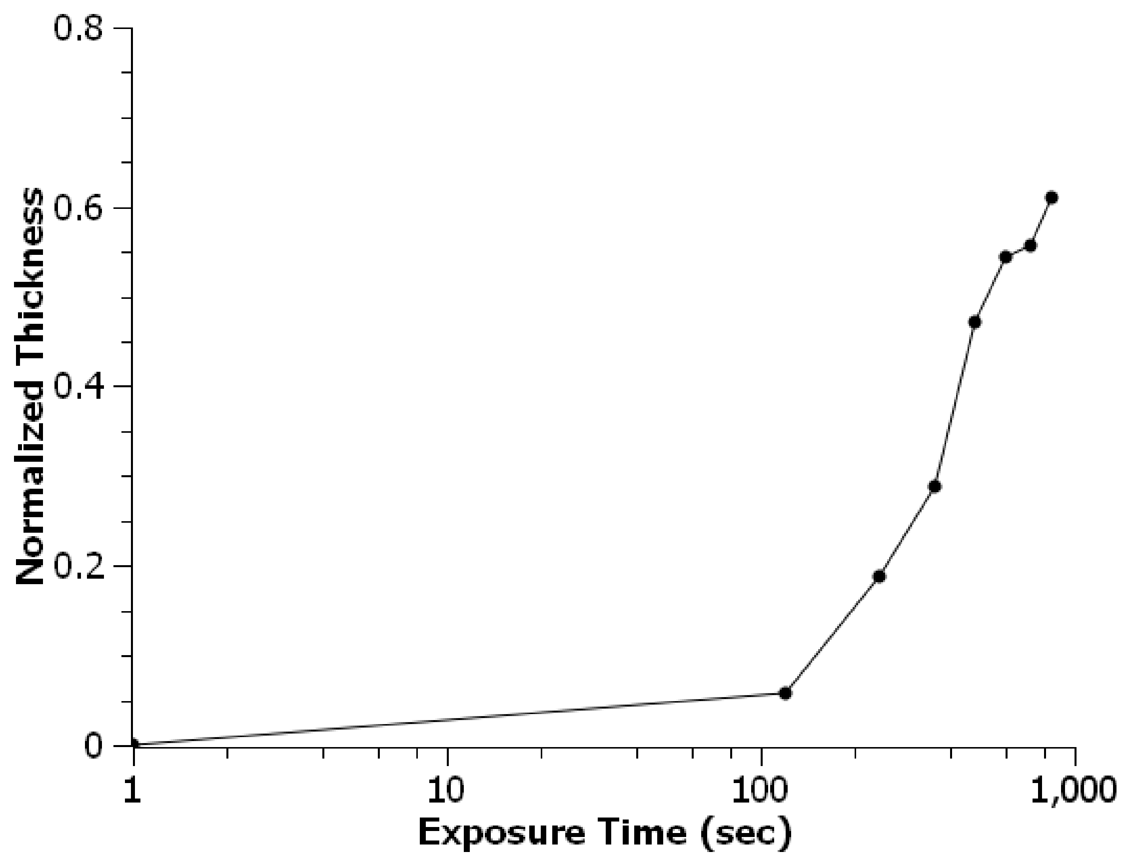

Figure 3-2. Time dependent characteristic contrast curve for UV exposed ZircSOx. The curve exhibits a contrast of 0.7. The film was developed in 0.1 M HCl for 45 s.

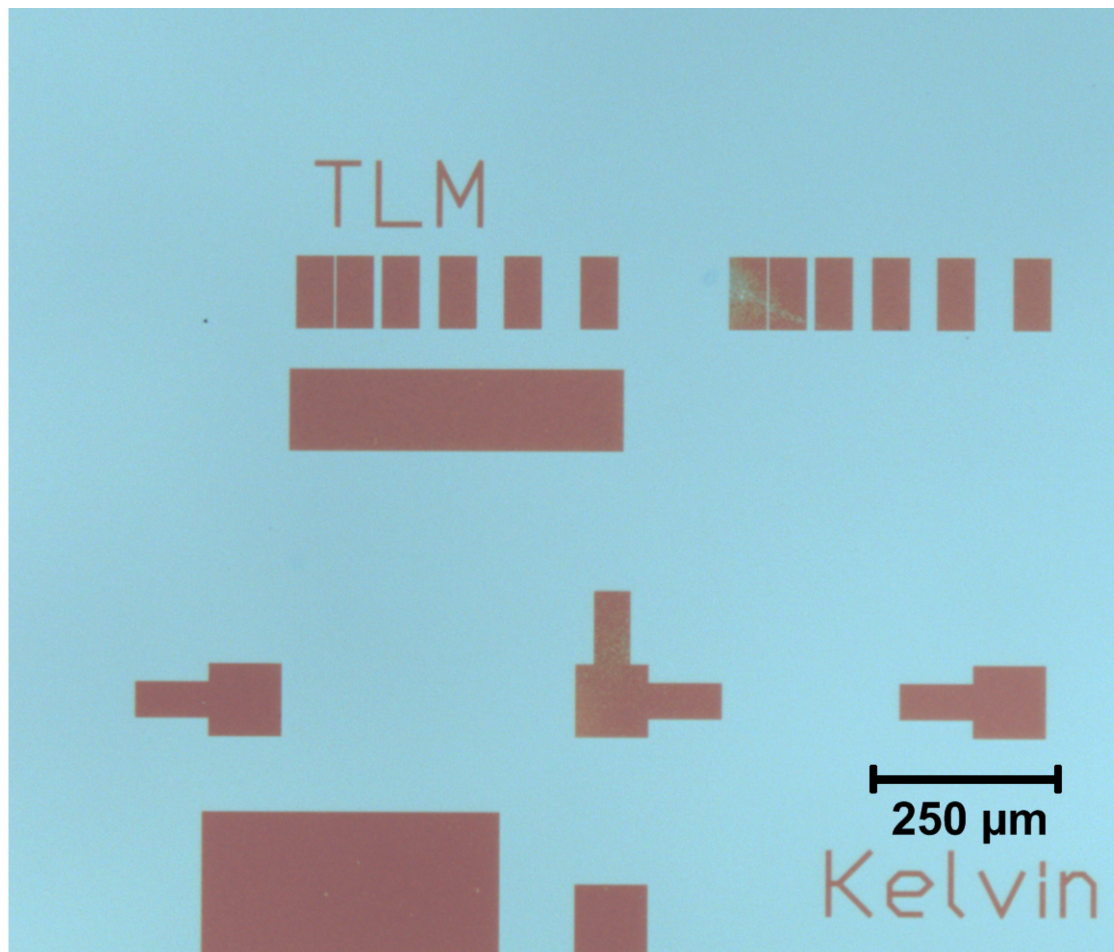

Figure 3-3. Optical microscope image of UV patterned negative-tone ZircSOx. The dark regions are ZircSOx and the light areas are substrate.

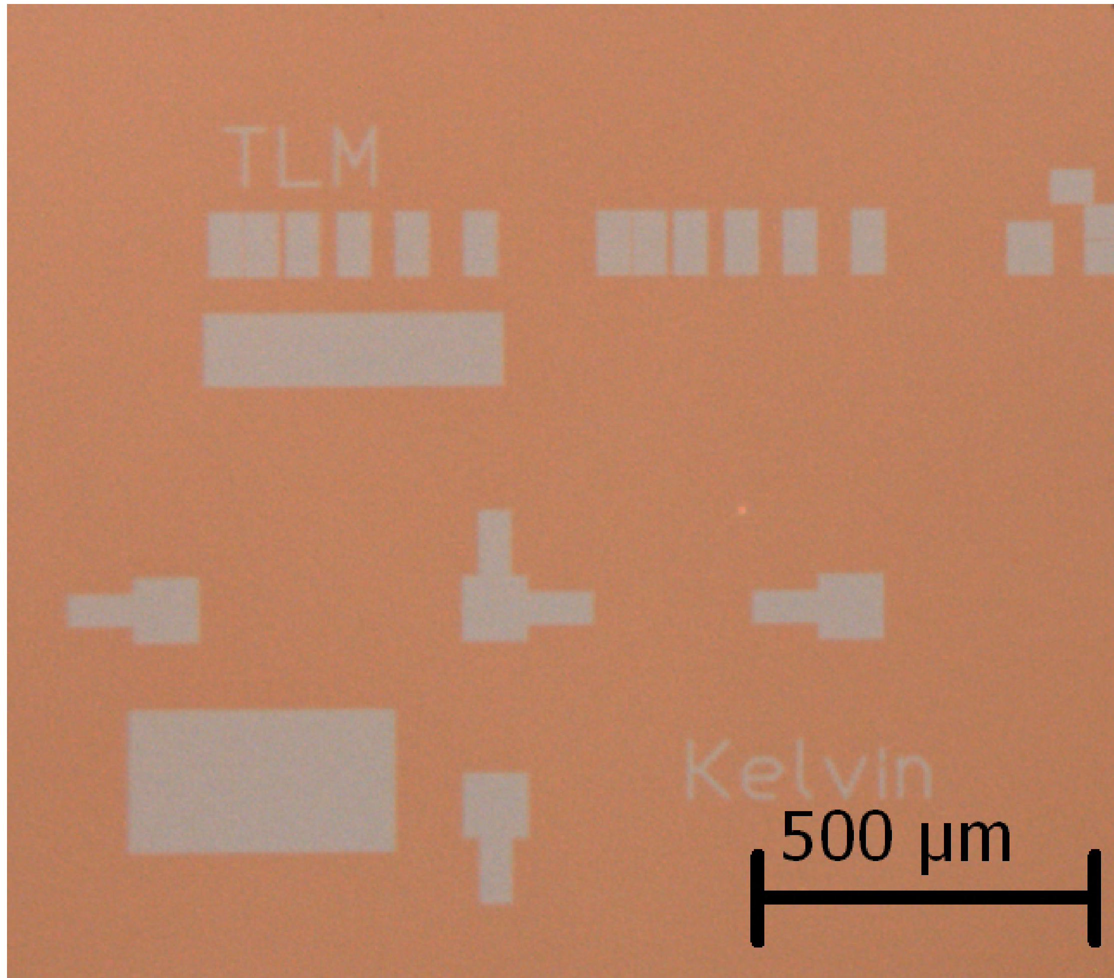

Figure 3-4. Optical microscope image of UV patterned positive-tone ZircSOx. The dark regions are ZircSOx and the light areas are substrate.

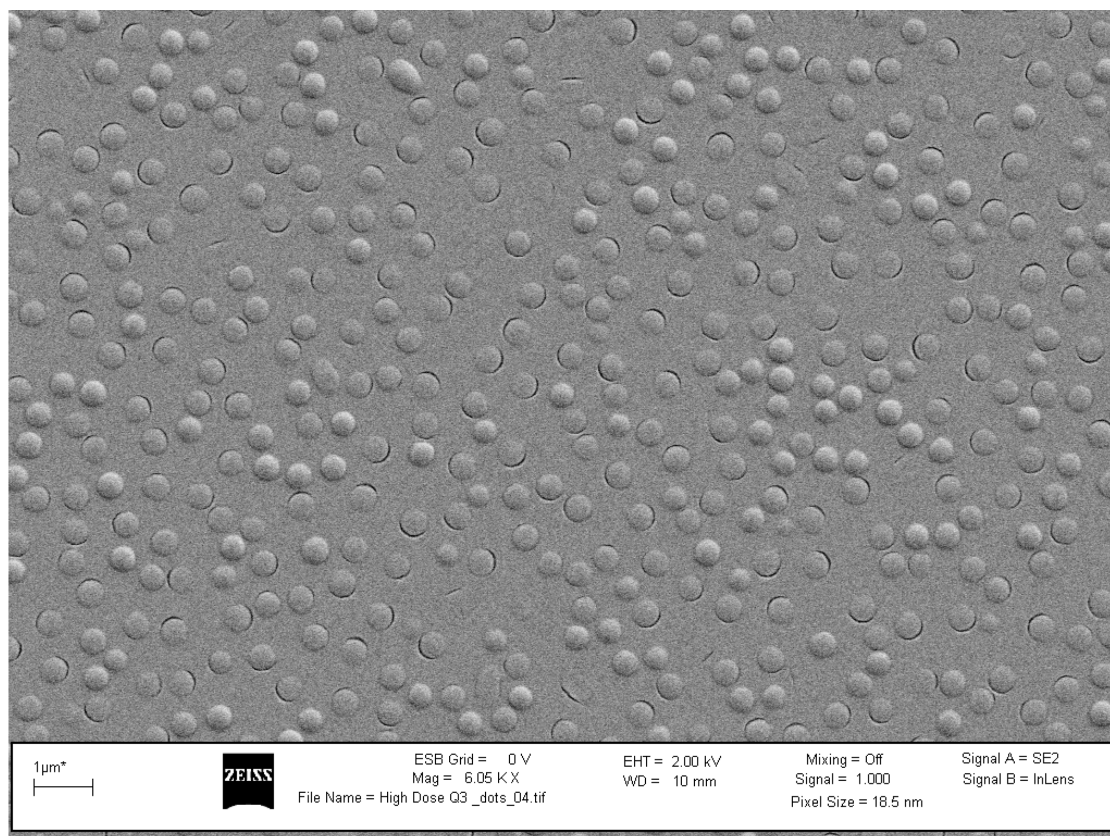

Figure 3-5. SEM of EUV exposed sample degradation. The image was taken in the middle of area of blanket exposure. The bubbles covering the sample are approximately 500 nm in diameter.

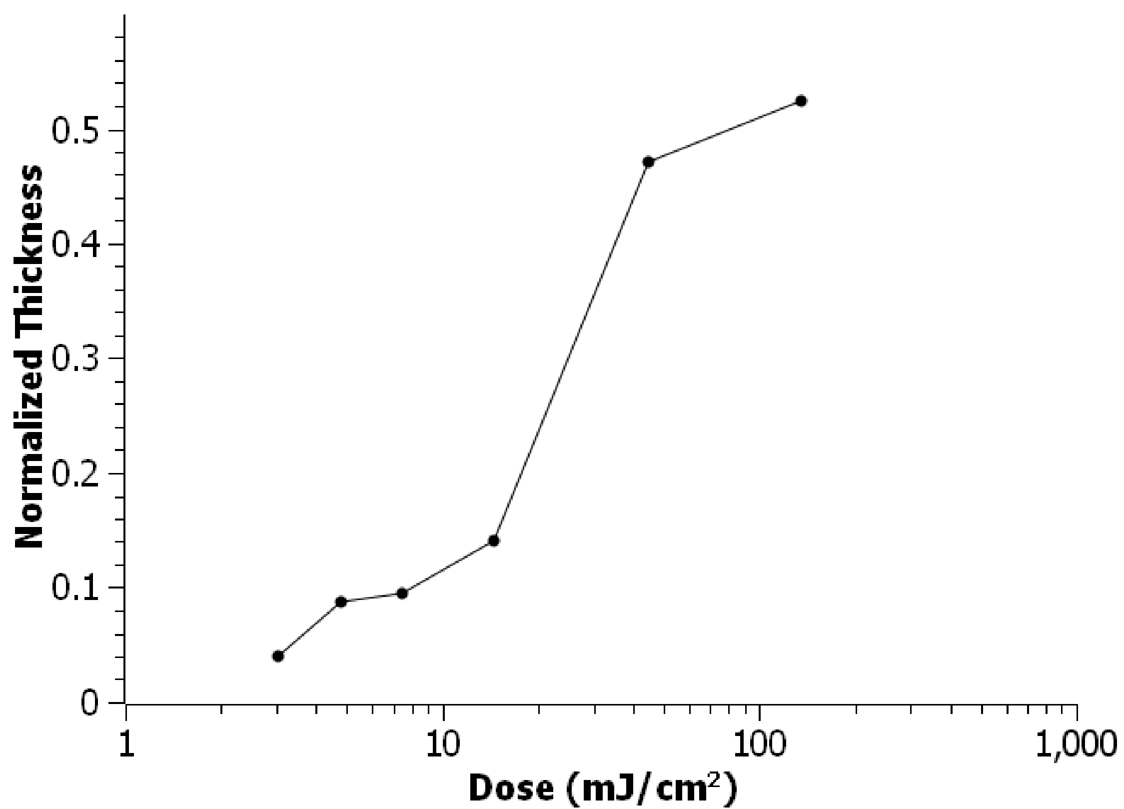

Figure 3-6. Characteristic contrast curve for EUV exposed HafSOx. The curve exhibits a contrast of 0.3 and a sensitivity of $D_{0.8}$ = 194 mJ/cm^2. The film was developed in 12 M HCl for 50 s.

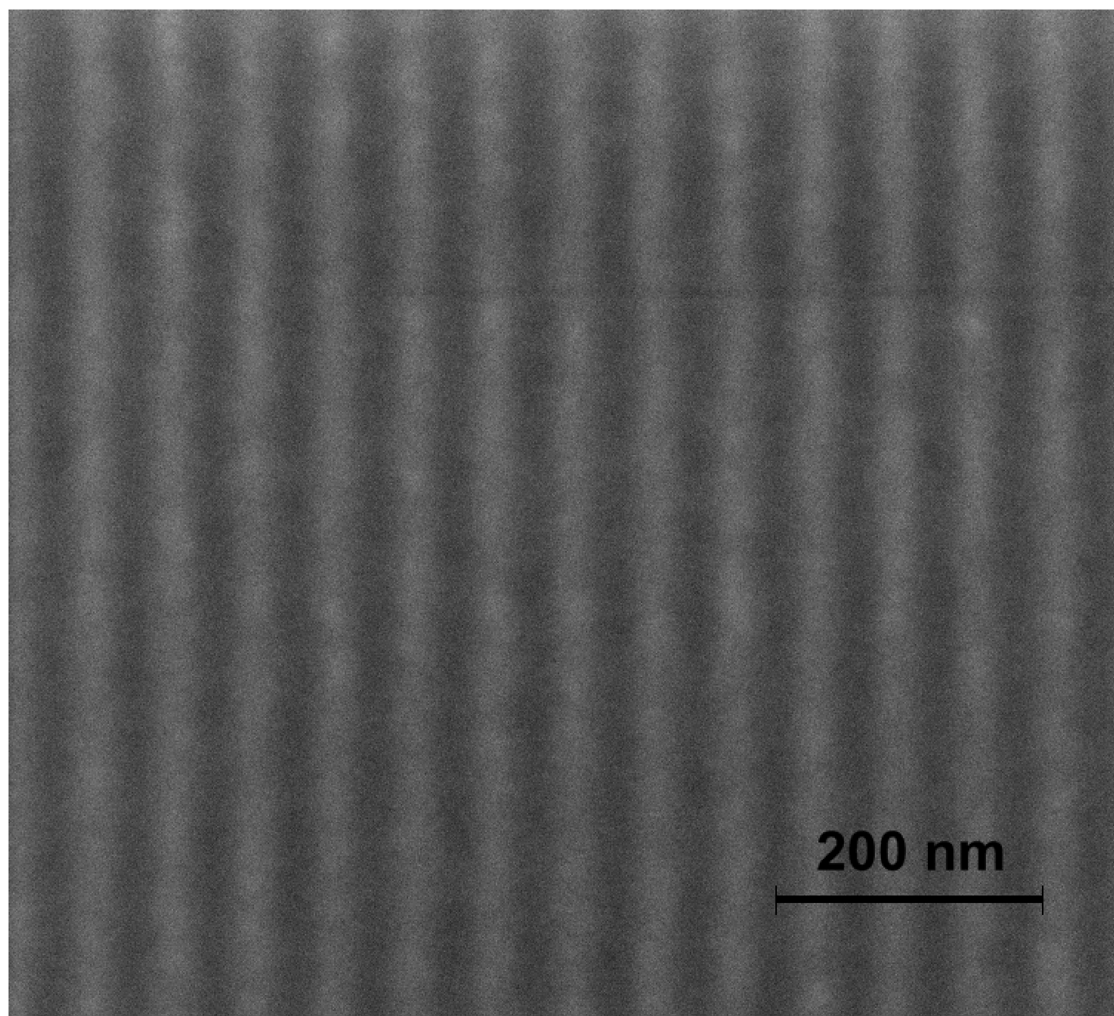

Figure 3-7. SEM image of 30 nm lines and spaces patterned by EUV interference lithography. The dose to print these features was 289 mJ/cm^2.

CHAPTER 4

NOVEL INORGANIC RESIST FOR NANOMETER SCALE PATTERNING

Abstract

We present here a unique, high-sensitivity solution-deposited inorganic resist. This material has been generated on the basis of our recently published work on the high-performance dielectric HafSOx. HafSOx, a hafnium oxide sulfate, and its zirconium analog ZircSOx are spin-coated materials that exhibit extraordinary film qualities. These materials has been deposited in thickness ranges of 3 to 500 nm, and throughout this range, they are characterized as atomically smooth, amorphous, and pinhole free films. When modified for use as a resists, they exhibit several unique characteristics. Their versatility is demonstrated by exposure sensitivity to essentially any energy source – photo, EUV, X-ray, and electron beam. In electron-beam exposures at 30 keV, a dose to gel as low as 8 $\mu C/cm^2$ and a contrast of 3 have been observed. We have already demonstrated a feature resolution of 16 nm, which simply reflects the capabilities of the available electron-beam system. The resulting patterned oxide also exhibits excellent resistance (5x > SiO_2) during plasma etching. Since the materials also serve as high quality dielectrics, they provide an unprecedented, direct route to patterned functional inorganic materials. Unlike exposure chemistries unique to HSQ imaging chemistries associated with HafSOx and ZircSOx are quite general. For the first time, a path for directly patterning a variety of metal oxide compositions that cover a significant portion of the periodic table is envisioned.

Introduction

Nanometer scale fabrication has significant implications for advancing future electronic devices. Using a high energy electron beam with a width of a few nanometers, electron beam lithography has become one of the major tools for nanolithography. Many other types of lithography, e.g., extreme ultra violet, deep ultra violet, and nanoimprint lithography, are dependent on the flexibility and resolution of electron beam lithography to produce the masks and templates necessary for their implementation.

Inorganic resist systems have for many years shown potential as high resolution materials. The highest resolution patterned with electron beam lithography has been with metal fluoride systems [1-3]. The problem plaguing these fluoride systems has been an impractically low sensitivity. The lowest sensitivity a flouride system has demonstrated is $\sim 10^5$ $\mu C/cm^2$ [4]. This dose is several orders of magnitude greater than required for PMMA, a traditional polymer electron beam resist. Despite this limitation, these fluoride systems demonstrated the potential of a fine-grained or amorphous inorganic material in terms of resolution, if the sensitivity could be reduced to a reasonable value.

The greatest volume of research currently being directed at inorganic resists is aimed at hydrogen silsesquioxane (HSQ). HSQ is a polymer consisting of $HSiO_{1.5}$ units with a three-dimensional network structure. This network structure leads to advantages over a linear chain polymer found in most polymer resists. The three dimensional structure causes a smaller radius of gyration and less aggregation [5].

The molecular weight of this material is typically > ~10^4. These factors result in higher resolution and a lower line edge roughness. HSQ undergoes a Si-H bond scission under electron beam exposure that enables subsequent crosslinking. Using electron beam lithography isolated lines as small as 6 nm and dense lines and spaces of 10 nm have been produced [6]. The dose required to print these features was 5.5 and 33 mC/cm^2, respectively.

Though HSQ is a promising material for e-beam lithography, it is a typical inorganic resist limited by a low sensitivity. The sensitivity level is dictated by the activation energy for breaking the Si-H bond. This reaction is only active to electrons and photons at very high energies associated with EUV lithography.

We present here a high-sensitivity solution deposited inorganic resist. This resist has the potential for pattern formation at a higher resolution than obtainable with HSQ at a significantly lower dose. By breaking the limitations of low sensitivity associated with inorganic resist, it has been observed to function at a dose comparable to a chemically amplified polymer resist. In addition, at this sensitivity the resist also has application in lower resolution, high speed patterning.

HafSOx and ZircSOx , the materials which are a basis for these new resists, have previously been reported [7]. These amorphous materials are aqueous solution deposited metal oxides that find applications as high-k dielectrics in thin film transistors. Films made of these materials are characterized as being atomically smooth, dense, and pin hole free. Films have been demonstrated as thin as 3 nm with retention of film quality. This material system serves as a significant starting point for

the creation of an inorganic resist.

HafSOx and ZircSOx resists have significantly different characteristics from a traditional polymer resist. With a traditional polymer resist, the molecules in the resist film are identical to those solvated in the resist solution and do not change over a wide range of conditions. The SOx materials undergo polymerization during and after deposition. As such the species in solution are different from those deposited in a film. These species in solution are oligomers of several metal ions but are difficult to characterize. The zirconyl ion is known to exist as a discrete tetrameric complex $[Zr_4(OH)_8(H_2O)_{16}]^{8+}$ in oxychloride compounds. This complex was first found to exist in the crystal structure of $ZrOCl_2 \bullet 8H_2O$ [8] and later proven to exist in solution [9]. In zirconium sulfate solutions, the chemistry is quite different because the sulfate anion strongly bonds with the zirconium and can serve as a bridge, promoting polymerization. A large number of hydroxo sulfato species have been identified in zirconum sulfate solutions, depending on conditions [10]. None of them has been reported as stable over a range of condutions indicating that the zirconium sulfate system is governed by a series of complicated equilibra. In the resist solution chloride, peroxide, and sulfate are present. Identification of species in the resist solution is further complicated by the ligand exchange equilibrium between each anion and hydroxl groups.

During the spin-coating process, the resist solution experiences rapidly changing conditions. As the water is driven off, the increase in the concentration of the solvated species induces polymerization. Further polymerization is induced during

later processing. Since this polymerization process is reserved for deposition and later processing, there is not a set radius of gyration or aggregate size in the resist solution which can be measure and applied to the resist. A way in which the radius of gyration demonstrates its self in traditional polymer resists is in how thin they can be deposited. HSQ, an inorganic polymer, has a radius of gyration lower than that of other polymer resists. For HSQ the roughness has a minimum for films of 40 nm and builds in roughness in thickness below this [11]. Namatsu et al. reported a radius of gyration for HSQ of 2-5 nm. They also reported aggregation resulting in particles 10-15 nm in diameter. This limits the thickness of deposited HSQ to a minimum of 10 nm. As a way of comparison, HafSOx has been deposited as thin as 2-3 nm in a film characterized as being atomically smooth and pin-hole free. No attempts have yet been made to deposit films thinner than this. This serves to demonstrate a fundamental difference of SOx materials from traditional polymer resists.

As stated, during spin coating solvent is lost from the resist, but not completely. Residual solvent content in deposited films is something common to all resist materials. Efforts are usually made to remove some or all solvent. The issue of solvent content in the deposited SOx material is obfuscated by the roll water plays as both a solvent and a polymerization agent. The polymerization of this material is conducted through condensation reactions which exclude water from the material. Removal of all of the solvent would necessitate complete polymerization of the film. Because of the roll of water, the application of either a prebake or a postbake to remove solvent takes on an added dimension. Due to the added complexity of the

influence of various bake steps, no attempt has yet been made to optimize these variables.

Experimental

Unlike traditional polymer resists, HafSOx and ZircSOx must be prepared from dry chemicals and concentrated stock solutions. Aqueous precursors solutions of 1 M $ZrOCl_2$ (aq), 1M $HfOCl_2$ (aq), 2 M H2SO4 (aq), and 2 M H_2O_2 (aq) were prepared. To make these, $ZrOCl_2 \cdot 8H_2O$ (Alfa Aesar 98%), $HfOCl_2 \cdot 8H_2O$ (Alfa Aesar, 99+ % excluding 1.5%Zr), H_2SO_4 (EMD 17.8M), or H_2O_2 (Mallinckrodt, 30%) were combined with 18-MΩ purified water. Prior to deposition these precursor solutions were combined to produce a working solution which is directly spin coated. Working solutions were prepared by combining the $ZrOCl_2$ (aq) or $HfOCl_2$ (aq) with H_2O_2 (aq) to give a metal to peroxide ratio of 1 to 0.75. This was allowed to rest for 15 minutes to enable ligand exchange to reach equilibrium. Then, H_2SO_4 (aq) was added to give a metal to sulfate ratio of 1 to 0.5-0.7. Again the solution was allowed to rest for 15 minutes. Solutions were diluted with 18 MΩ purified water to give a final metal concentration of 0.5 M.

Silicon n-type conductive wafers were cleaved into one inch square chips for use as substrates. The substrates were prepared for spincoating by sonication in Decon Labs, Contrad 70 at 45°C for 60 minutes. Working solutions were then spin coated at 3000 rpm for 30 seconds and exposures were conducted at 30 keV beam voltage on a Zeiss Ultra FEG SEM with a Nabity lithography system. Development was conducted

by immersion in the selected developer. A low contrast process could be obtained by development in 6-12 M HCl (aq) or a higher contrast and higher sensitivity can be obtained by using 10-25% w/w tetramethylammonium hydroxide (TMAH). A final hardbake was performed at 325C for 5 minutes.

Contrast curves were generated from step heights across 16 μm^2 pads. The step heights were collected on an Asylum Research MFP-3D AFM. Images were taken on the same Zeiss Ultra FEG SEM used for lithographic exposure.

Electron probe microanalysis (EPMA) was performed on a Cameca SX-100 Electron Microprobe. To approximate condition within the SEM chamber, samples for EMPA analysis were placed in vacuum of $3*10^{-5}$ Torr for 1 hour, removed, and then exposed with a Oriel Series Q 30-W deuterium lamp. This allowed for blanket patterned areas which electron beam lithography cannot generate with a negative tone resist.

Films were tested for resistance to reactive ion etching (RIE). These films were prepared in the same way as films for EPMA. A Plasmatherm System VII RIE tool, that uses parallel plates to produce a capacitively coupled plasma, was used to test etch resistance. The etch recipe used was; 15 SCCM of CHF_3 at a chamber pressure of 30mTorr. Etching was done at 75W 374V DC Bias for 5 minutes. Etch depths were collected with by AFM.

Results

The materials exhibit significantly varying characteristic contrast curves

depending on the developer used. Figure 4-1 shows a contrast curve for electron beam exposure of HafSOx with development in HCl. Figure 4-2 shows a contrast curve using TMAH as the developer. Both cases results in negative tone patterning. The higher sensitivity and contrast of the basic developer, 8 $\mu C/cm^2$ dose to gel and contrast of 3, make it the the best candidate for almost all lithography applications. The acidic developer exhibits a higher sensitivity and low contrast, 400$\mu C/cm^2$ dose to gel and contrast of 0.5. The acidic developer with its low contrast is most suitable for application in gray scale lithography, in which dose is varied to impart topographical information to the resist.

The acidic developer, exhibiting low contrast, can still be used to generate high quality patterns. A SEM of 100-nm lines and spaces patterned at 60 $\mu C/cm^2$ can be found in Figure 4-3. A SEM of 30 nm wide isolated lines patterned at 300 $\mu C/cm^2$ can be found in Figure 4-4.

Using the basic developer, ZircSOx films were exposed to determine the highest resolution obtainable with our 30 keV electron beam lithography system. It has been observed that 16 nm wide isolated features can be patterned at a dose of 112 $\mu C/cm^2$. An example of these isolated features is shown in Figure 4-3. Figure 4-4 shows dense features of 28 nm lines on a 100 nm period which have been patterned at 50 $\mu C/cm^2$. These features are the smallest that can be patterned with our current lithography system. They demonstrate the resolution limit of the exposure system, not an intrinsic resolution limit of the resist. A dedicated electron beam lithography system operating at 100 keV is required to fully test the resolution of these resist materials.

The sensitivity of this resist is comparable to chemically amplified resists. A clue to the source of this remarkable sensitivity can be found in the density of these metal oxides. The stopping power of a high energy electron by a material is dependent on the electron density and the average ionization potential of a material. The modified Bethe stopping power equation proposed by Joy and Luo [12] is as follows:

$$\frac{dE}{ds} = -785 \frac{\rho Z}{AE} \ln\left[\frac{1.166(E+kJ)}{J}\right] \qquad eV/Å$$

where E is the instantaneous energy of the electron (in eV), s is the path length along the trajectory (in Å), ρ is the density (in g/cm^3), Z is the average atomic number, A is the atomic weight, J is the mean ionization potential of the material (in eV), and k is a variable which is dependant on the material but is always close to, but less than, unity. To accurately calculate the stopping power of the SOx materials, it will be necessary to determine the density under exposure conditions. This work is ongoing. Because of the metal content, ZircSOx and particularly HafSOx have a higher density than other resists like HSQ (1.4 g/cm^3) or PMMA (1.19 g/cm^3). If a reasonable density of 4 g/cm^3 for ZircSOx and 5 g/cm^3 for HafSOx were assumed, a rough comparison of the stopping power of SOx materials to HSQ and PMMA can be made. For a 30 keV electron energy the stopping power of HSQ and PMMA are almost equal while the stopping power of ZircSOX is 2.5x greater and HafSOx is 3x greater; illustrating a possible explanation for the high sensitivity of the SOx materials. Furthermore the stopping power of these materials also applies to secondary electrons as well. Secondary electrons are generated as the primary beam passes through the resist.

They serve to widen the effective diameter of interaction for the primary electron beam. The higher stopping power of the SOx materials limits the distance secondary electrons travel through the resist , minimizing the effective diameter of interaction. The high density of these materials benefits both the resolution the sensitivity of these materials.

The 3 σ line edge roughness (LER) of lines in Figures 4-3 and 4-4 are 2.4 and 4.6 nm, respectively. This is slightly higher than the LER reported for HSQ by Namastu et al. in their original investigation of that material [5]. It should be noted that the exposure dose to generate both of these patterns is significantly lower than required by HSQ. The lower dose is in the realm of statistical variation of dose due to a small number of electrons. At 50 $\mu C/cm^2$, the width of a 30 nm line is defined by 94 electrons. A small variation of the placement of a few electrons can result in a significant noise in width of this feature, affecting the LER. It is not known what the fraction of the roughness in this case is a property of the resist and what can be attributed to exposure statistics. It will likely be beneficial to LER in moving to a lower sensitivity through the application of a stronger developer. From this perspective, this resist material has the unique property of functioning in two resolution/dose regimes. The resist can be employed at a high resolution with a lower LER by sacrificing sensitivity or can be employed at a high speed at the cost of a higher LER.

It is known from previous work that when these materials are not fully cured they can undergo ion exchange when treated with concentrated basic solutions [13]. This

allows the sulfate and chloride anions to be exchanged with hydroxyl groups. The resulting metal oxo-hydroxide is easily dehydrated to produce the metal oxide. To confirm that this phenomenon was present during the development process electron probe microanalysis was conducted on films that underwent various process conditions. The results of this analysis can be found in Table 4-1.

Table 4-1. EPMA data for HafSOx/ZircSOx under varying processing conditions. The atomic ratios are scaled to a total metal concentration of 1.

		Atomic ratios				
Sample	Developer Type	Hf	Zr	S	Cl	Development time (sec)
HafSOx	Undeveloped	0.99	0.01	0.41	0.12	NA
HafSOx	20% TMAH	0.99	0.01	0.01	0.04	105
HafSOX	25% TMAH	0.99	0.01	0.14	0.05	10
ZircSOx	Undeveloped	0.01	0.99	0.56	0.12	NA
ZircSOx	20% TMAH	0.01	0.99	0.02	0.05	10
ZircSOX	12M HCl	0.01	0.99	0.54	0.03	180

During the development process, it can be seen in a basic or an acidic developer that a significant amount of chemical modification of the film occurs. This modification during the development process is unique to this resist system. The impact of this exchange process on the development characteristics is unknown, but it is clear in the case of HafSOx developed in different concentrations of TMAH that the

time needed to exchange anions does not always coincide with the time needed to fully develop a film. The kinetics between development and ion exchange in exposed and unexposed regions could play a significant role in obtaining a high contrast. The role of ion exchange in the development process merits further study.

The EPMA results also illustrate a small difference in the sulfate concentration in as deposited HafSOx and ZircSOX. This subtle difference has significant implications for using TMAH as a developer in electron beam exposure. HafSOx films with the lower sulfate level are more resistant to development in TMAH, leading to difficulty in patterning. It is believed that higher sulfate levels inhibit dehydration of films while under vacuum. It is possible to vary the sulfate level by modifying the formulation of the original working solution. Though not tested for resist performance, it has been observed that HafSOx films prepared with higher sulfate levels are more soluble in TMAH after vaccum treatment. The formulation recipes require further optimization for this reason.

Reactive ion etching was used to determine the ability of this material to transfer a pattern to an underlying substrate. An SiO_2 etch process was selected because of the application of a patterning SiO_2 films to nano-imprint lithography master template fabrication. Using the etch process designed to remove thermally grown SiO_2 at a rate of 20 nm/min, ZircSOx and HafSOx exhibited etch rates of 2.9 and 2.2 nm/mi,n respectively. This translates to a (Zr/Hf)SOx etch selectivity to thermal SiO_2 of 1:7 and 1:9 respectively. This demonstrates the chemically inert nature of these metal oxides and their resulting expected high etch resistance.

There are several traditional avenues to optimize patterning performance. The prebake and postbake, neither of which have been sufficiently explored at this point, can be adjusted for temperature and time. It has been observed that by applying a mild postbake of 50°C for 30 s that the sensitivity can be pushed even lower, to 4 μC/cm^2. The trade off is a poor contrast of 0.7, which indicates that a stronger developer should be used when applying a postbake. The choice of developer plays significant role in resist performance. We have demonstrated how different developers can drastically modify the characteristics of the resist. It is expected that a stonger developer will be needed to increase the contrast and lower the sensitivity to a level more appropriate to high resolution patterning. Transitioning to a stronger developer is also expected to lower the LER. Specific developers will need to be optimized for target applications, for example, gray scale versus high resolution.

There are several less traditional variables that do not apply to polymer resists, which can be optimized for resist performance. The ratios of metal to peroxide to sulfate are all variable and careful experimentation will be useful in determining the optimal ratios. There exists the possibility of novel developer mixes for high contrast development. It has been reported recently that contrast in HSQ can be increased 3x over the standard high contrast development using 25% TMAH by changing the developer to 1% wt NaOH with 4% wt NaCl [14]. As it has already been shown the development in the HafSOx/ZircSOx resist system is a dynamic chemical process and should prove to be influenced by the presence of additional salts in the developer. The solution chemistry of HafSOx/ZircSOx is amenable to the addition of secondary metal

ions in moderate ratios. This opens up a large portion of the periodic table as candidates for modification of this resist system. These modifying elements can function a variety of roles, as sensitizers for photolithography or as hardeners for reactive ion etch resistance.

This resist system also needs to be considered in the larger tapestry of directly patterned materials. Since the original application of these materials is solution deposited high-k dielectrics, this resist system is also a directly patterned dielectric system. Furthermore, unlike the unique chemistry associated with HSQ, the exposure chemistry here should be quite general and can be applied as a direct patterning method for a host of metal oxides covering the periodic table.

Conclusions

We have presented here a unique high-sensitivity solution deposited inorganic resist. Sensitivities comparable to chemically amplified resists have been demonstrated at a reasonable contrast. Isolated features as small as 16 nm, exhibiting a LER of 2.4 nm, have been patterned. The development process has been explored, demonstrating that there are chemical modifications taking place during development that are unique to this system. High RIE resistance to a CHF_3 plasma show that this resist is applicable to the patterning of thermally grown SiO_2. At present these materials system exhibits significant promise as a new inorganic resist system. With further optimization, they could find application in both high speed and high resolution patterning.

References

[1] M. Isaacson, A. Muray, M. Scheinfein, A. Adesida, E. Kratschmer, Microelectronic Engineering, 2 (1984) 58-64.

[2] E. Kratschmer, M. Isaacson, Journal of Vacuum Science & Technology B: Microelectronics and Nanometer Structures, 4 (1986) 361.

[3] E. Kratschmer, M. Isaacson, Journal of Vacuum Science & Technology B: Microelectronics and Nanometer Structures, 5 (1987) 369.

[4] J. Fujita, H. Watanabe, Y. Ochiai, S. Manako, J.S. Tsai, S. Matsui, Applied Physics Letters, 66 (1995) 3064.

[5] H. Namatsu, Y. Takahashi, K. Yamazaki, T. Yamaguchi, M. Nagase, K. Kurihara, J. Vac. Sci. Technol. B, 16 (1998) 69-76.

[6] A.E. Grigorescu, M.C. van der Krogt, C.W. Hagen, P. Kruit, Microelectronic Engineering, 84 (2007) 822-824.

[7] J.T. Anderson, C.L. Munsee, C.M. Hung, T.M. Phung, G.S. Herman, D.C. Johnson, J.F. Wager, D.A. Keszler, Adv. Funct. Mater, 17 (2007) 2117-2124.

[8] A. Clearfield, P.A. Vaughan, Acta Crystallographica, 9 (1956) 555-558.

[9] G.M. Muha, P.A. Vaughan, J. Chem. Phys., 33 (1960) 194-199.

[10] A. Clearfield, Reviews of Pure and Applied Chemistry, 14 (1964) 91.

[11] M.J. Word, I. Adesida, P.R. Berger, J. Vac. Sci. Technol. B, 21 (2003) L12-L15.

[12] D.C. Joy, S. Luo, Scanning, 11 (1989) 176-180.

[13] P.A. Hersh, *Wide band gap semiconductors and insulators: synthesis, processing and characterization*, Oregon State University, 2007.

[14] J.K.W. Yang, K.K. Berggren, Journal of Vacuum Science & Technology B: Microelectronics and Nanometer Structures, 25 (2007) 2025.

Figures

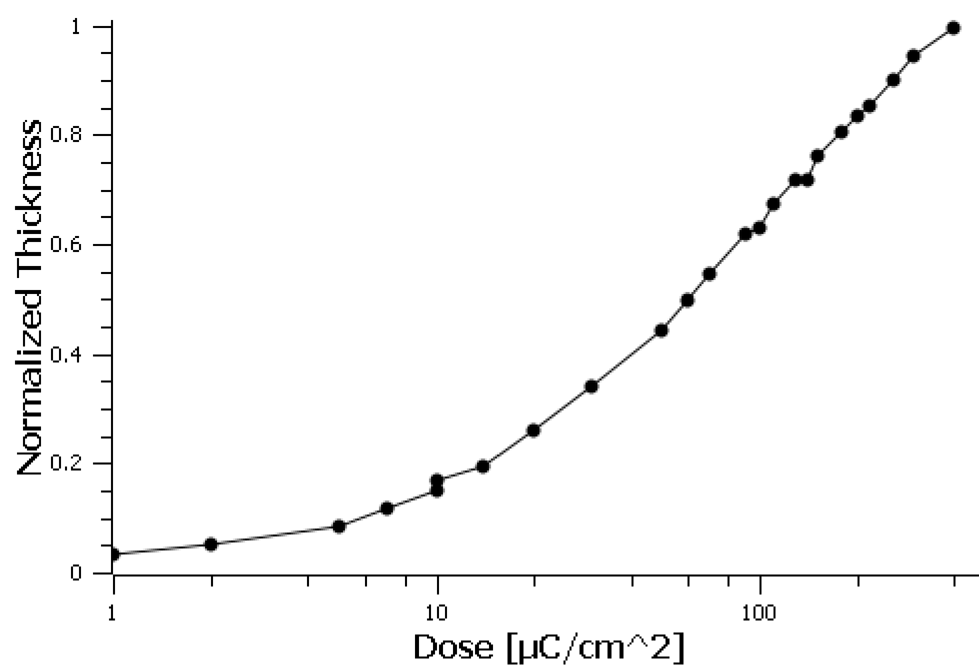

Figure 4-1. Contrast curve for a HafSOx film developed in 12 M HCl. The curve shows a dose to gel of ~ 400 µC/cm^2. The curve shows no real zero dose, as the lowest dose delivered 1 µC/cm^2 creates a non zero thickness. The region around 10 µC/cm^2 showing a negative second derivative is atypical resist behaviour. The contrast of the resist is 0.4.

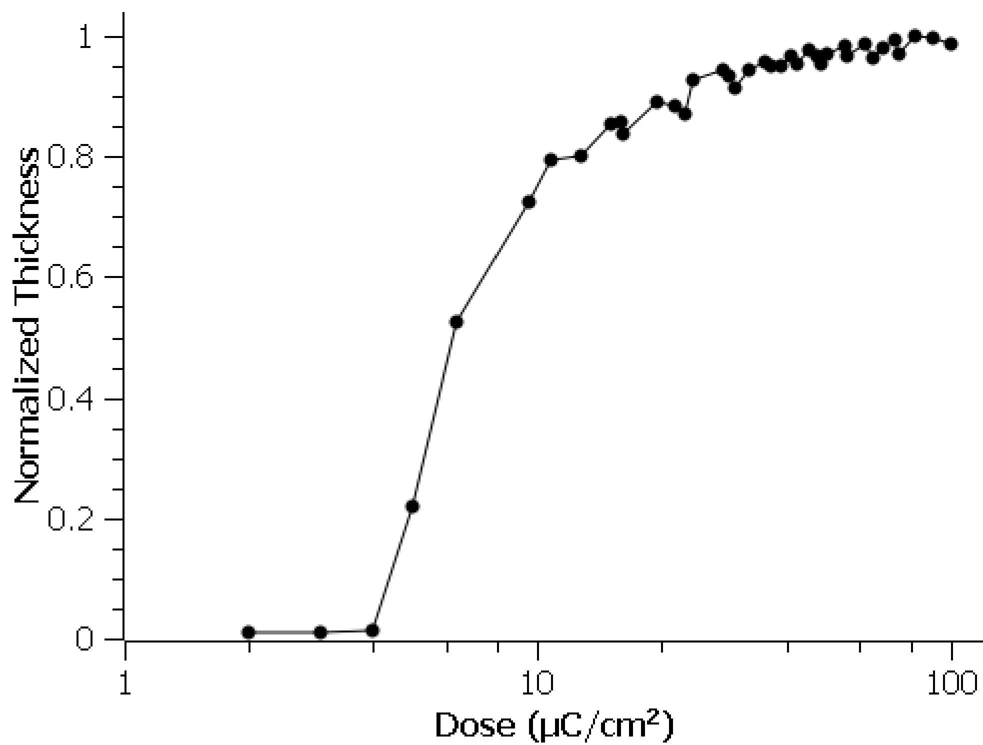

Figure 4-2. Contrast curve for a ZircSOx film developed in 20% TMAH for 4 minutes. The curve shows a dose to gel of 8 µC/cm^2 and a zero dose of 4 µC/cm^2. The contrast of the resist is 3.

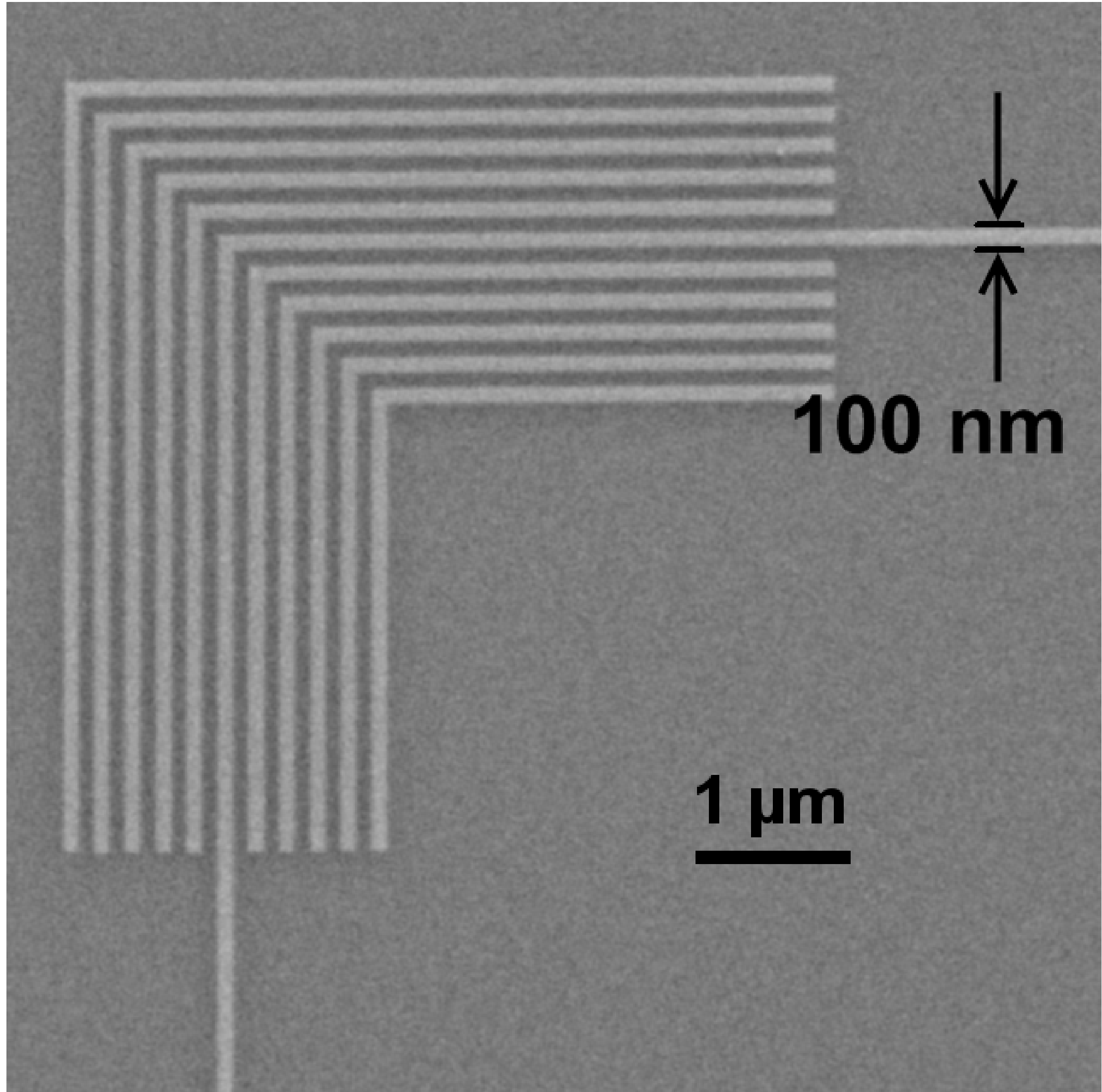

Figure 4-3. SEM images of 100-nm lines and spaces patterned in HafSOx with a dose of 60 μC/cm² with a 30 keV electron beam. A low contrast acidic developer was used.

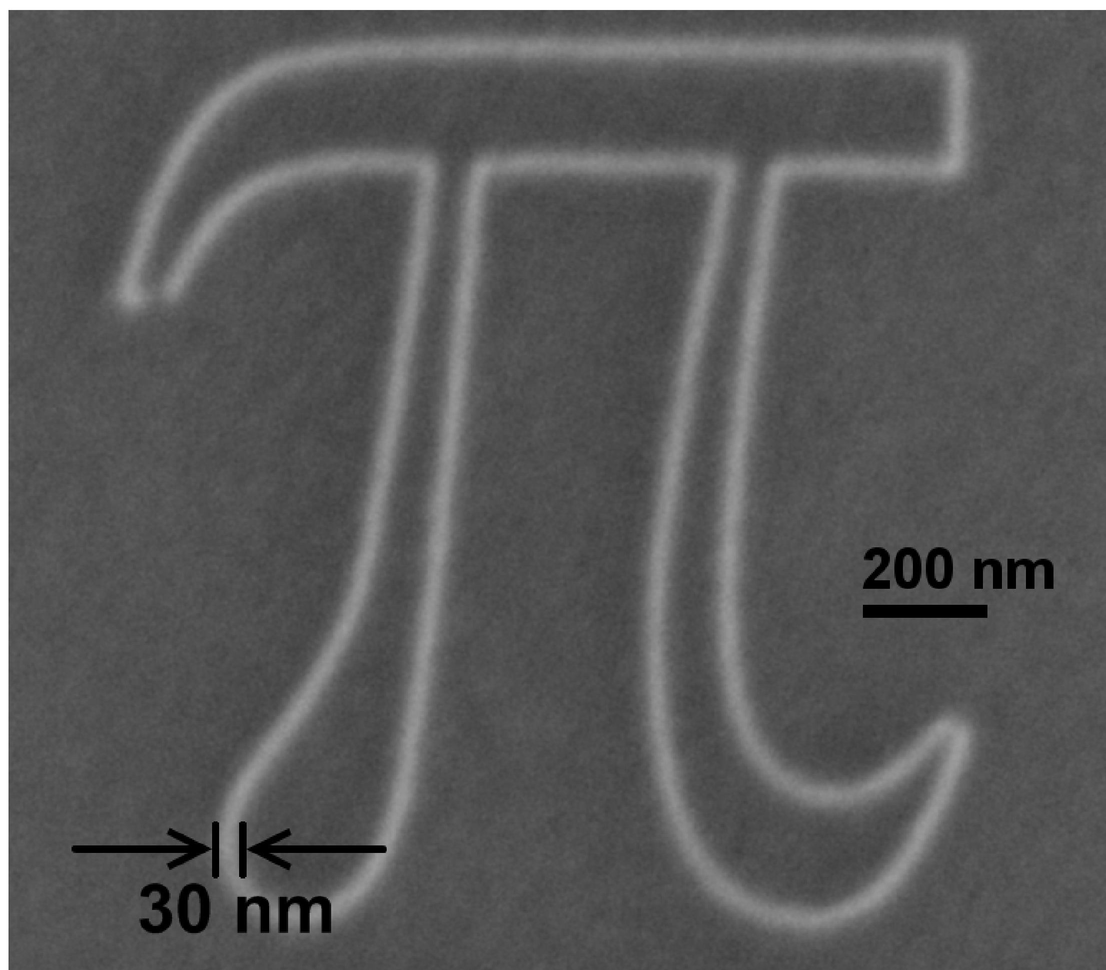

Figure 4-4. SEM images of 30-nm isolated lines patterned in HafSOx with a dose of 300 μC/cm^2 with a 30 keV electron beam. A low contrast acidic developer was used.

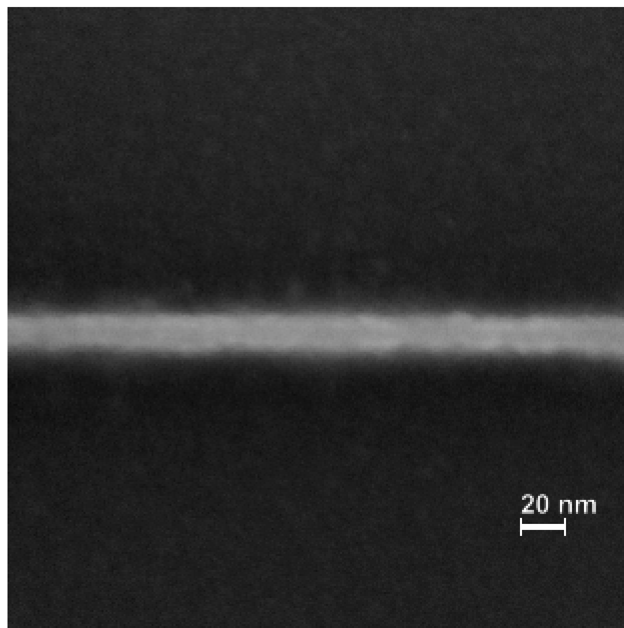

Figure 4-5. SEM of a 16-nm isolate line printed in ZircSOx at a dose of 112 μC/cm^2 with a 30 keV electron beam. The three sigma line edge roughness of this feature is 2.4 nm.

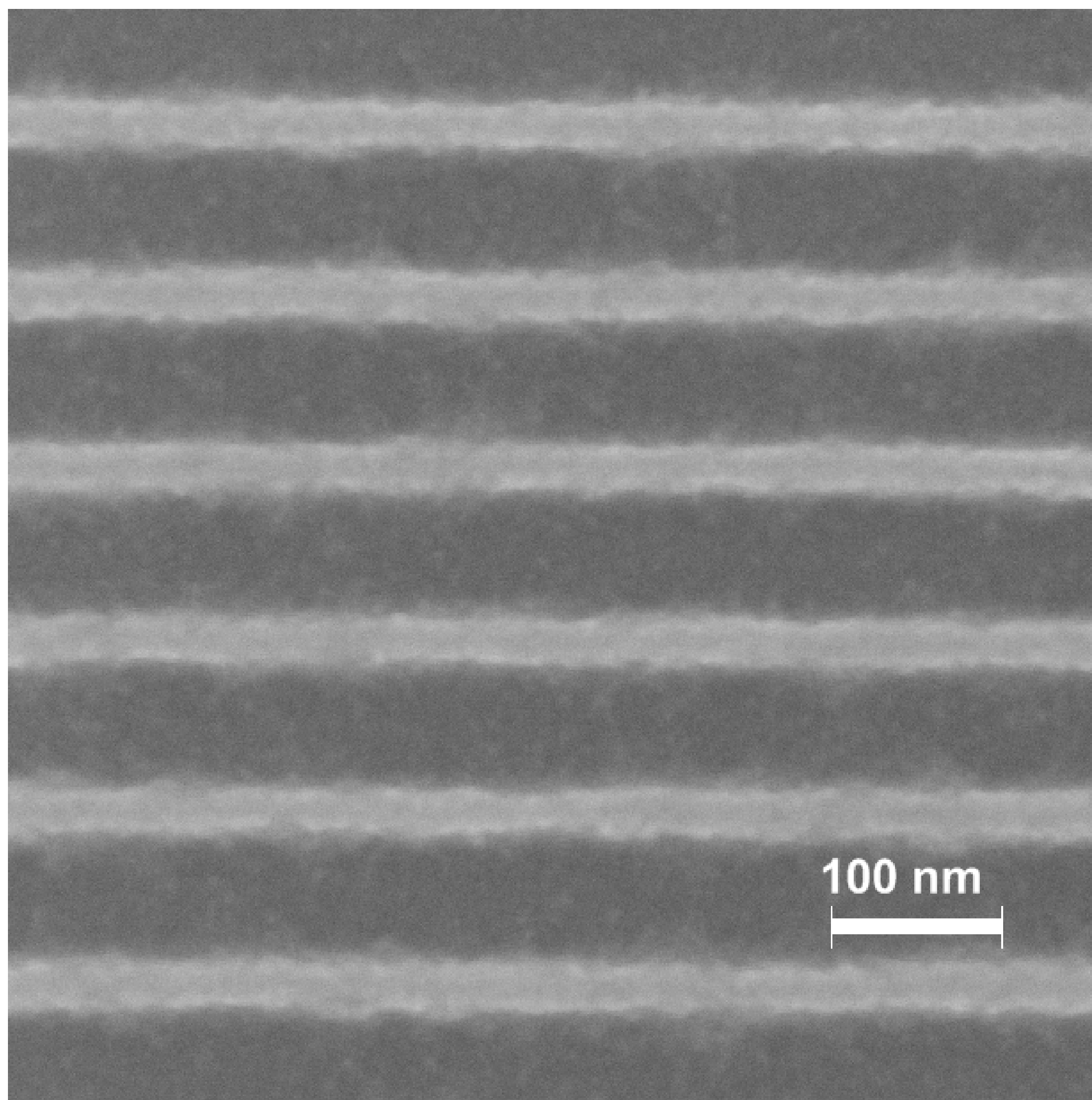

Figure 4-6. SEM of 28-nm lines printed on a 100 nm period at a dose of 50 μC/cm^2 with a 30 keV electron beam. The three sigma line edge roughness of these features is 4.6 nm.

CHAPTER 5

PATTERNING OF SOLUTION DEPOSITED TITANIA

Abstract

A system for the solution deposition of high-quality TiO_2 films is found to be directly patternable. This system is sensitive to UV and electron-beam exposures. The sensitivity and contrast to electron beam exposure is reported.

Introduction

A novel chemistry allowing high quality TiO_2 thin films deposited from aqueous titanium-peroxo solutions via spin coating has previously been reported [1]. This system enables the deposition of anatase TiO_2 films at temperature as low as 250 °C as seen in X-ray diffraction patterns in Figure 5-1. Scanning Electron Microscope (SEM) images demonstrating the high quality of these films can be found in Figure 5-2. A unique property of this chemical system is that it enables direct patterning of TiO_2, a significant advance for the integration of TiO_2 into functional devices. Previously high quality patterned TiO_2 films could only be obtained by etching. TiO_2 can be wet etched with boiling H_2SO_4 or a HF/NH_4F mixture [2]. Dry etching of TiO_2 is possible but it requires high power inductively coupled plasma reactive ion etching [3]. Such processing, however, does not offer any significant etch selectivity over any traditional substrate material. Without an etch stop layer, patterning by dry etching needs to be tightly controlled to ensure complete removal of the TiO_2 and prevent significant etching of the substrate.

Direct patterning of TiO_2 can also be obtained with Titanium n-butoxide derived sol-gels.[4, 5] These sol-gels have been employed as a directly patterned hardmask for the transfer of patterns to compound semiconductors and for deep etching of silicon. These patterned sol-gel films have not been used to provide functional TiO_2. As we have previously shown, our system generates TiO_2 of a superior quality to that derived from a sol-gel. While sol-gel systems, employed as resists, have demonstrated high resolution patterns, they do so at doses greater than competing resists like

hydrogen silsesquioxane.[6]

Experimental

To prepare precursor solutions, 8 mL of a 0.64 M aqueous solution of ammonium bis(oxalate)oxotitanate (99.998%, Alfa Aesar) or titanium oxide sulfate (Alfa Aesar) was rapidly combined with 8 mL of 4 M NH_3•H_2O (29.3%, Mallinckrodt Chemicals). The resulting precipitates were centrifuged and repeatedly washed with deionized water to remove $C_2O_4^{2-}$ or SO_4^{2-} counter-ions and ammonia. Ultra pure, 18-MΩ, water was used for the preparation of all solutions. The precipitates were then dissolved in 6 mL concentrated H_2O_2 (29.0-32.0%, Mallinckrodt Chemicals) at 5 °C. This resulted in an orange-colored solution with pH=3. The acidic precursor is stable for approximately one day at 5 °C. As the solution ages, the pH rises and the color changes from orange to yellow, eventually leading to the formation of transparent gels.

The basic precursor solution with pH=10 was obtained by adding 2 mL of 8M NH_3•H_2O to a freshly prepared acidic precursor solution and mixed quickly. The color of the basic precursor solution is yellowish green. The precursor solution is stable for 3-5 days at 5 °C; beyond this time precipitation was observed.

Thin films were cast from spin coating the precursor solution. Spin coating was conducted immediately after the precursor solutions were prepared. Silicon substrates with a coating of 200 nm thermally grown SiO_2 were used. The substrates were cleaned by ultrasonic agitation in Decon Labs, Contrad-70 solution at 45 °C for 60 min, followed by a thorough rinse with deionized water before deposition. A thin film

of TiO_2 was deposited on the substrate by spin coating at 3000 rpm for 30 s, followed by immediate hot-plate polymerization at 80 °C for 1 min. This procedure was repeated until the desired thickness was obtained. The typical film thickness with 0.45 M Ti solution was ~ 18 nm for one deposition cycle.

For patterning purpose, TiO_2 thin films were deposited from the basics precursor with two deposition cycles, between which an 80ºC curing temperature was applied. The acidic precursor solution was not used due to a higher required between coat cure temperature. Photolithographic patterning of TiO_2 was achieved by exposing films through a chrome-on-fused-silica mask, placed in contact with the films. The exposure source was an Oriel Series Q 30-W deuterium lamp with an exposure time of 1 to 3 min. Electron beam exposures were conducted at 30 keV beam voltage on a Zeiss Ultra FEG SEM with a Nabity lithography system. The images were developed by immersion in 6 M HCl for 3 min, which removed the regions that were not exposed to light or electron beam. After patterning the films were annealed at 300 °C for 5 min to fully cure them. Atomic Force Microscope (AFM) images were collected on an Asylum Research MFP-3D AFM.

Results and Discussion

patternes generated from exposure to UV light over a range times are displayed in Figure 5-3. It can be observed from these images that after development more material is present in the exposed areas when exposed for 2 min in comparison to a 1 min exposure. The increase in thickness can be marked by a change in the color of

the patterned area. There is no significant color change in the main exposed region when comparing 2 and a 3 min exposure. This indicates that the minimum exposure time for retention of maximun material is approximately 2 min for these exposure conditions.

An additional example of photo-patterning TiO_2 films can be found in Figure 5-4. Upon development, TiO_2 forms a negative image of the applied exposure. The smallest feature on the mask used was 3 µm, cf., Fig. 5-4. It can also be seen in Figure 5-4 that the edges of features are not abrupt. The faint yellow outline present around all features indicates that this material is functioning at a low contrast.

The photolithography setup employed does not allow for the accurate determination of sensitivity or contrast. To generate a more quantitative view of sensitivity and contrast, TiO_2 films were exposed with an electron beam. An AFM of an exposed pattern can be found in Figure 5-5, showing significant blurring of the exposed pattern. This maybe due in some part, to the low contrast of pattern formation for this TiO_2 precursor. Following these expariments, however, we were informed that the lithography system was not operating properly. Similar patterns formed at the same time with highly developed resists exhibited a similar image degradation. When equipment has been working properly these systems have generated far superior results. The pattern in Figure 5-5 can be used to generate a contrast curve and to calculate a sensitivity, but at the time this pattern was made, the lithography tool was not capable of testing the resolution of the present precursor.

The contrast curve generated from these data is displayed in Figure 5-6. This

contrast curve exhibits a contrast of 0.5 and a sensitivity of 1.1 mC/cm^2. This contrast is very low, and the shape of the curve indicated that the material may not be etched fully to the substrate. A stronger developer is required to improve the contrast and etch fully through the film. The sensitivity of this material to electron beam exposure is unfortunately quite low, and increasing the strength of the developer will have a negative impact on the sensitivity of the film. To improve both contrast and sensitivity at the same time will require improvements to the processing conditions for the film. The film patterned by electron beam experienced a long delay, >12 hrs, between deposition and all subsequent processing. Minimizing this delay will have a positive influence on patterning properties. The film was heated to 80 °C after deposition of each layer allowing multiple layers to be deposited. Limiting the film deposition to a single layer and removing this annealing step will also likely have a positive influence on both contrast and sensitivity. However, the trade off in depositing a single layer would be a limitation to the thickness available for functional applications.

The multilayer deposition and subsequent patterning demonstrate significant differences between the TiO_2 and HafSOx/ZircSOx systems. We have demonstrated that the TiO_2 can be patterned after deposition of multiple layers, opening the possibility of patterning much thicker films. HafSOx and ZircSOx have not yet demonstrated the ability to be patterned in more than a single layer. This limits the thickness of HafSOx/ZircSOx that can be patterned to the thickness that can be deposited in a single layer.

Conclusion

These results demonstrate the application of this material system as a directly patterned functional material. The direct patterning of this material negates the use of a photoresist and removes the need for a high power RIE step. This simplifies the integration of this material into future applications. The patterning process that has been demonstrated has significant potential for future processing with multiple avenues for optimization.

References

[1] K. Jiang, D. Keszler, J. Tate, D. McIntyre , J. Stowers, A. Zakutayev, In Press, (2008).

[2] P. Walker, W.H. Tarn, *CRC Handbook of Metal Etchants*, 1st ed., CRC, 1990.

[3] S. Norasetthekul, P.Y. Park, K.H. Baik, K.P. Lee, J.H. Shin, B.S. Jeong, V. Shishodia, E.S. Lambers, D.P. Norton, S.J. Pearton, Applied Surface Science, 185 (2001) 27-33.

[4] W. Hu, K. Sarveswaran, M. Lieberman, G.H. Bernstein, J. Vac. Sci. Technol. B, 22 (2004) 1711-1716.

[5] M. Saifullah, K. Subramanian, E. Tapley, D. Kang, M. Welland, M. Butler, Nano Lett., 3 (2003) 1587-1591.

[6] A.E. Grigorescu, M.C. van der Krogt, C.W. Hagen, P. Kruit, Microelectronic Engineering, 84 (2007) 822-824.

Figures

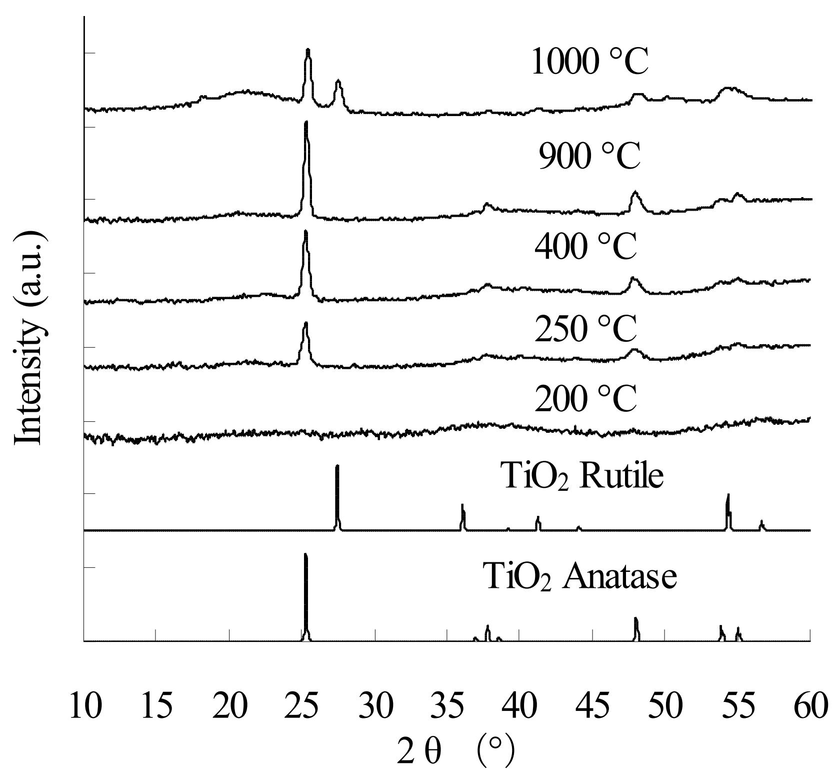

Figure 5-1. XRD patterns of TiO_2 films annealed at different temperatures.

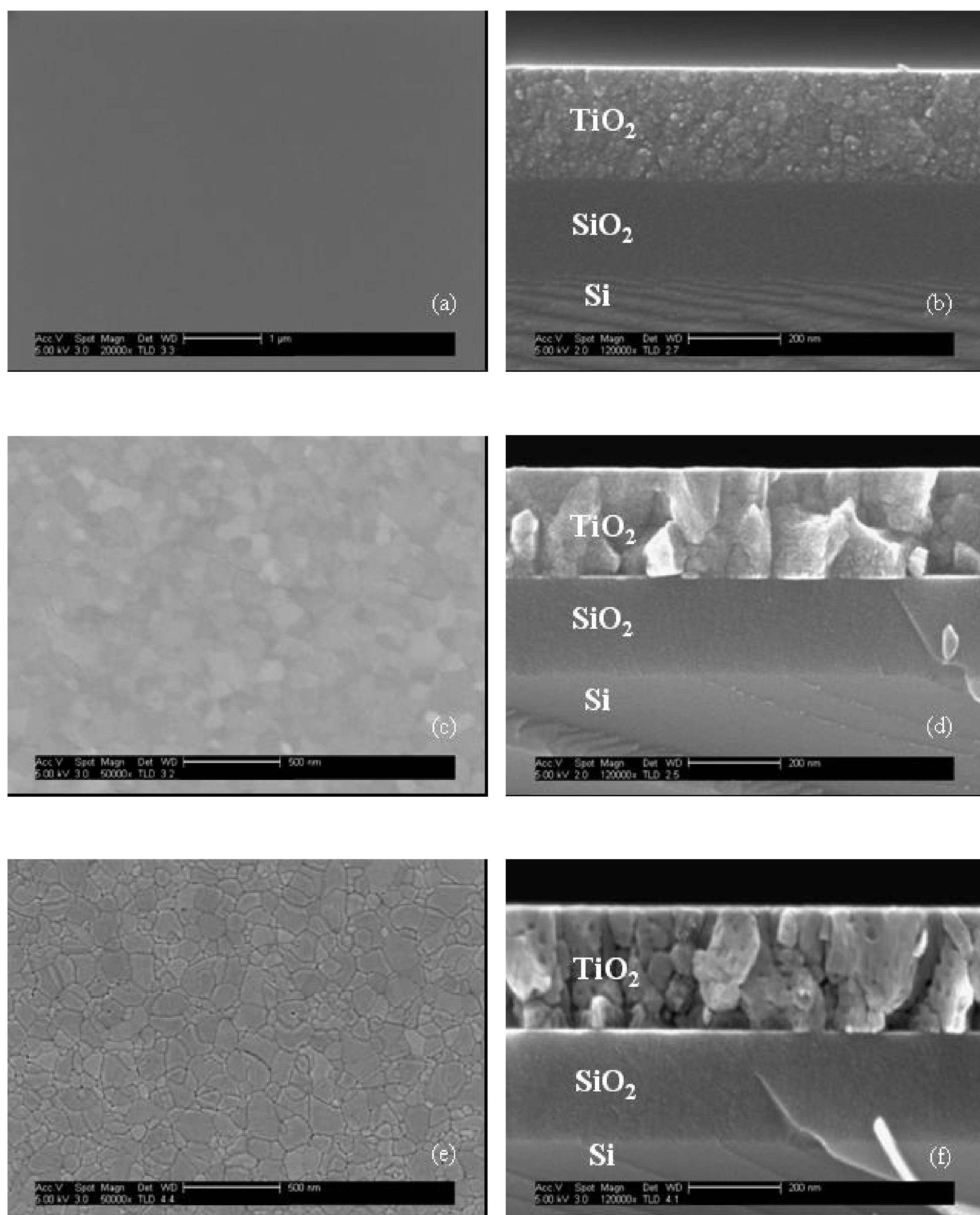

Figure 5-2. SEM images of TiO_2 thin films deposited from acidic precursor solution with (a) (b) 200 ºC, (c) (d) 300 ºC and (e) (f) 500 ºC final anneal.

Figure 5-3. Patterned TiO_2 films with exposure times of a) 1 min, b) 2 min, and c) 3 min.

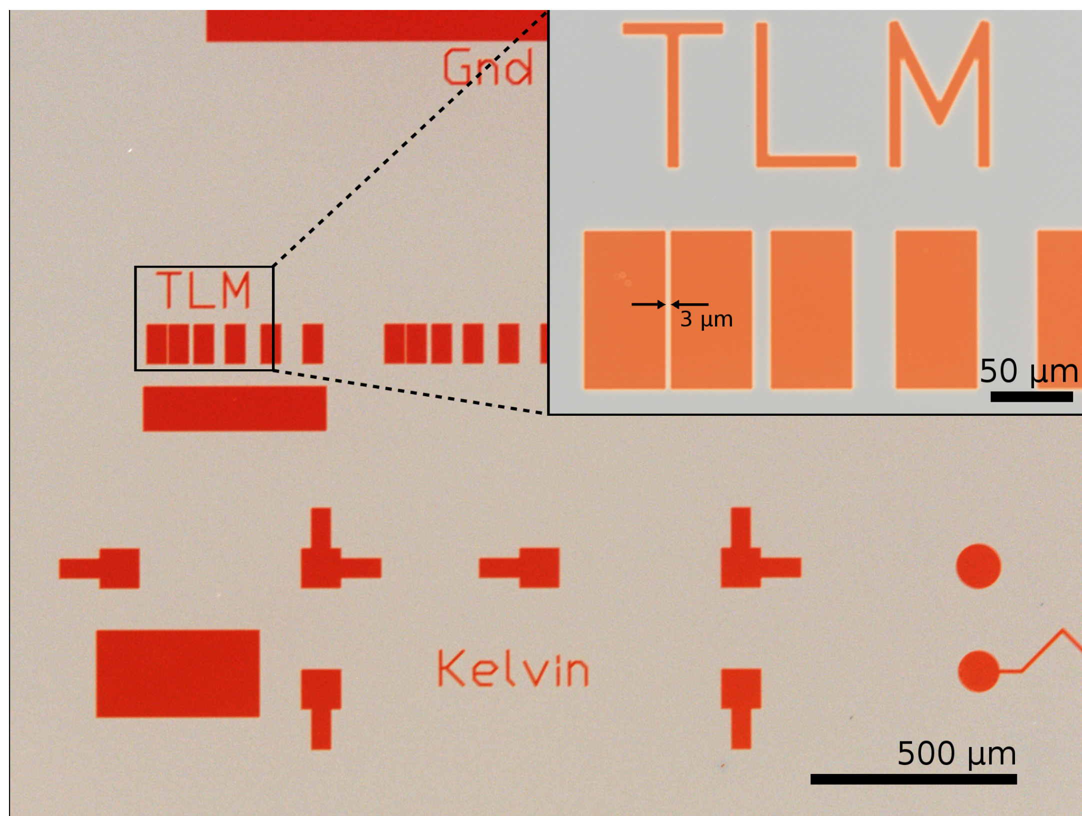

Figure 5-4. Photolithographically patterned TiO_2. The darker regions are TiO_2, while the light region is the substrate.

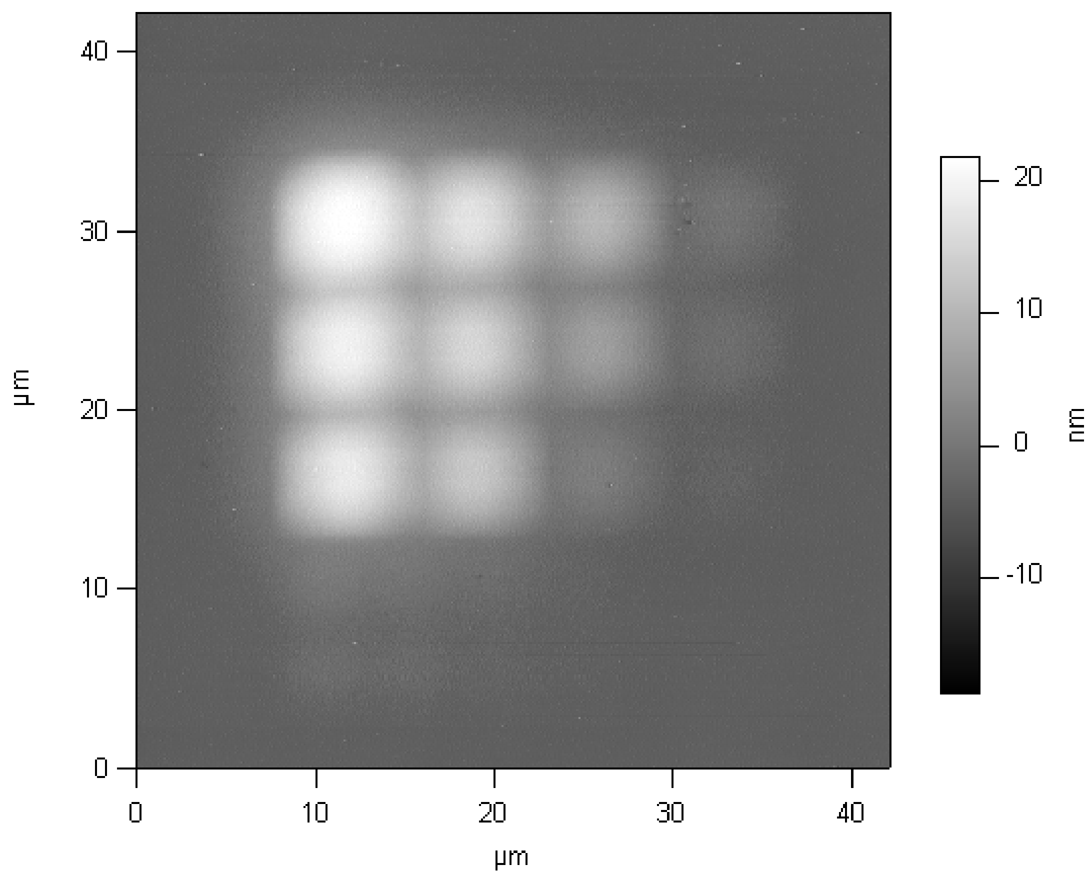

Figure 5-5. AFM image of an electron beam lithography pattern. The pattern has a 4x3 grid of exposure doses. The doses range from 678 μC/cm^2 in the upper left to 7 μC/cm^2, barely visible, in the lower right.

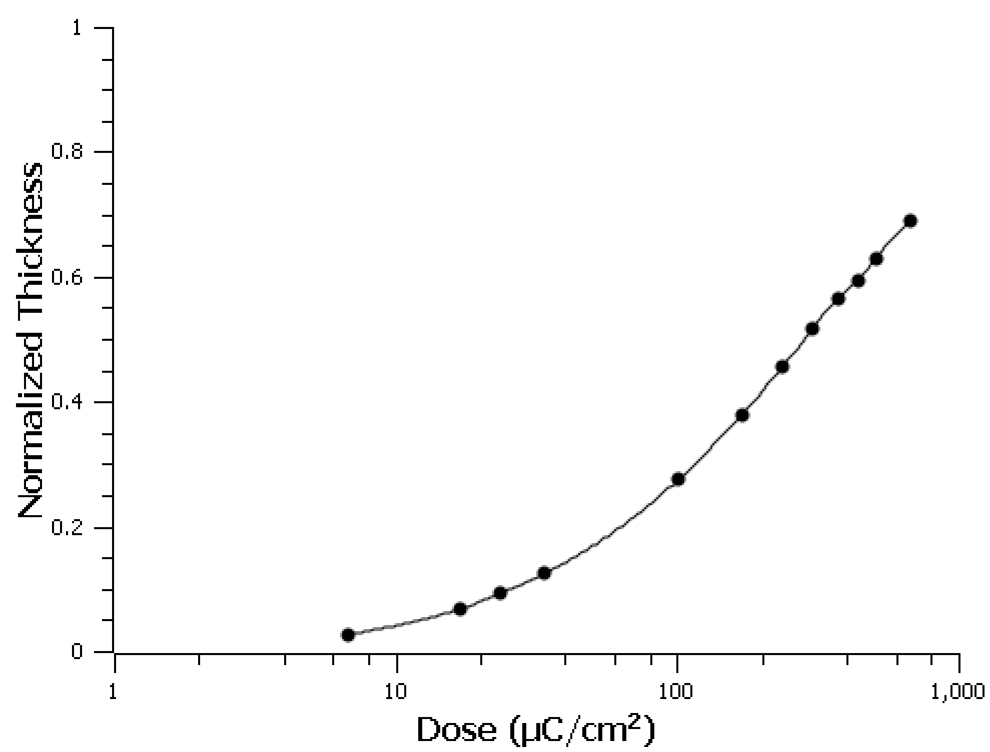

Figure5-6. Characteristic contrast curve for electron-beam exposure of TiO_2 precursor film.

CHAPTER 6

SOLUTION DEPOSITION AND SOLID STATE MODIFICATION OF MOLYBDENUM OXIDES

Abstract

A system for the direct patterning of peroxopolymolybdate has been developed. Features as small as 3 μm have been defined with photolithography. Annealing films in air results in MoO_3. In a reducing atmosphere, the films are converted to conductive and transparent MoO_2.

Introduction

Directly patterned metal oxides can be used as resists in lithographic processing. In this application, they have exhibited better resolution and etch resistance than polymer resists [1, 2]. Focusing on evaluating these metal oxides by just the metrics used to evaluate polymer resists limits the potential application for these materials. A directly patterned metal oxide can be used to transfer a pattern to a substrate just as a polymer resist, but the metal oxide also serves a functional purpose by itself. Depending on its physical properties, a metal oxide can be used as a dielectric, semiconductor, or conductor. Directly patterned metal oxides have even greater flexibility than a polymer resist. Considering that after a metal oxide is patterned, the physical properties can be drastically modified by conversion of the oxide through solid state chemical methods. We demonstrate here the direct patterning of a metal oxide and a method to convert that metal oxide from a semiconductor to a conductor.

Peroxopolytungstate has been previously examined as a directly patternable metal oxide. This material exhibited sensitivity to UV light, electrons, and x-rays [1]. After processing, WO_3 is a semiconductor that has functional application in gas sensors [3], as an electrochromic material [4], and passive application in optical wave guides [5]. Solid state chemical modification has been employed to modify directly patterned WO_3. After the patterning process, WO_3 was subject to high temperatures in flowing H_2 resulting in a directly patterned W metal film [6].

The chemistry of the molybdenum analog, peroxopolymolybdate, is quite similar to that of peroxopolytungstate. The MoO_3 that results from the thermal decomposition

of peroxopolymolybdate has been well characterized [7, 8] and finds use in electrochromic applications [9]. Though the chemistry of these two peroxopolymetalates is similar, surprisingly, patterning of the molybdenum analog has not previously been reported. We report here the direct patterning of peroxopolymolybdate by photolithography. As a resist, this material does not perform as well as the peroxopolytungstate, but as a directly patterned oxide, the molybdenum system allows access to materials with interesting properties. In conjunction with this patterning process, we report a method for the conversion of peroxopolymolybdate films to MoO_2.

MoO_2 is potentially far more useful in electronic applications than MoO_3, the standard decomposition product of peroxopolymolybdate. While the trioxide is a poorly performing semiconductor, the dioxide is a metallic conductor [10]. The conductivity arises from Mo d-orbital overlap and strong covalent mixing with oxygen s and p orbitals. MoO_2 has a monoclinic distorted rutile-type structure with Mo atoms grouped in pairs along the *c* axis. The Mo couplet is tilted in the [100] direction and has a short Mo-Mo distance of 2.51 Å. Single crystal MoO_2 has exhibited a resistivity of 8.55×10^{-5} Ω cm. Thin films of MoO_2 have been deposited by numerous methods, including DC magnetron sputtering [11, 12], pulsed laser deposition [13, 14], chemical vapor deposition [15], electrochemical deposition [16], and thermal evaporation [17]. The conductivity of MoO_2 is great enough that very thin films can retain a reasonably low sheet resistance. The absorption of light in the visible spectrum by MoO_2 is also low enough that very thin films would exhibit a reasonable transparency. These two

properties allow application of very thin films of MoO_2 as directly patterned transparent conductors.

As a transparent conductive oxide (TCO) MoO_2 would need to out perform the standard material for this application, Indium Tin Oxide (ITO). The properties of ITO vary with processing conditions but typical values are an electrical resistivity of 0.2 mΩ cm, a hall mobility of 25 cm^2/VS, a carrier concentration of 1×10^{21} cm^{-3}, and a transparency of 85% over the visible spectrum [18]. An alternative to ITO would be desirable because of the high cost of materials and the necessary use of vacuum deposition equipment. If a direct performance advantage can not be found with MoO_2, it may still be possible to find application with a cost advantage.

Experimental

Precursor solutions for spin coating were prepared in a method similar to that found in the literature [9]. Solutions of peroxopolymolybdate were prepared by slowly adding 7.2 g of Mo powder (Alfa Aesar, 3-7 μm, 99.95 % metals basis) to 50 mL of 30% H_2O_2 (Mallinckrodt) that is maintained in an ice bath. This resulted in a strongly acidic solution, orange in color with a small amount of dark blue precipitate. The solution was filtered and stored under refrigeration, resulting in solutions with Mo concentrations of 1.3 M. Using this solution, films were made by spin coating at 3000 rpm for 30 seconds. Highly doped n-type conductive silicon was used for substrates for X-ray diffraction (XRD) analysis and Scanning Electron Microscope (SEM) imaging. Corning 1734 glass was used for electrical and optical measurements. Due

to softening of the corning glass, fused silica was substituted as a substrate for anneal temperatures above 600 °C. The substrates were prepared for spin coating by sonication in Decon Labs, Contrad 70 at 45°C for 60 min. It should be noted that a less concentrated solution can be prepared but requires that excess peroxide be catalytically removed with activated platinum.

Patterning of peroxopolymolybdate was achieved by exposing films through a contact mask. The exposure source was an Oriel Series Q 30-W deuterium lamp with an exposure time of 10 min. The pattern was developed by immersion for 2 min in a mixture of absolute methanol and ethylene glycol at a ratio of 1:3, followed by a rinse in isopropanol, and drying in a stream of Ar (g).

Reduction of the films and patterns was carried out in flowing H_2/Ar (5% H_2) at temperatures of 400 – 700ºC. Ramp rates were 7ºC/min with a 10 or 30 minute dwell time. X-ray diffraction (XRD) analysis on the thin films was performed on a Rigaku R-axis Rapid with Cu Kα radiation. The incident beam angle was 7.6°, while the diffracted beam was collected with an image plate. Powders for thermogravimetric analysis (TGA) were prepared by drying solutions at room temperature under flowing Ar. TGA data was collected with a Shimadzu TGA-50 by heating samples (10–20 mg) in a Pt crucible under flowing Ar, at a rate of 5 °C/min. Electrical conductivity and Hall mobility were measured at room temperture by using the Van der Pauw configuration [19, 20] on a Lakeshore 7504 Hall measurement system at fields of 17-20 kG with field reversal. Optical transmission was measured using a Ocean Optics HR4000 spectrometer and Ocean Optics DH-2000-BAL lamp.

Results and Discussion

Because deposited films are completely soluble in water until annealed to 175ºC for 30 s, identifying an appropriate developer made pattering more difficult.. The films dissolve more slowly in water as the anneal temperature is progressively increased above 175ºC. At an anneal of 300ºC for 30 s the film becomes insoluble in water. These temperatures are not compatible with the patterning process. For this reason a non-aqueous developer was explored. We found that unannealed films were slightly too soluble in methanol and not sufficiently soluble in ethylene glycol. It was determined that a mix of these two solvents would be tunable to a appropriate developer strength for optimal patterning. The ratio of 1 part methanol to 3 parts ethylene glycol was found to be an effective developer. A volatile non-aqueous residue free rinse was needed to halt the development process. Isopropanol was found to be an effective rinse. An example of photolithographic patterning of peroxopolymolybdate can be found in Figure 6-1.

Before attempting to reduce this material it is beneficial to understand how peroxopolymolybdate behaves upon annealing in air. XRD data were collected from as deposited films and films annealed at 325ºC and 600ºC for 5 min, the data in Figure 6-2. As-deposited, the film exhibits a faint nano-crystalline MoO_3 x-ray pattern. MoO_3 is clearly represented in the patterns for 325ºC and 600ºC. In both cases, preferential orientation is evident and is visible at 325ºC as a diminishing of the (021) reflection at 27.4º 2θ and at 600ºC as strong reflection from the (0*k*0) family of peaks

at 12.8º and 25.7º 2θ.

The orientation found in the XRD data for films annealed in air is reflected in SEM images. Rod like structures are visible in an SEM image of a film annealed at 325 ºC in air, Figure 6-3. To generate the orientation evident in the XRD data, these rods have to be grown in the (021) direction, thus placing the (021) reflection in plane. An SEM image of peroxopolymolybdate annealed at 600ºC in air can be found in Figure 6-4. Considering the strength of the (0*k*0) reflections, the obvious plate like structures must be presenting the (0*k*0) face parallel to the plane of the substrate. The disconnected nature of these plates likely arises from the high vapor pressure and sublimation of MoO_3 at 600 ºC.

The decrease in solubility over the temperature range 175 to 300 ºC coincides with features found in the thermogravimetric analysis. Thermal Gravimetric Analysis (TGA) data for peroxopolymolybdate can be found in Figure 6-5. Powders for TGA were prepared from three solutions that varied in age; 3 months, one week, and freshly prepared. Due to aging of the solution, it was expected that these solutions would vary in the peroxide concentration. The TGA curves have been normalized to a final mass of 1 to enable run to run comparison. The initial mass loss occurring upto 170ºC is associate with dehydration, while the sharp mass loss initiated around 178ºC is likely due to decomposition of peroxide. It is possible that this second mass loss is associated with loss of tightly bound water. A final mass loss at 280ºC is associated with the loss of excess oxygen upon crystallization of MoO_3.

Determining if the second mass loss is associated with the decomposition of

peroxide could be done with Thermally Programmed Desorption (TPD). TPD employs a mass spectrometer to identify the desorbate at each temperature of the TGA curve. This technique is not available to us, but TPD analysis has been performed on the tungsten analog, peroxopolytungstate [21, 22]. The amorphous peroxopolytungstate desorbs O_2 associated with the decomposition of peroxide at 137ºC. The crystalline peroxopolytungstate desorbs O_2 at 170ºC. Considering the similarities between the tungsten and molybdenum systems, it is reasonable to assume that the mass loss in question is due to decomposition of peroxide.

Due to the presence of MoO_3 found by the XRD analysis in peroxopolymolybdate films, it was decided to minimize the thermal treatment of the films prior to attempting to reduce them. Films were spin coated and were promptly placed in the reducing furnace. While an anneal would remove residual water in the film, it was preferred to minimize the growth of any existing MoO_3 nucleation sites. XRD patterns of films from varying reduction temperatures can be found in Figure 6-6. At 400ºC the XRD pattern exhibits predominantly Mo_4O_{11} with a small amount of MoO_3. Mo_4O_{11} is an intermediate phase in the reduction of MoO_3 to MoO_2 [23]. At 450ºC the XRD exhibits a weak MoO_2 pattern. At 700ºC the XRD pattern is strongly MoO_2. Based on these results, 450ºC was selected for longer anneals.

The influence of peroxide on the reduction to MoO_2 also needs to be considered. It was theorized that the reduction of Mo^{6+} to Mo^{4+} was inhibited by the presence of peroxide, an oxidizing agent. Furthermore, if the peroxide decomposition is thermally initiated at elevated temperatures, the nucleation and growth of MoO_3 will proceed

before the available H_2 can reduce the molybdenum. The reduction of a nucleated MoO_3 crystal will be kinetically unfavorable. To test this theory, films were halved and one part exposed to UV light for 10 min. Both halves of the film were then reduced in one anneal.

Exposed and unexposed films were reduced at 450ºC for 10 and 30 min. XRD data of the films can be found in Figure 6-7. In all cases the MoO_2 pattern is present. This pattern is stronger at 30 min than at 10 min and for exposed films in comparison to unexposed films. Though very faint, the MoO_3 (110) peak is visible in films reduced for 30 min. This peak location has been marked in Figure 6-7.

Resistivity, Hall mobility, and carrier concentration for various samples can be found in Table 6-1.

Table 6-1. Electrical data for peroxopolymolybdate films reduced to MoO_2

Reduction Temp.	Reduction Time	Exposed?	Resistivity [mΩ cm]	Carrier Density [1/cm³]	Hall Mobility [cm²/(VS)]
450	10	No	53.38	4.34×10^{22}	0.003
450	10	Yes	21.22	2.66×10^{22}	0.011
450	30	No	2.45	1.76×10^{22}	0.145
450	30	Yes	1.24	1.69×10^{22}	0.298

The effect the UV exposure and resulting increased crystallinity of MoO_2 is apparent. In the films reduced for 30 min, the effect of the exposure is less pronounced but electrical results are better overall. The lowest measured resistivity is greater than reported for single crystal MoO_2 by more than an order of magnitude. In all cases a small but positive Hall mobility is measured, indicating p-type behavior.

The film that was exposed and reduced at 450ºC for 30 min was also subjected to thermoelectric measurements. These thermoelectric data can be found in Figure 6-8. From this plot, a Seebeck coefficient of -4.94 μV/ºK was calculated, an unexpected result. Considering the Hall mobility and the resistivity, this value was expected to be small but positive. To reconcile this, it is necessary to recall that XRD determined a small amount of MoO_3 to be present in this film. MoO_3 has a Seebeck coefficient of -30 μV/ºK. Since MoO_2 is metallic and should have a very small positive Seebeck coefficient, it is theorized that the small amount of MoO_3 in the film is dominating the Seebeck coefficient and driving it negative. This theory will be tested by following the Seebeck coefficient in future films as the reduction process is optimized and conversion to MoO_2 is improved.

SEM images of the exposed and unexposed films reduced for 30 min emphasize the effect of the UV exposure, Figure 6-9 and Figure 6-10. There would appear to be two phases in each image. For the film exposed before reduction the lighter of the two phases is greater in area. This further emphasize that these films are not single phase MoO_2 and that the reduction process requires optimization. SEM analysis was also used to determine that film thickness was ~100 nm.

Optical transmission data for peroxopolymolybdate films reduced in flowing H_2 at 450ºC for 30 min can be found in Figure 6-11. The average transmission across the visible spectrum is 20% for the unexposed film and 24% for the exposed film. The films being produced at present are too absorbing for transparent applications. There remains several options to improve upon this result. Optimization of the reduction to

MoO_2 is expected to increase the transparency and lower the resistivity. A lower resistivity would enable a thinner film to provide the same sheet resistance while transmitting more light. The 100-nm thickness of the current films offers a significant available range for application of thinner films. This system demonstrates significant promise in generating a low cost alternative to ITO.

The patterning, deposition, and reduction process are still under development. It is promising that the exposure step required for patterning of films is beneficial to the reduction process. Future work will be directed at integrating these two process to produce patterned conductive films. As the reduction process is optimized, films with a higher mobility and lower resistivity are expected. It appears the greatest limitation of this system could be the limited transparency.

Conclusion

A system has been developed for the direct patterning of peroxopolymolybdate. Annealed in air, this system results in patterned MoO_3. Annealed in a reducing atmosphere of flowing H_2 the system converts to MoO_2. MoO_2 films exhibiting resistivity as low as 1.24 mΩ cm have been deposited. The transmission of these films is 24% over the visible spectrum and as film thickness is reduced this transmission will increase. This system represents a directly patterned transparent conductive oxide and demonstrates the versatility of solution deposited metal oxide thin films. These materials are amenable to chemical modification, providing access to a host chemical and physical of properties.

References

[1] H. Okamoto, T. Iwayanagi, K. Mochiji, H. Umezaki, T. Kudo, Appl. Phys. Lett., 49 (1986) 298-300.

[2] H. Namatsu, Y. Takahashi, K. Yamazaki, T. Yamaguchi, M. Nagase, K. Kurihara, J. Vac. Sci. Technol. B, 16 (1998) 69-76.

[3] A. Labidi, C. Jacolin, M. Bendahan, A. Abdelghani, J. Guerin, K. Aguir, M. Maaref, Sensors and Actuators B, 106 (2005) 713-718.

[4] J. Choy, Y. Kim, J. Yoon, S. Choy, J. Mater. Chem., 11 (2001) 1506-1513.

[5] K. Itoh, T. Okamoto, S. Wakita, H. Niikura, M. Murabayashi, Applied Organometallic Chemistry, 5 (1991) 295-301.

[6] H. Okamoto, A. Ishikawa, Appl. Phys. Lett., 55 (1989) 1923-1925.

[7] A. Klisinska, A.S. Mamede, E.M. Gaigneaux, Thin Solid Films, 516 (2008) 2904-2912.

[8] E. M. Gaigneaux, K. Fukui, Y. Iwasawa, Thin Solid Films, 374 (2000) 49-58.

[9] K. Hinokuma, K. Ogasawara, A. Kishimoto, S. Takano, T. Kudo, Solid state ionics, 53 (1992) 507-512.

[10] D.B. Rogers, R.D. Shannon, A.W. Sleight, J.L. Gillson, Inorganic Chemistry, 8 (1969) 841-849.

[11] S.H. Mohamed, O. Kappertz, J.M. Ngaruiya, T.P. Leervad Pedersen, R. Drese, M. Wuttig, Thin Solid Films, 429 (2003) 135-143.

[12] J. Okumu, F. Koerfer, C. Salinga, M. Wuttig, J. Appl. Phys., 95 (2004) 7632-7636.

[13] V. Bhosle, A. Tiwari, J. Narayan, Journal of Applied Physics, 97 (2005) 083539.

[14] R. Patil, M. Uplane, P. Patil, Applied Surface Science, 252 (2006) 8050-8056.

[15] S. Ashraf, C.S. Blackman, G. Hyett, I.P. Parkin, J. Mater. Chem., 16 (2006) 3575-3582.

[16] R. Patil, M. Uplane, P. Patil, Applied Surface Science, 252 (2006) 8050-8056.

[17] F. Chen, Y. Lin, T. Chen, L. Kung, Electrochem. Solid-State Lett., 10 (2007) H186-H188.

[18] H. Kim, J.S. Horwitz, G. Kushto, A. Pique, Z.H. Kafafi, C.M. Gilmore, D.B. Chrisey, J. Appl. Phys., 88 (2000) 6021-6025.

[19] L.J. van der Pauw, Philips Technical Review, 20 (1958) 220224.

[20] L.J. van der Pauw, Philips Res. Rep, 13 (1958) 1-9.

[21] H. Okamoto, A. Ishikawa, T. Kudo, Journal of photochemistry and photobiology. A, Chemistry, 49 (1989) 377-385.

[22] H. Okamoto, A. Ishikawa, T. Kudo, Journal of The Electrochemical Society, 136 (1989) 2646.

[23] E. Lalik, W. David, P. Barnes, J. Turner, J. Phys. Chem. B, 105 (2001) 9153-9156.

Figures

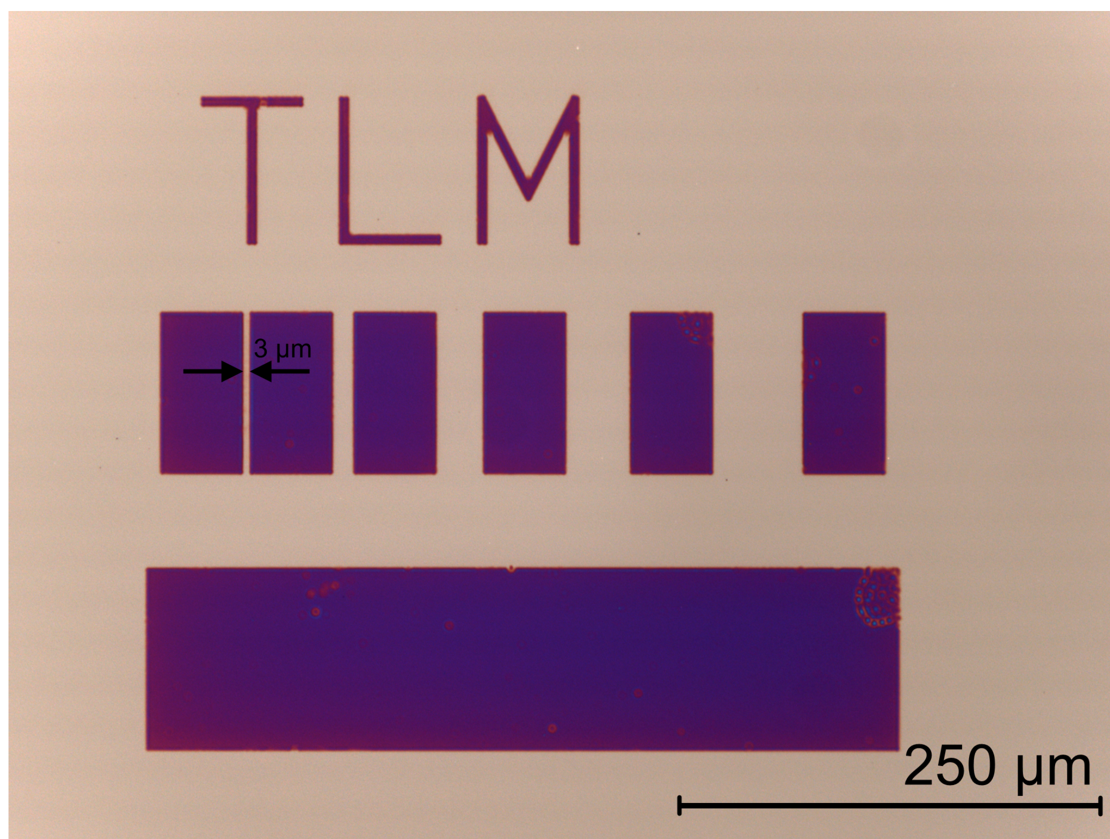

Figure 6-1. Optical image of photolithographically patterned peroxopolymolybdate. The dark region is the peroxopolymolybdate and the light region is the substrate. The smallest feature patterned, 3 µm, is noted on the image The defects, for example in the top right corner of the largest rectangle, are due to dust on the photomask shadowing the film.

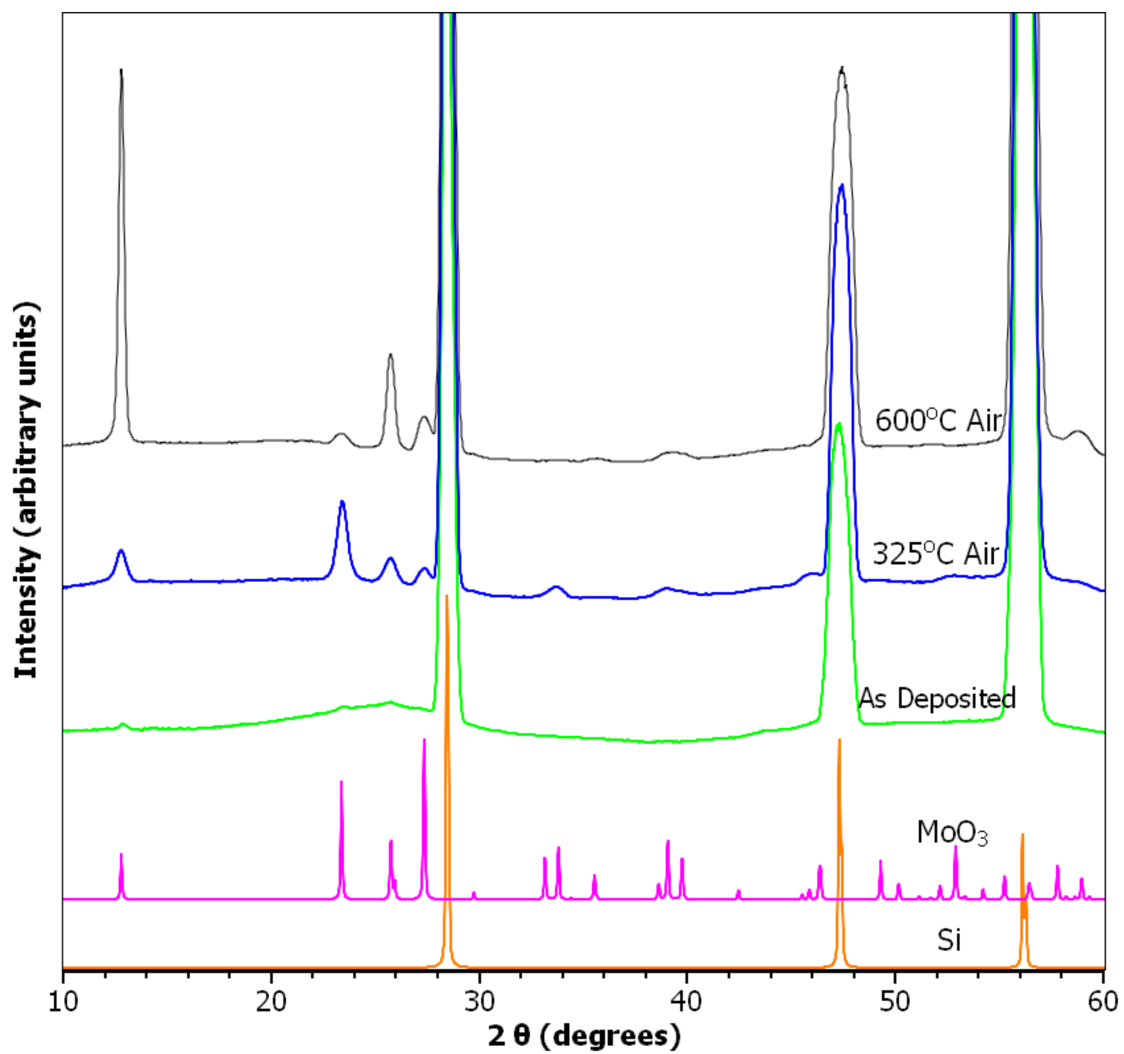

Figure 6-2. XRD data for peroxopolymolybdate films, as deposited and annealed in air to 325 and 600ºC. Reference patterns for MoO_3 and Si have been included.

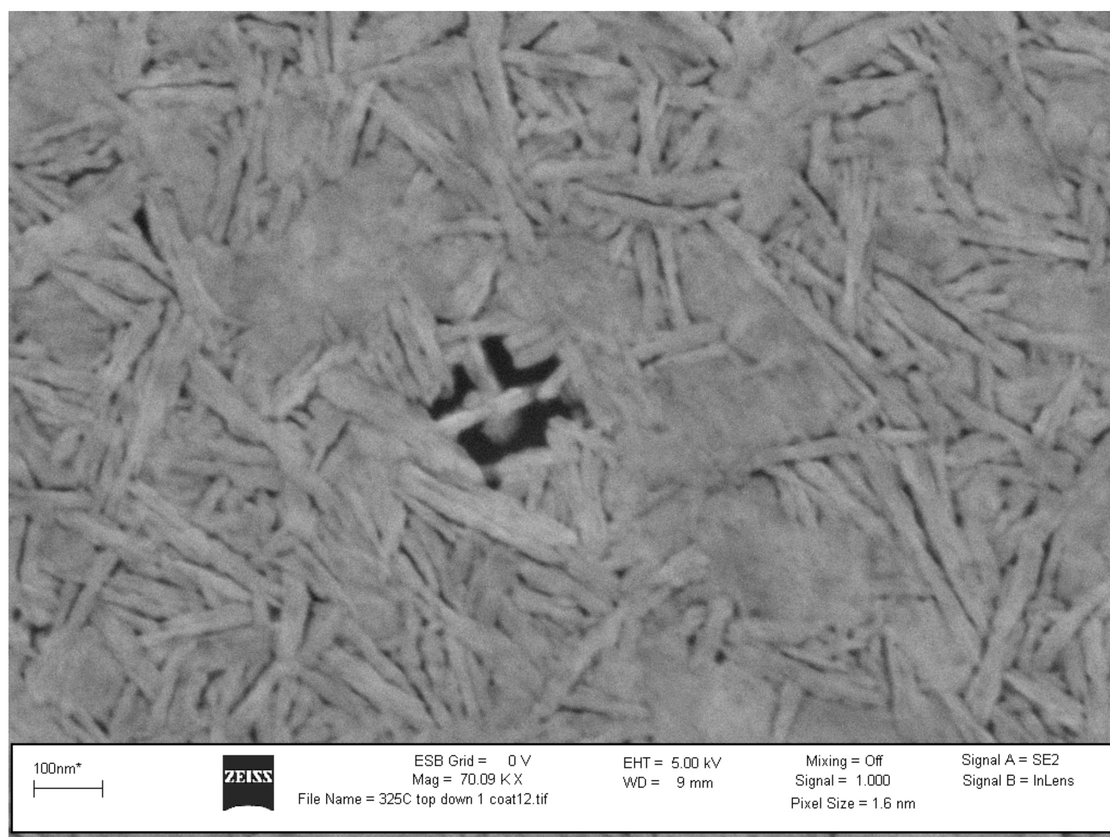

Figure 6-3. SEM image of an oriented MoO_3 film from a peroxopolymolybdate film annealed in air to 325ºC for 5 min.

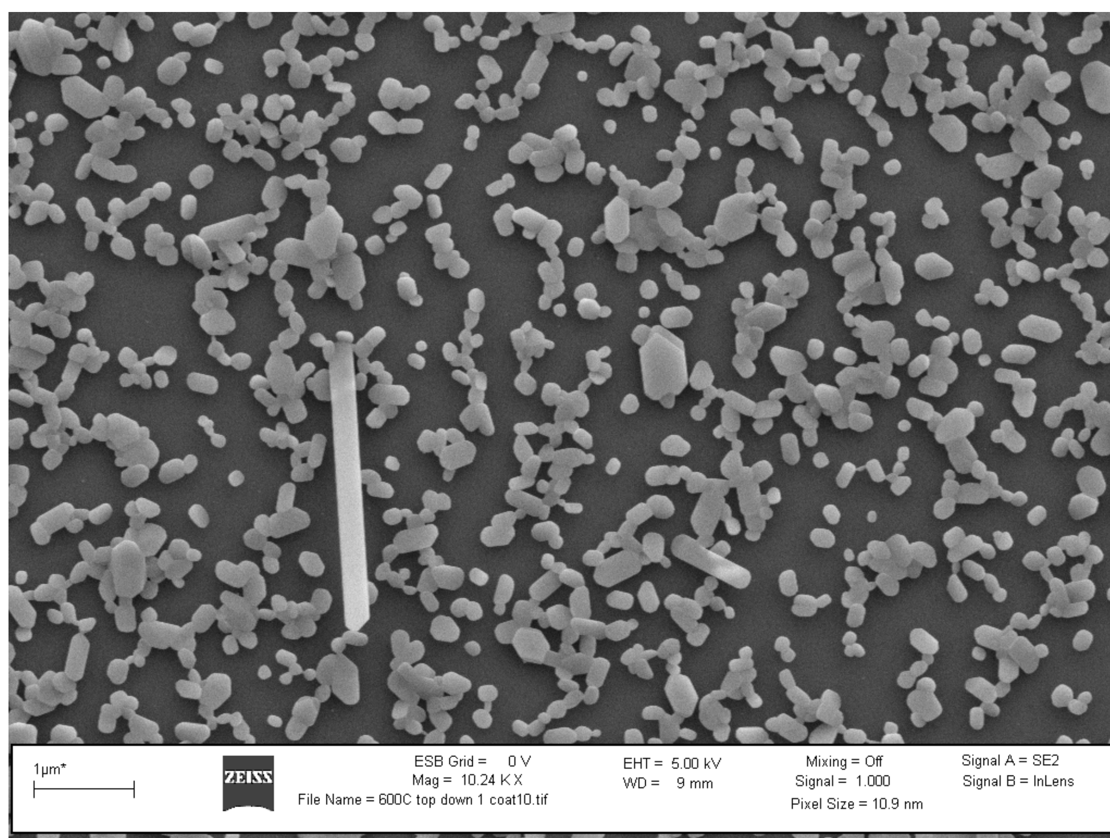

Figure 6-4. SEM image of an oriented MoO_3 film from a peroxopolymolybdate film annealed to 600ºC for 5 min in air.

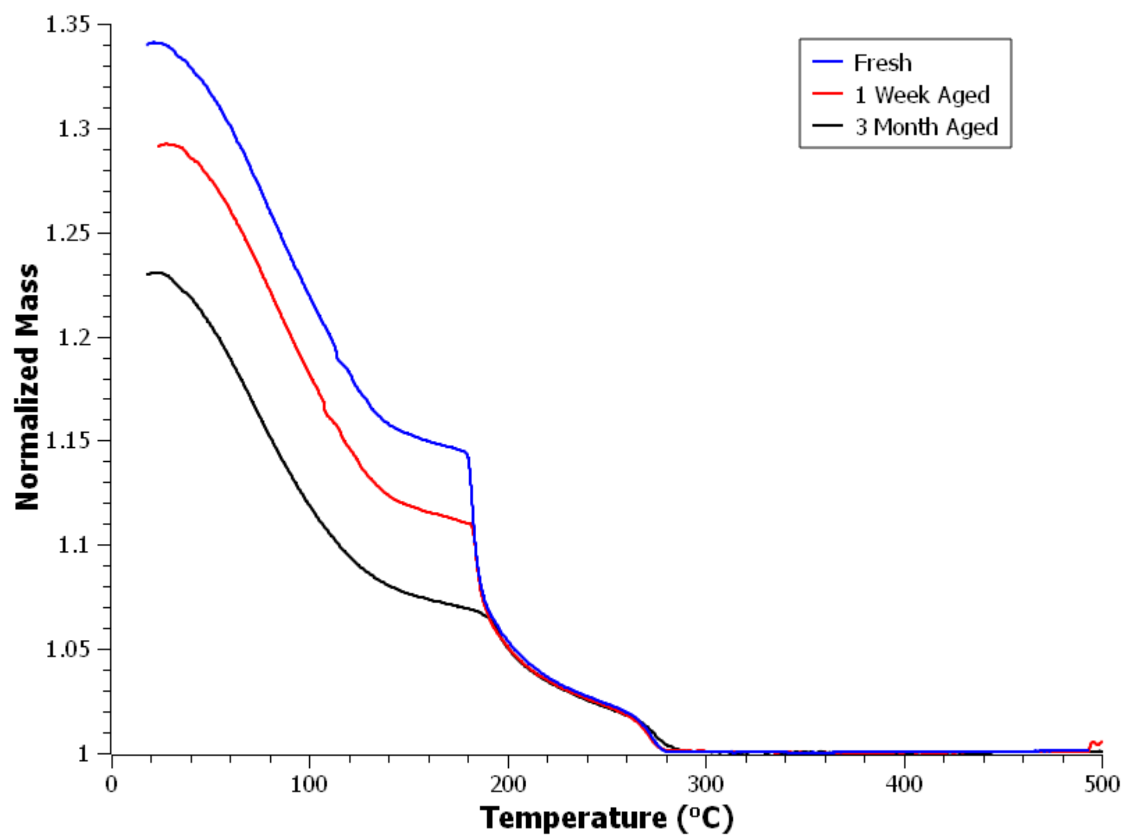

Figure 6-5. TGA data for peroxopolymolybdate powders prepared from solutions of three different ages. The mass of each run has been normalized to the final mass.

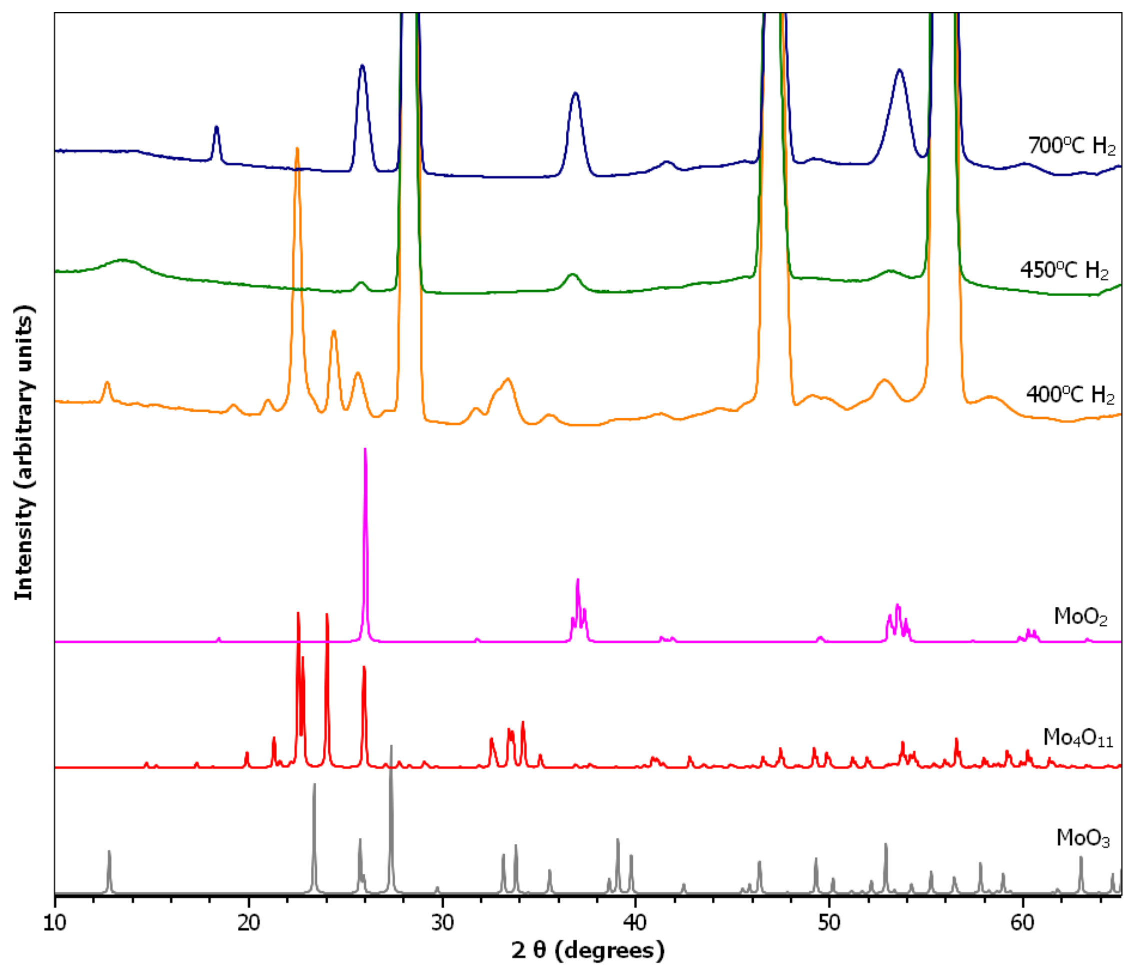

Figure 6-6. XRD of peroxopolymolybdate films reduced in flowing H2 at various temperatures. Reference patterns for MoO_3, Mo_4O_{11} and MoO_2 have been included.

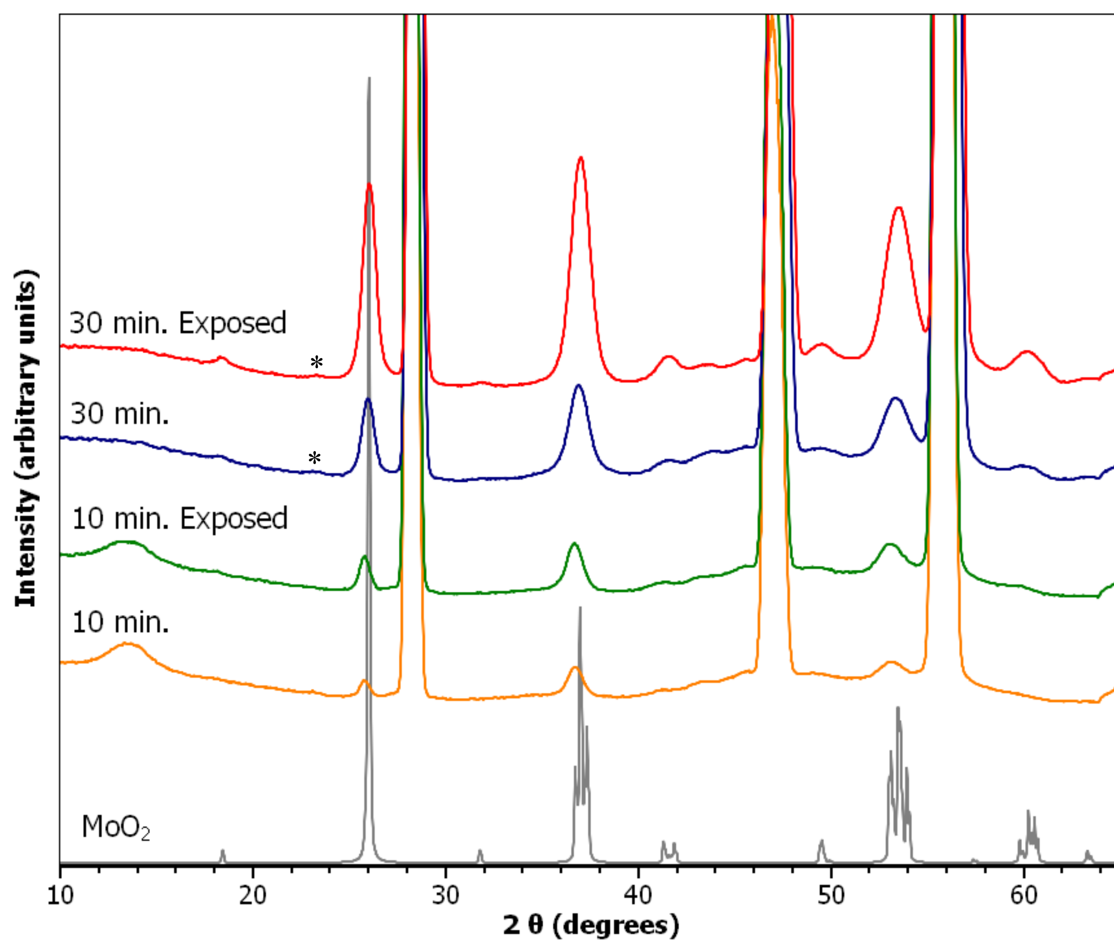

Figure 6-7. XRD of peroxopolymolybdate films reduced to MoO2 at 450ºC for 10 or 30 min. For each reduction time half of a film was exposed to UV light for 10 min. A very faint MoO_3 (110) peak can be seen in the 30 minute reduction patterns. This has been marked with *. The reference pattern for MoO_2 has been included.

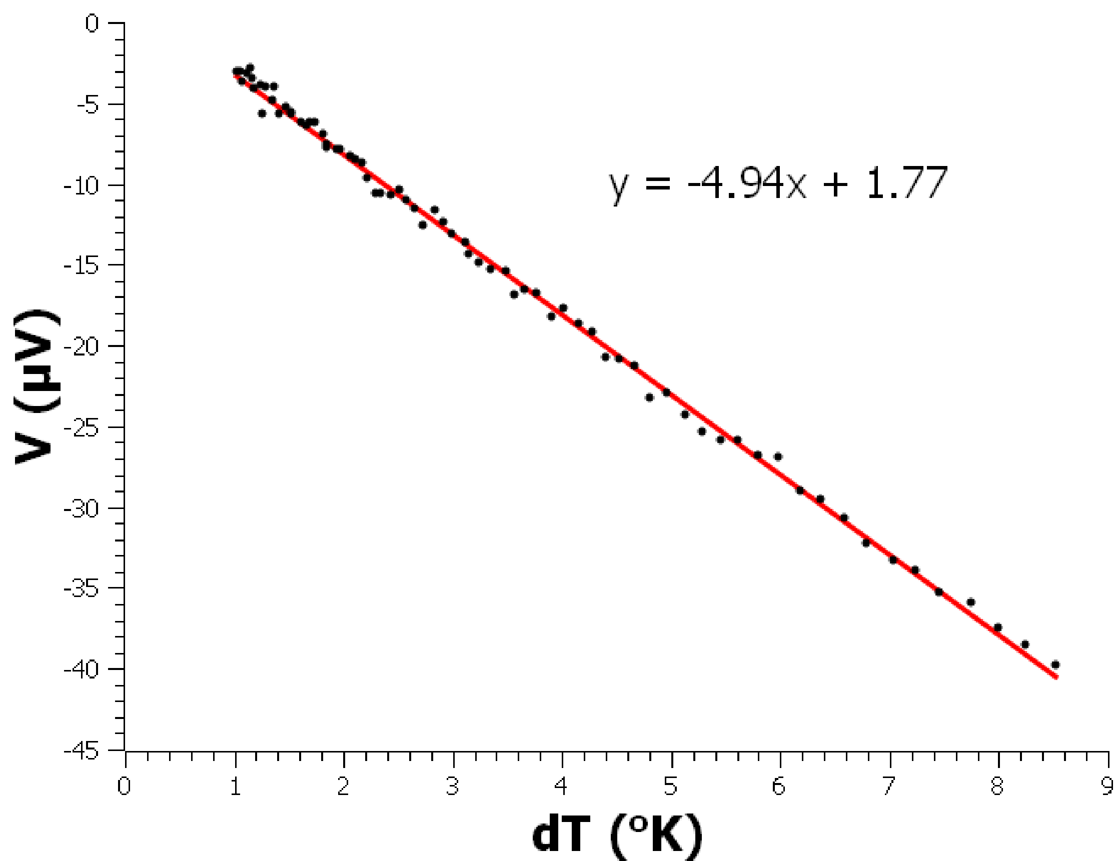

Figure 6-8. Thermoelectric data for a peroxopolymolybdate reduced at 450ºC for 30 min after an exposure to UV light for 10 min. The slope of this curve, -4.94 dµV/dºK, is the Seebeck coefficient for this film.

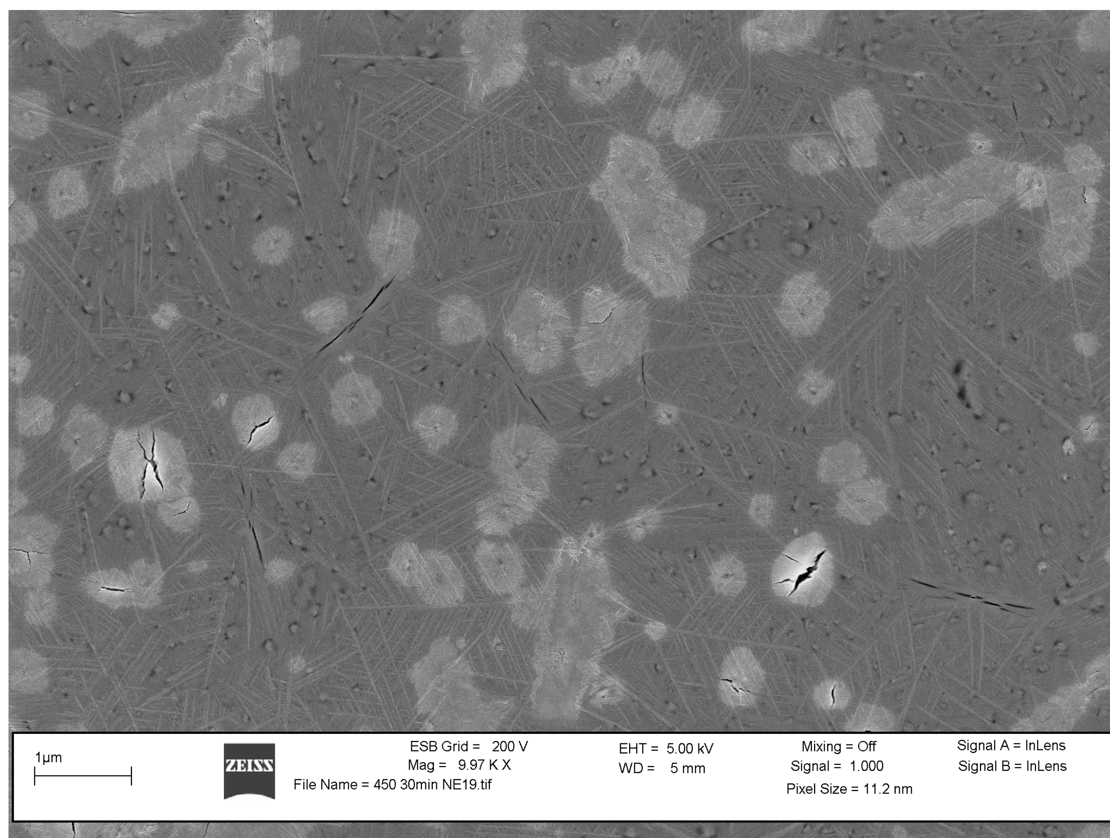

Figure 6-9. SEM image of peroxopolymolybdate after reduction at 450ºC in flowing H_2 for 30 min.

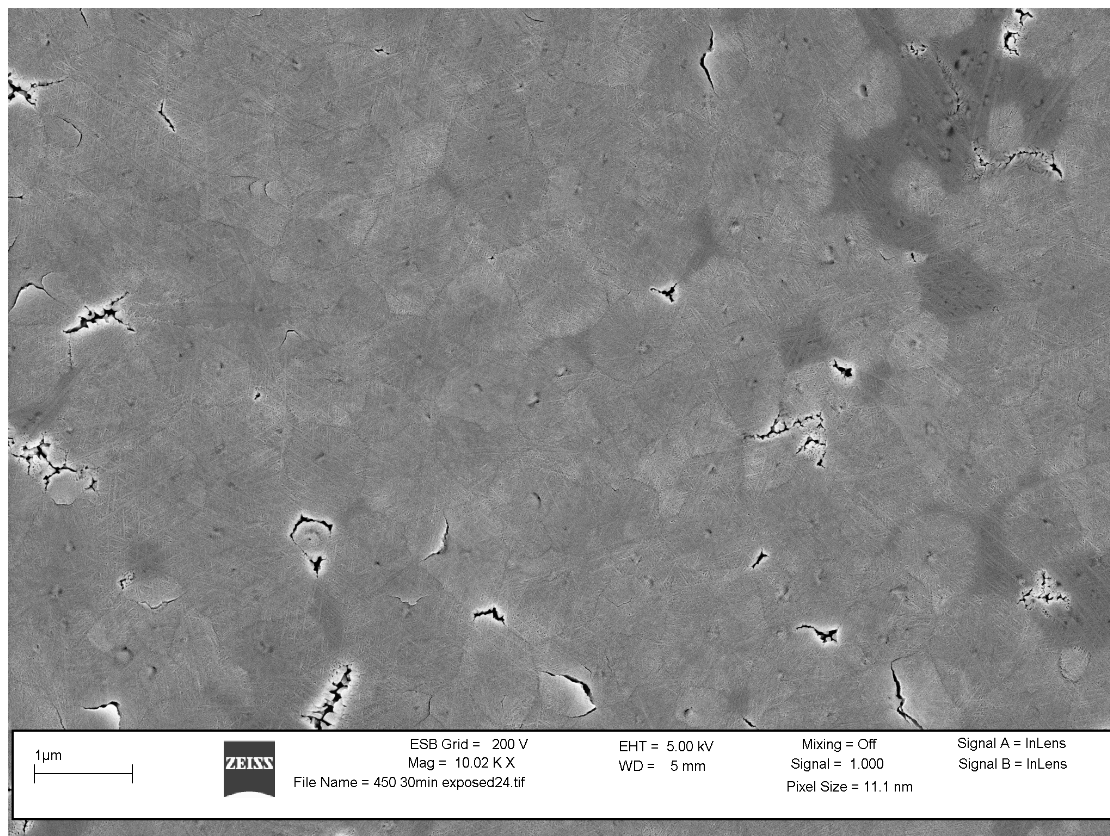

Figure 6-10. SEM image of peroxopolymolybdate after exposure to UV light for 10 min followed by reduction at 450ºC in flowing H_2 for 30 min.

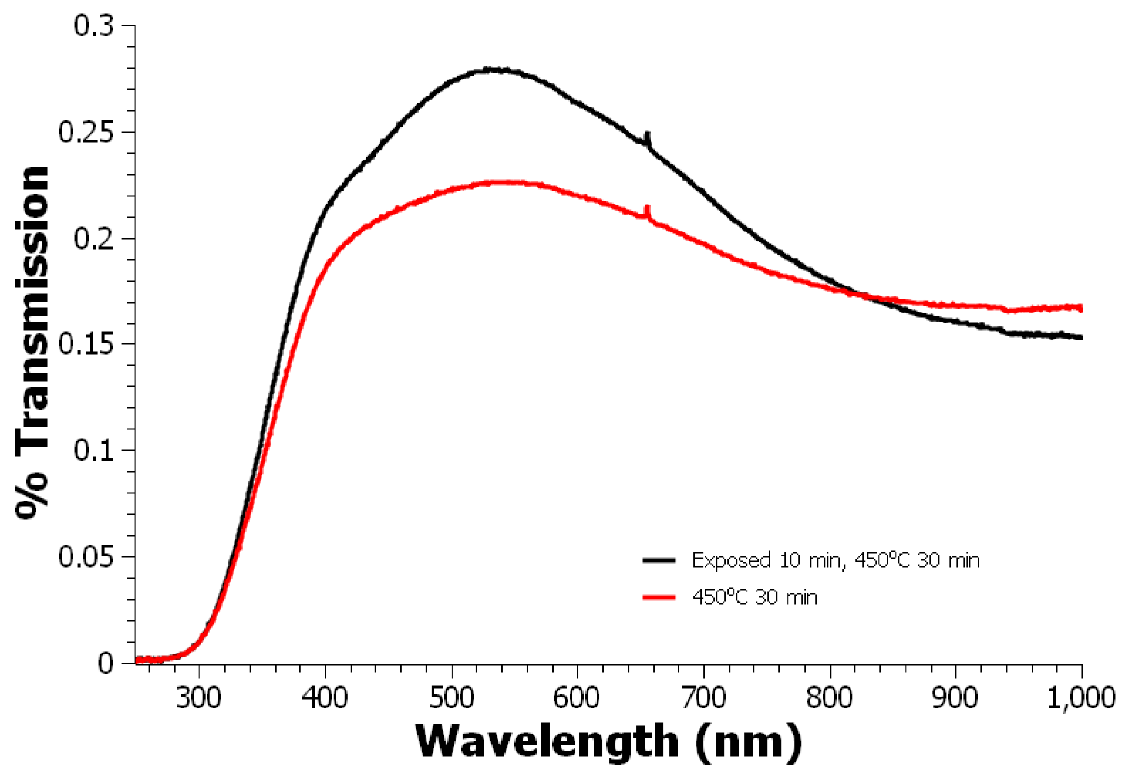

Figure 6-11. Optical Transmission for exposed and unexposed films reduced in flowing H_2 at 450ºC for 30 min.

CHAPTER 7

CONCLUSIONS

The ability to do direct patterning adds a significant advantage to solution deposited metal oxides. In comparison, other methods for the deposition of metal oxides rely on the use of a polymer resist and plasma etching to achieve the same patterning result.

In Chapter 2, HafSOx and ZircSOx have been patterned using a bilayer diffusion process. Though the ability to pattern these materials through this process was exceeded by later work, this patterning system represents a novel method for the selective elemental modification of a metal oxide.

In Chapter 3, the patterning of HafSOx and ZircSOx was significantly improved on by changing chemistries to a peroxide based system. Sensitivity to UV ($\lambda <$ 254nm) and EUV light was demonstrated. The contrast of the unoptimized photolithographic process was generally found to be low. In the future, photolithography deserves revisiting using the knowledge gained using electron-beam lithography.

In Chapter 4, patterning of the SOx materials with electron beam lithography produced excellent results. A sensitivity of 8 $\mu C/cm^2$ and a contrast of 3 was exhibited. Isolated lines 16-nm in width with a LER of 2.4 nm were patterned at 112 $\mu C/cm^2$. The SOx materials exhibited excellent dry etch resistance. These results indicate that this system performs well as an inorganic resist. With a small amount of continued development this resist will exceed the ability of the negative-tone resists used by industry.

In Chapter 5, a material system for the solution deposition of TiO_2 was found to be

directly patternable. This system was found to be sensitive to UV and electron beam exposure. A sensitivity of 1.1 mC/cm^2 and a contrast of 0.5 are exhibited for exposure by electron beam. These results represent a method to generate high quality patterned TiO_2 films. In comparison to physical vapor deposition or sol-gel methods this result demonstrates a significant advantage for this method in terms of quality and ease of patterning.

In Chapter 6, patterning thin films of peroxopolymolybdate is demonstrated. This system was converted to MoO_3 upon annealing in air. The films are converted to a conductive transparent MoO_2 upon reduction in flowing H_2. A resistivity as low as 1.4 mΩ cm is demonstrated. The transmission of these films across the visible spectrum is 24%. This system exhibits the potential to be employed as a patterned thin film transparent conductive oxide. From a larger perspective, the results here are an example of the flexibility of aqueous solution-deposited metal oxides.

The focus of this dissertation has been enabling the direct patterning of aqueous solution-deposited metal oxides. This research will play a critical role in future integration of these functional materials in to a variety of applications. The patterning ability of these materials can be useful itself as a potential replacement for polymer resists used in photolithography and electron-beam lithography.

Bibliography

[1] J.T. Anderson, C.L. Munsee, C.M. Hung, T.M. Phung, G.S. Herman, D.C. Johnson, J.F. Wager, D.A. Keszler, Adv. Funct. Mater, 17 (2007) 2117-2124.

[2] G.E. Moore, Electronics,, 38 (1965).

[3] C. Mack, Future Fab International, (2007).

[4] “Intel Technology Journal”; http://www.intel.com/technology/itj/2008/v12i1/7-evaluation/2-intro.htm.

[5] J.A. Liddle, G.M. Gallatin, L.E. Ocola, Three-Dimensional Nanoengineered Assemblies as held at the 2002 MRS Fall Meeting, (2002) 19-30.

[6] S.W. Chang, R. Ayothi, D. Bratton, D. Yang, N. Felix, H.B. Cao, H. Deng, C.K. Ober, Journal of Materials Chemistry, 16 (2006) 1470-1474.

[7] H. Gernsheim, A. Gernsheim, *The History of Photography: From the Camera Obscura to the Beginnings of the Modern Era*, McGraw Hill, New York, NY, 1969.

[8] J.L. Marignier, in: V.V. Krongauz, A.D. Trifunac (Eds.), Processes in Photoreactive Polymers, Springer, 1995, p. 409.

[9] W.S. Deforest, *Photoresist: Materials and Processes*, Mcgraw-Hill (Tx), 1975.

[10] A. Reiser, *Photoreactive Polymers: The Science and Technology of Resists*, John Wiley & Sons, 1989.

[11] J.G. Jorgensen, H.M. Bruno, *The Sensitivity of Bichromated Coatings*, Lithographic Technical Foundation, New York, NY, 1954.

[12] H. Stobbe, A. Lehfeldt, Ber, 58 (1925) 2418.

[13] R.K. Agnihorti, F. D.L, F.P. Hood, L.G. Lesoine, C.D. Needham, J.A. Offenbach, Photogr. Sci. Eng., 16 (1954) 443.

[14] O. Süss, Liebeg's Ann. Chem., 566 (1944) 65-84.

[15] O. Süss, M. Schmidt, U.S. Patent 2 766 118, (1956).

[16] J.P. Fouassier, J.F. Rabek, *Radiation Curing in Polymer Science and Technology*, Springer, 1993.

[17] T. Iwayanagi, S. Ueno, H. Nonogaki, C.G. Willson, in: M. Bowden, S. Turner (Eds.), Electronic and Photonic Applications of Polymers, American Chemical Society, 1988, p. 372.

[18] S.A. MacDonald, C.G. Willson, J.M.J. Frechet, Accounts of Chemical Research, 27 (1994) 151-158.

[19] E. Reichmanis, L.F. Thompson, Chemical Reviews, 89 (1989) 1273-1289.

[20] J.M.J. Frechet, H. Ito, E. Eichler, C.G. Wilson, Polymer, 24 (1983) 995-1000.

[21] C.P. Umbach, A.N. Broers, C.G. Willson, R. Koch, R.B. Laibowitz, Journal of Vacuum Science & Technology B: Microelectronics and Nanometer Structures, 6 (1988) 319.

[22] G. Wallraff, R. Allen, W. Hinsberg, C. Willson, L. Simpson, S. Webber, J. Sturtevant, Journal of imaging science and technology, 36 (1992) 468-476.

[23] M. Isaacson, A. Muray, M. Scheinfein, A. Adesida, E. Kratschmer, Microelectronic Engineering, 2 (1984) 58-64.

[24] E. Kratschmer, M. Isaacson, Journal of Vacuum Science & Technology B: Microelectronics and Nanometer Structures, 4 (1986) 361.

[25] E. Kratschmer, M. Isaacson, Journal of Vacuum Science & Technology B: Microelectronics and Nanometer Structures, 5 (1987) 369.

[26] W. Langheinrich, A. Vescan, B. Spangenberg, H. Beneking, Microelectronics Eng, 23 (1994) 287.

[27] J. Fujita, H. Watanabe, Y. Ochiai, S. Manako, J.S. Tsai, S. Matsui, Applied Physics Letters, 66 (1995) 3064.

[28] G.H. Chapman, Y. Tu, M.V. Sarunic, J. Dhaliwal, 2001, pp. 557-568.

[29] H. Nagai, A. Yoshikawa, Y. Toyoshima, O. Ochi, Y. Mizushima, Appl. Phys. Lett., 28 (1976) 145-147.

[30] V. Lyubin, M. Klebanov, I. Bar, S. Rosenwaks, N.P. Eisenberg, M. Manevich, J. Vac. Sci. Technol. B , 15 (1997) 823-827.

[31] J. Teteris, Journal of Non-Crystalline Solids, 299 (2002) 978-982.

[32] G.C. Chern, I. Lauks, J. Appl. Phys., 53 (1982) 6979-6982.

[33] S. Shtutina, M. Klebanov, V. Lyubin, S. Rosenwaks, V. Volterra, Thin Solid Films, 261 (1995) 263-265.

[34] K. Tanaka, Current Opinion in Solid State and Materials Science, 1 (1996) 567-571.

[35] A. Yoshikawa, O. Ochi, H. Nagai, Y. Mizushima, Applied Physics Letters, 29 (1976) 677.

[36] M. Frumar, T. Wagner, Current Opinion in Solid State and Materials Science, 7 (2003) 117-126.

[37] J.M. Lavine, M.J. Buliszak, J. Vac. Sci. Technol. B, 14 (1996) 3489-3491.

[38] A. Yoshikawa, S. Hirota, O. Ochi, A. Takeda , Y. Mizushima , Jpn. J. Appl. Phys. , 20 (1981) L81-L83.

[39] H. Okamoto, T. Iwayanagi, K. Mochiji, H. Umezaki, T. Kudo, Appl. Phys. Lett., 49 (1986) 298-300.

[40] H. Okamoto, A. Ishikawa, T. Kudo, Thin Solid Films, 172 (1989) L97-L99.

[41] H. Okamoto, A. Ishikawa, T. Kudo, Journal of photochemistry and photobiology. A, Chemistry, 49 (1989) 377-385.

[42] H. Okamoto, A. Ishikawa, T. Kudo, Journal of The Electrochemical Society, 136 (1989) 2646.

[43] M.S.M. Saifullah, K. Kurihara, C.J. Humphreys, J. Vac. Sci. Technol. B, 18 (2000) 2737-2744.

[44] K.R.V. Subramanian, M.S.M. Saifullah, E. Tapley, D. Kang, M.E. Welland, M. Butler, Nanotechnology, 15 (2004) 158-162.

[45] M. Saifullah, K. Subramanian, E. Tapley, D. Kang, M. Welland, M. Butler, Nano Lett., 3 (2003) 1587-1591.

[46] H. Namatsu, Y. Takahashi, K. Yamazaki, T. Yamaguchi, M. Nagase, K. Kurihara, J. Vac. Sci. Technol. B, 16 (1998) 69-76.

[47] A.E. Grigorescu, M.C. van der Krogt, C.W. Hagen, P. Kruit, Microelectronic Engineering, 84 (2007) 822-824.

[48] Y. Ekinci, H.H. Solak, C. Padeste, J. Gobrecht, M.P. Stoykovich, P.F. Nealey, Microelectronic Engineering, 84 (2007) 700-704.

[49] H. Okamoto, A. Ishikawa, Appl. Phys. Lett., 55 (1989) 1923-1925.

[50] C.G. Willson, R.R. Dammel, A. Reiser, Proc. SPIE, 3049 (1997), 28-41.

[51] A.E. Grigorescu, M.C. van der Krogt, C.W. Hagen, (2007).

[52] C. Mack, *Fundamental Principles of Optical Lithography: The Science of Microfabrication*, Wiley-Interscience, 2008.

[53] H.J. Levinson, *Principles of Lithography, Second Edition*, 2nd ed., SPIE Publications, 2005.

[54] R.P. Meagley, Future Fab International, (2006).

[55] G.H. Bernstein, W.P. Liu, Y.N. Khawaja, M.N. Kozicki, D.K. Ferry, L. Blum, J. Vac. Sci. Technol. B, 6 (1988) 2298-2302.

[56] K. Nomura, H. Ohta, A. Takagi, T. Kamiya, M. Hirano, H. Hosono, Nature, 432 (2004) 488-492.

[57] A. Clearfield, P.A. Vaughan, Acta Crystallographica, 9 (1956) 555-558.

[58] G.M. Muha, P.A. Vaughan, J. Chem. Phys., 33 (1960) 194-199.

[59] A. Clearfield, Reviews of Pure and Applied Chemistry, 14 (1964) 91.

[60] M.J. Word, I. Adesida, P.R. Berger, J. Vac. Sci. Technol. B, 21 (2003) L12-L15.

[61] D.C. Joy, S. Luo, Scanning, 11 (1989) 176-180.

[62] P.A. Hersh, *Wide band gap semiconductors and insulators: synthesis, processing and characterization*, Oregon State University, 2007.

[63] J.K.W. Yang, K.K. Berggren, Journal of Vacuum Science & Technology B: Microelectronics and Nanometer Structures, 25 (2007) 2025.

[64] K. Jiang, D. Keszler, J. Tate, D. McIntyre , J. Stowers, A. Zakutayev, In Press, (2008).

[65] P. Walker, W.H. Tarn, *CRC Handbook of Metal Etchants*, 1st ed., CRC, 1990.

[66] S. Norasetthekul, P.Y. Park, K.H. Baik, K.P. Lee, J.H. Shin, B.S. Jeong, V. Shishodia, E.S. Lambers, D.P. Norton, S.J. Pearton, Applied Surface Science, 185 (2001) 27-33.

[67] W. Hu, K. Sarveswaran, M. Lieberman, G.H. Bernstein, J. Vac. Sci. Technol. B, 22 (2004) 1711-1716.

[68] A. Labidi, C. Jacolin, M. Bendahan, A. Abdelghani, J. Guerin, K. Aguir, M. Maaref, Sensors and Actuators B, 106 (2005) 713-718.

[69] J. Choy, Y. Kim, J. Yoon, S. Choy, J. Mater. Chem., 11 (2001) 1506-1513.

[70] K. Itoh, T. Okamoto, S. Wakita, H. Niikura, M. Murabayashi, Applied Organometallic Chemistry, 5 (1991) 295-301.

[71] A. Klisinska, A.S. Mamede, E.M. Gaigneaux, Thin Solid Films, 516 (2008) 2904-2912.

[72] E. M. Gaigneaux, K. Fukui, Y. Iwasawa, Thin Solid Films, 374 (2000) 49-58.

[73] K. Hinokuma, K. Ogasawara, A. Kishimoto, S. Takano, T. Kudo, Solid state ionics, 53 (1992) 507-512.

[74] D.B. Rogers, R.D. Shannon, A.W. Sleight, J.L. Gillson, Inorganic Chemistry, 8 (1969) 841-849.

[75] S.H. Mohamed, O. Kappertz, J.M. Ngaruiya, T.P. Leervad Pedersen, R. Drese, M. Wuttig, Thin Solid Films, 429 (2003) 135-143.

[76] J. Okumu, F. Koerfer, C. Salinga, M. Wuttig, J. Appl. Phys., 95 (2004) 7632-7636.

[77] V. Bhosle, A. Tiwari, J. Narayan, Journal of Applied Physics, 97 (2005) 083539.

[78] R. Patil, M. Uplane, P. Patil, Applied Surface Science, 252 (2006) 8050-8056.

[79] S. Ashraf, C.S. Blackman, G. Hyett, I.P. Parkin, J. Mater. Chem., 16 (2006) 3575-3582.

[80] R. Patil, M. Uplane, P. Patil, Applied Surface Science, 252 (2006) 8050-8056.

[81] F. Chen, Y. Lin, T. Chen, L. Kung, Electrochem. Solid-State Lett., 10 (2007) H186-H188.

[82] H. Kim, J.S. Horwitz, G. Kushto, A. Pique, Z.H. Kafafi, C.M. Gilmore, D.B. Chrisey, J. Appl. Phys., 88 (2000) 6021-6025.

[83] L.J. van der Pauw, Philips Technical Review, 20 (1958) 220–224.

[84] L.J. van der Pauw, Philips Res. Rep, 13 (1958) 1-9.

[85] E. Lalik, W. David, P. Barnes, J. Turner, J. Phys. Chem. B, 105 (2001) 9153-9156.